UNIVERSITY OF GENOVA

PHD PROGRAM IN BIOENGINEERING AND ROBOTICS

Tactile sensors for robot bodies

by

Giulia Baldini

Thesis submitted for the degree of *Doctor of Philosophy* (35° cycle)

July 2026

Prof. Giorgio Cannata	Supervisor
Prof. Paolo Massobrio	Head of the PhD program

Thesis Jury:

Perla Maiolino, *University of Oxford*	External examiner
Federico Carpi, *Università di Firenze*	External examiner
Giorgio Cannata, *University of Genoa*	Internal examiner

Dibris

Department of Informatics, Bioengineering, Robotics and Systems Engineering

I would like to dedicate this thesis to my blood family and to the one I choose every day . . .

Declaration

I hereby declare that except where specific reference is made to the work of others, the contents of this dissertation are original and have not been submitted in whole or in part for consideration for any other degree or qualification in this, or any other university. This dissertation is my own work and contains nothing which is the outcome of work done in collaboration with others, except as specified in the text and Acknowledgements.

Giulia Baldini
January 2023

Acknowledgements

I would like to thank my supervisor Prof. Giorgio Cannata, who gives me the opportunity to work on this project.
This work was supported by the European Community's Framework Programme Horizon 2020 (grant agreement number 820767, project CoLLaboratE) and by the European Union's Horizon Europe project "Sestosenso" under grant agreement No. 101070310.

Abstract

Tactile sensing technology has been studied for a long time, and a significant number of technologies have been proposed in the literature. This technology has also found growing relevance in the robotics field, including robot manipulation and safe human–robot interactions, where force/torque sensors are frequently used. Despite their accuracy, these kind of sensors do not allow dealing with complex physical interactions as in the case of multiple contacts (where only the resultant force would be detected, and therefore information on internal forces and contact locations are lost) or when major internal forces arise. Conversely, skin-like sensors used to measure and process distributed contacts, allow the reconstruction of the pressure distribution applied to the entire contact area.

The goal of this thesis is to investigate the design of skin-like capacitive sensors for robot bodies, based on inkjet printing technique. Tactile sensors are devices based on the transduction of a component due to induce contact stresses, and they are often built as matrices of sensitive interconnected elements called taxels. The challenges for the manufacturing of tactile sensors are related to the maximization of their dynamic range and sensitivity, and to the use of a fabrication method that allows to optimize the sensor placement especially on curved surfaces, with the embedded electronics. To enhance the sensors dynamic range and sensitivity, the approach of exploiting the sensors vertical direction has been adopted, by creating stacks of capacitors. The validation of the proposed mathematical model is conducted by means of finite element simulations and the effectiveness of stacked capacitors in sub-optimal configurations has been experimentally tested by using inkjet printing as the main fabrication technique. The use of printed electronics has been chosen since it simplifies the fabrication process of tactile sensors with respect to conventional fabrication methods and it contributes to overcome the difficulties arising in the development of tactile sensors for real robot applications. From the system-level in the thesis we have design a front-end electronics for data acquisition and early tactile data processing based on embedded microcontrollers which can do both the acquisition and transmission part and programmed with an event-based algorithm to test the reliability about the touch detection.

Results show that the stacked capacitors exhibit an enhanced dynamic range and sensitivity with respect to common single capacitors, for a given sensors area budget, and this suggests a method for designing tactile sensors with higher spatial resolution, higher transduction sensitivity and dynamic range. Furthermore, it has been verified that the new architecture can be connected and integrated with the manufactured sensors, detecting touches, and showing the resulting output capacitances on the host PC with low noise. This is a low-cost solution which allows to increase the number of sensors from which gather data and process them, meaning that a large contact area of the robot can be covered by the sensors and its electronic components. The result is the design of an embedded system that combines the manufactured part with electronics, creating an optimal blueprint for a future real implementation.

Keywords: Capacitive tactile sensing, robotics, skin, stack, inkjet printing, sensitivity.

Table of contents

List of figures

List of tables

Nomenclature

Acronyms / Abbreviations

P(VDF-trFE) Polyvinylidene Fluoride-Triflouroethylene

AgNP Siver Nanoparticle

CAD Computer Aided Design

CDC Capacitance to Digital Converters

CIJ Continous Inkjet Printing

CNT Carbon Nanotube

CSD CapSense Sigma Delta

CSX CapSense Crosspoint

DoD Drop-on-Demand

EDA Electronic Design Automation

IDE Integrated Design Environment

MPTMS (3- mercaptopropyl)trimethoxysilane

FDM FusedDeposition Modeling

PCBs Printed Circuits Boards

SLA Stereolithography

SLS Selective Laser Sintering

PDMS Polydimethylsiloxane

PEN Polyethylene Naphthalate

PET Polyethylene Terephthalate

PVA Polyvinyl Alcohol

SNR Signal to Noise Ratio

SRR Split Ring Resonator

TPU Thermoplastic Polyurethan

TRL Technology Readiness Level

VHB Very High Bond

Introduction

Tactile sensing began to develop in the 1970s— albeit at a slower pace, when compared with the development of other sensing modalities. Early surveys on the state of tactile sensing show a wide diversity in the types of sensing device that were developed in the 1980s (87; 177). The application domain of robotics has been continuously developing and rapid technological progress and rising expectations of machines have changed the face of robotics. The concept of a robot as an industrial machine working in a human-less area though controlled by humans is fading, and a new generation of robots such as humanoids, bio-robots, social robots, assistive and medical robots, etc. are entering our lives. Humanoids robots simulate human structure and behavior; bio-robots help provide insight into how biological systems work; social robots enable human-robot interaction; exoskeletons and artificial limbs assist humans; and medical robots help perform surgical procedures more accurately and less invasive. All these new types of robots are expected to learn autonomously, interact safely with the environment, with the humans, among themselves and also feature additional characteristics, such as self-maintenance, and more.

Achieving this goal is not straightforward even the model of the environment would be available and the robot actuators could perfectly execute motion commands relative to that model. Unfortunately, in most cases, a complete model of the world is not available, and robots must plan and successfully execute tasks while taking into account uncertainties in the environment. For this reason, current robots and the next generation robots must be equipped with advanced sensors, which enable the development of techniques in order to manage the interaction with the environment and with humans.

In general, sensory information from multiple sensory modalities (e.g., touch, vision, hearing, etc.) is needed to interact with and perceive the environment. The sensor information may come from a single sensory modality or simultaneously from multiple sensory modalities to obtain a robust perception (63). Touch is an essential modality that allows us to evaluate contact parameters such as shape, surface texture, stiffness, and temperature, etc. It helps develop body awareness, enables us to distinguish between "me" and "not me," and helps us roll an object between our fingers without dropping it. Tactile perception is also required in human-robot interaction for safe interaction and robot training. Without adequate touch feedback, performing normal tasks that require a high degree of dexterity is extremely difficult, if not impossible. Thus, it is clear that the sense of touch is critically important on many different levels, from controlling the body to perceiving the environment to learning and interacting with it.

Historically, sensor-based robotics emerged when traditional motion strategies proved insufficient to reduce uncertainties in the relative positioning of objects. For example, when a robot is asked to place a book on a table, one motion strategy was to move the book at a reasonable height above the table and then simply drop it (52). Such strategies are simple and fast, but the result is flawed due to inevitable control and model errors. The inadequacy of such strategies for the ever-changing robotics paved the way for sensor-based strategies. Sensors provide information about the state of the environment and the state of the robotic system, which serves as the basis for control, decision making, and interaction with other agents/objects in the environment. In this thesis we focus on particular sense modality which is "touch", or more specifically "tactile sensing". The sense of touch is different from sensory modalities such as vision and hearing because it is distributed over the body and involves physical contact with objects. What a robot can or cannot do without a "sense of touch" can be seen in many of the difficulties that humans might face in its absence. The interaction behavior with objects in the real world can be better understood when robots physically interact with them -just as humans do. The "sense of touch" helps to understand the interaction behavior of real-world objects, which depends on the weight and stiffness of the object, how their surfaces feel when touched, how they deform on contact, and how they move when pushed, etc (52). In biomedical robotics, tactile and force feedback together can improve the ability of robots to detect lumps (or hard tissue) during minimally invasive surgery (MIS). Information obtained through the sense of touch is used for reflexes and automatic responses (e.g., regulation of grasping force) without requiring cognitive effort. In daily life, we use tactile sensors to feel objects, measure the comfort of shoes through touch receptors in the foot, and more, where sensory modalities such as vision would be of little help (52). The tasks mediated by the sense of touch can be divided into three categories: Manipulation (perception for action), Exploration (action for perception), and Response or Haptics (210). It should be noted that all of these tasks are dynamic in nature and require relative movement of the sensors. Grasping is an essential capability for a general-purpose robot operating in an industrial or domestic environment. It is a manipulation task where touch data is used as a control parameter or for grip stability. Using tactile sensors to maximize the contact area for removing a book from a bookshelf is an example where tactile sensing is used for control (173). Similarly, touch sensing can prevent slippage when holding an object, contributing to stable grasping. Information of interest during gripping typically includes contact point estimation, surface normal and curvature measurement, position, shape, weight, slip detection, and/or material properties (66; 210). Often the environment is unstructured, making it difficult to estimate the parameters of interest and thus challenging traditional approaches to achieving a stable grip. For example, visual sensing has traditionally been used to determine touch information such as the shape and position of an object. However, the accuracy of vision is limited, and small errors in object position are common, even for known objects, and even small errors can lead to errors in grasping. Uncertainties arising from the softness or deformability of an object also lead to errors in grasping, since most analytical methods used for grasping stability focus on rigid objects. Studies of the kinematics and dynamics of dexterous manipulation with robotic hands also indicate that the equations of motion of the combined hand-object system are very sensitive to the contact conditions or events between the fingers and the object. That is, stable grasping requires detection of changes in the state of the contacts (between the fingertips and the object and between the grasped object and the external environment), and tactile feedback can be very useful for this purpose. Equipping robotic hands with appropriate touch sensors (i.e., tactile and joint force sensors) is therefore urgently needed to extend the possibilities offered by using only other sensing modalities. The sense of touch plays an important role in exploring objects and distinguishing them from each other. In robotics, this is done by touching the objects, by multiple grasping, or by various manipulations using haptic inputs. For example, when the robot moves its finger over a surface or object, it can extract data/features from multiple points to obtain a tactile image that can be used to create or improve a model using learning techniques. The contact information can be used to derive information about the properties of the object, such as: is the object stiff or is it compliant? Is there a texture? What is the coefficient of friction? etc. Tactile perception is also important for the safe interaction of robots with humans, objects, and possibly in unstructured environments. In classical robot interaction tasks, such as the peg-in-hole problem, certain robot parts (typically the tip of the end effector) are involved during the interaction, and force/torque sensors have been widely and successfully used for this purpose (52). However, a robot's physical interaction with the real world is not necessarily through touch with fingers or hands. Other body parts such as the arms are often involved as well. For example, a robot lifts an elderly or disabled person and transfers them from a wheelchair to bed. Advanced robotic systems such as humanoids must be able to control more complex forms of interaction (e.g., grasping and manipulating with the whole hand or arm, controlling gait stability, etc.). These tasks require monitoring the robot's contacts with the environment, which may occur at unpredictable positions and in unpredictable ways. Therefore, skin-like sensors, not only on the fingers and hands, but on the entire body, are needed for such complex forms of interaction to enable the implementation of safe interaction strategies.

Chapter 1

Tactile Sensing: Technological Issue

Tactile sensing has been studied for a long time and a significant number of technologies has been studied in the literature (218; 232; 267). As discussed in the Introduction, tactile sensors are used for sensing the location of contact and to measure surface properties, such as roughness, stiffness and temperature. The research on tactile sensing has attracted intense interest in different fields, from biomedical engineering to industry. There are several applications of tactile sensing systems, such as manual paalpation, minimally invasive surgery, prosthetic, sportswear as well as agriculture, food processing, aerospace and automobiles industry (226). Tactile sensing has also found growing relevance in the robotic field, including robot manipulation and safe robot-human interaction (28; 29; 32; 103; 130; 144; 160; 181). In the domain of robot control, this operations have been treated using force/torque sensors (54; 55; 77; 85; 144; 152; 159). Despite their accuracy, they do not allow to deal with complex physical interactions as in the case of multiple contacts or when major internal forces could arise. In case of multilple contacts, indeed, force resultant would only be detected and, therefore, information on internal forces and contact locations are lost. Conversely, skin-like sensors used to process the distribution of tactile information, allow to reconstruct the pressure distribution applied to the entire contact area (25; 58; 59; 93; 100; 109; 126; 139; 214). This chapter aims to introduce the state of art of tactile sensors, focusing on the problems that could arise during their development. Section 1.1 provides an overview of the requirements and major challenges arising in the design of large area tactile sensors, while in Section 1.2 the fundamental transduction principles used for tactile sensors are introduced. Section 1.3 provides a summary of the main fabrication techniques for tactile sensors, with a description of their pros and cons, while determining how inkjet printing behaves in respect to manufacturing.

1.1 Requirements and challenges in tactile sensors design

In general, a tactile sensor is a device based on the transduction of a component due to induced contact stresses. Different transduction principles based on different techniques have been used to measure contact information (178). Each method has its pros and cons, and, depending on the applications, some methods are more suitable than others (50; 135) . While tactile sensors are often built as matrices of sensitive interconnected elements (taxels), there is not a standard technology (in comparison to e.g. image transducers) for the development of these devices. Consequently, the overall system design can be linked to the type of application. In particular, for some applications, tactile sensing arrays built over large areas have been proposed. In this context, there are not specific numbers to define the requirements. Thus, we give the guidelines based on the task. Examples of large area skins (in which information on the size -cm^2- and number of sensitive elements can be found) are described in applications of *Tactile-based control* (in the works of (8; 127)) and *Tactile-based recognition* (in the works of (7; 20)). In *Tactile-based control* tasks, the fundamental requirement is often the coverage: in these applications, the robot needs to be covered with tactile sensors since contact can occur anywhere. An extended coverage allows to detect the forces acting on the entire robot and to react accordingly. As a result, the spatial resolution plays a minor role, as we do not need to reconstruct the contact shape but to detect the lumped forces acting on robots. Conversely, in *Tactile-based recognition* tasks a high spatial resolution is required, since the aim is to recognize the spatial distribution of the acting force.
The development of tactile sensing systems is affected by a large number of challenges and constraints (50; 51). One of these regards the fabrication of vertical vias in multi-layered tactile devices, in which functional devices from different layers need to be connected by vertical interconnects (195). Some works addressed the problem by manually creating vertical feedthrough (creating holes and metallizing them), during or even after the device fabrication (30; 79). This process is normally conducted in rigid double layer devices. More difficulties arise in the case of multi-layered sensors (more than two layers), as the drilling must be done with a perfect cut to ensure that the subsequent metallization contacts all the conductive layers involved. Furthermore, reliable interfacial adhesion of flexible sensing elements with electronic components, such as wiring, integrated circuits, or other conventional devices, still remains a problem. Since tactile sensors are devices subjected to significant mechanical stresses due to contacts, the problem of bonding and of sensor integration with the integrated electronics is an issue from the durability and robustness point of view. Then, the choice of materials is an important constraint in the design of a tactile sensor. The ageing of the

material used has to be considered, as it leads to a decrease in sensor lifetime and sensitivity. For large area tactile sensors, the interconnection of the sensitive elements strongly depends on the geometry of the surface on which they must adapt. Therefore, other fundamental constraints arise during the design of tactile sensors. The sensors conformability is an important parameter since they need to mechanically adapt to a generic geometry, either planar or curved. Furthermore, sensors placement to ensure the maximum surface covering is needed, as well as simple calibration procedures. Once interconnected, sensors need to communicate with each other via suitably routed wires (to not prevent, for example, the robot movement). As we will discuss later, the key challenges that can be treated with printed electronics technologies mainly regard the system-level integration of tactile sensors (i.e., conformability, sensors distribution and placement, spatial calibration, routing of wires) as shown in Figure 1.1, while the others still remain open problems.
In this section, we will limit to describe how the systeml-level requirements have been addressed in the past.

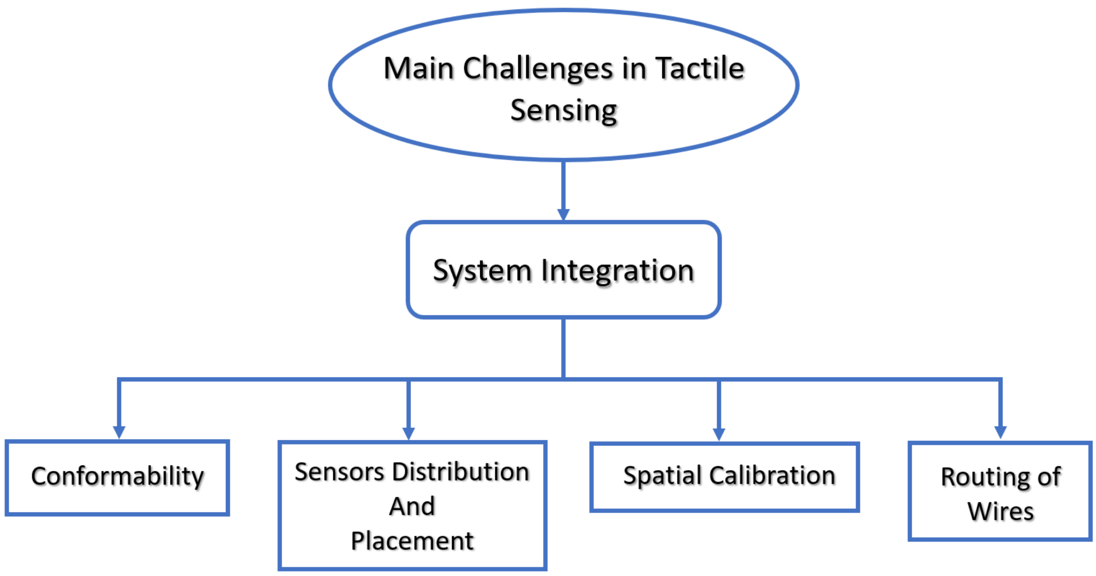

Figure 1.1 The main challenges in tactile sensing addressed with the inkjet printing technology.

1.1.1 Conformability

Tactile sensors should be conformable to cover arbitrary curved robot body parts easily. This is an important aspect especially when tactile sensors are distributed all over the body (51).

This goal has been pursued in the literature by implementing tactile sensors using flexible *printed circuits boards (PCBs)*, implementing discrete and interconnected tactile skin patches to improve the adaptability to the robot surface (26; 170; 175; 181; 202). The available mechanically flexible tactile sensing solutions tipically use PCB on rubber like substrates and flexible PCBs as substrate and the off-shelf sensing and electronic components are soldered. Examples of such solutions are based on tactile skin modules having triangular, hexagonal or other basic shapes, interconnected to form tree or comb or general shaped patches. These techniques ensure a pretty good conformability but also have major drawbacks. In fact, sometimes, the bending radius of flexible PCBs is large and such solutions are only suitable for body parts like arms of a humanoid. Furthemore, skin patches make the sensors easily adaptable to different surfaces, but, as we will discuss in the next paragraph, they lead to surface covering problems. Finally, the flexibility of a sensing structures does not always ensure conformability in all directions. Many available structures can bend only along one axis and hence can conform to surfaces as cylinders, which approximates the arm of a robot; in this context, many simple flexible PCBs fail. One way to address this issue could be based on the use of intrinsically stretchable sensors. As discussed in (51), this poses new challenges in introducing new materials and manufactuing processes. Bringing these ideas to the extreme, the concept of stretchability could also be proved from the electronic components level by manufacturing stretchable electronic devices. The realization of stretchable devices with traditional materials such as silicon is a challenge owing to their intrinsic properties such as brittleness that limit their ability to stretch or bend (53; 84). Furthermore, metals such as gold and copper have been preferred for interconnects and electrodes, owing to their high electrical and thermal conductivity that permits an influx of large current and fast transmission of signals (53). However, when it comes to flexibility the metals have been found to have limited use as they are not elastic enough (53).

1.1.2 Sensor distribution and placement

The surface covered with tactile sensors often has a complex geometry characterized by variable curvatures. Hence, the need to create customized sensors has emerged. The spatial distribution and placement is an essential challenge because the number of tactile sensors and their distribution across the sensing surface affects the quality of measurements and the effectiveness of tactile data utilization. An appropriate placement of the sensors can ensure the maximum surface covering, guaranteeing appropriate sensitivity and taxel distribution over large areas allowing to measure multiple touches over the whole surface of the device

(47). The state of the art of tactile technology does not allow the fabrication of sensors which can be easly adapted to arbitrary geometries. Custom solutions can be complex, time consuming and expensive since they might require a complete redesign and setup of the manufacturing process. Approximate covering solutions have been proposed to ensure sub-optimal placement of general-purpose tactile skin patches (50). Examples of such solutions include tactile skin patches with triangular (26), (202), hexagonal (170), or the tree– or comb– shaped modules (175), (181). These types of structures start from simple shapes, and they are further be extended to approximate complex geometries. For example, the triangles are inspired by computer graphics for creating complex solids. For this reason various large area tactile sensors are constructed as meshes of triangles or hexagons to simplify the approximate placement of the sensors on general robot body geometries. Once shapes have been obtained, the interconnections can be done by software that solves the optimization problem to generate the mesh. Preliminary works by Anghinolfi et al. (13), further extended by Wei et al. (240) and Mastrogiovanni et al. (161) have discussed the possibility of obtaining suboptimal covering of surfaces based on standard robot skin patches geometries, typically formed by triangular or hexagonal meshes. Software methods can be either separate or complementary to the hardware part, as the aforementioned geometries do not solve the problem by themselves, especially for their physical limits (if the sensor is bent beyond a certain limit, it breaks). Thus, the challenge is the quick design of ad hoc components.

1.1.3 Spatial Calibration

As previously discussed, currently, sensor patches are placed on the surface to be sensorized with significant uncertainty in the displacement of the tactile elements. This requires time-consuming geometrical calibration procedures to obtain specific calibration files (27; 57; 123; 171; 179; 190). These procedures are tedious and may require specific equipment.

1.1.4 Wiring

Wiring of large area tactile sensors is one of the most critical problems related to the development of tactile sensors (48; 49). In robotics applications, the large number of wires bring to the fore such problems as routing cables through the robot's joints and optimizing the use of the limited available space in the robotic shell, due to existing motors and electronic components (50). Available wireless technologies (60; 96) can not be used for robotics applications because they are not reliable and they are not deterministic, and so problems on robots control arise (49). In general, as the number of sensors increases, so is the number of wires needed to address elements, acquire and transmit the data, and power the sensors. As reported in (49), the number of wires has an inverse relation with dexterity and a direct relation with the time needed to scan a set of taxels or array. Fewer wires call for the serial access of data, which is slower than parallel access that requires a large number of wires (49). So, the challenge is related to how many wires have to be integrated. If many wires are involved, the problem of routing arises, but if there are few wires with a serial access, the bus generates band saturation. In order to find optimal routes and avoid wire collisions, Wasserfall et al. (238) propose an algorithm solution for local, topology-aware wire routing.

1.2 Tactile Sensing Principles

This section introduces the fundamental transduction principles of tactile sensors and their relative advantages and disadvantages. In the literature a huge number of transduction principles have been proposed (115; 136; 143; 204; 232; 267). Piezoresistive, capacitive, piezoelectric, optical, inductive and magnetic methods have been often the preferred choice of sensor designers.

1.2.1 Piezoresistive

The mechanism of piezoresistive sensors is based on the transduction of pressure into the variation of resistance. The resistance variation of piezoresistive sensors mainly comes from the contact resistance between two conductive electrodes subject to an external pressure. The voltage–current characteristic of a simple resistive element can be expressed as, $V = IR$; where V is the voltage, I is the current and R is the electric resistance of the material. A standard piezoresistive sensor is composed of a thin film of material applied to a plastic substrate. Piezoresistive sensors have been widely studied for their simple fabrication, structure, low cost and easy signal acquisition. They allow to transduce pressure input stimuli starting from zero frequency (constant pressure) up to frequencies of the order of kHz. Piezoresistive sensing is less susceptible to noise, but it is affected by hysteresis, leading to lower frequency response compared to capacitive stactile sensors, and they can only be used for dynamic measurements with limited spatial resolution (226). The reported maximum piezoresistive sensing sensitivity can reach 0.25 mV/nm (68).

1.2.2 Capacitive

Capacitive tactile sensors are based on the change in capacity by mechanically changing the geometry of the capacitor. The capacitive pressure sensors are mainly based on the parallel plate capacitor, and the capacitance is determined by the equation: $C = \frac{\varepsilon_0 \varepsilon_r A}{d}$, where $\varepsilon_0, \varepsilon_r$ are, respectively, the vacuum electric permeability and the dielectric constant of the material used. A represents the electrode area and d is the distance between the electrodes. When applying pressure perpendicularly to the electrodes, d changes leading to the variation of capacitance, whereas in some design also A can change as the effect of shear force components (135). Parallel plate capacitors are the fundamental structure for capacitive sensing. Rectangular stripes, pyramidic structures, spheres, and pillars are all other structures used (267). Capacitive touch sensors have been well received for their low power consumption, high sensitivity, high repeatability, and simple device construction (228). They generally have a high spatial resolution and large dynamic ranges, though they might be susceptible to multiple types of noises (226). Furthermore, as for piezoresistive sensors, capacitive sensors can measure input stimuli starting from constant pressures (zero frequecy) up to frequencies limited by the required output sampling frequency and by the acquisition electronics. The best performance of capacitive tactile sensors ever reported is a minimum resolution of 3 Pa with a sensitivity of 0.55 kPa^{-1} (157).

1.2.3 Piezoelectric

Piezoelectric devices produce an electric charge proportional to the mechanical stress they are subject to. A typical readout mechanism is based on the usage of a charge amplifier leading to an output voltage which is proportional to the mechanical stress. The sensing principle leads to sandwich configurations as the general sensing structures for piezoelectric tactile sensors, where piezoelectric layers are deposited between two electrode layers. Like the capacitive tactile sensors, convex structures like mesas and spheres have been integrated as a contact promoter. The peculiar characteristic of piezoelectric transducers is that they cover wide measuring ranges. The maximum measurable pressure range has been reported as 100 MPa (15). So, it is possible to use the same sensor to measure very small or very large forces. Furthermore, piezoelectric tactile sensors are attractive due to their fast response, high dynamic sensitivity and low material costs. They exhibits very high-frequency response, making them the best choice for dynamic signal sensing (226). Unlike capacitive or piezoresistive tactile sensors, piezoelectric tactile sensors can not transduce the effect of constant input stimuli, i.e. constant pressures (zero frequency input).

1.2.4 Optical

Optical tactile sensing is implemented by coupling geometric change of electromagnetic waveguide with the modulation of wavelength, phase, polarization or intensity of the wave. Usually transduction occurs when changes in the tactile medium modulate the transmission or reflectance intensity, or the spectrum of the source light, as the applied force varies. Key sensing structures for tactile sensing are optic fibers vertically placed towards the sensing surface and waveguides sandwiched between substrate and contact interface structures (267). Optical tactile sensing is immune to common lower frequency electromagnetic interference generated by electrical systems, which is its major advantage. Optical sensors generally have high spatial resolution and wide dynamic response range. As reported in (267), optical tactile sensing can be used for sensing surface roughness, compliance, shear and vertical stress . For roughness measurements, the reported best resolution is around 100 nm level (241). For stress and mechanical forces, a resolution of 0.02 N has been reported for optical sensors used for minimally invasive surgery (192). Optical tactile sensing has shown great potential in applications requiring flexibility and portability (120; 180). Although they have many benefits, their size and rigidness are the major disadvantages (226).

1.2.5 Inductive and magnetic

In inductive and magnetic tactile sensors, a primary coil induces a magnetic field which is sensed in a secondary sense coil. Modulating the mutual inductance between the coils, for example by changing the length of an iron core in the case of a linear variable differential transformers, in turn modulates the amplitude and phase of the voltage measured in the sense coil. These sensors have a very high dynamic range and an often rugged construction, but are bulky in size, which leads to a very low spatial resolution when arrayed. Due to their mechanical nature, they have low repeatability as coils do not always return to the same position between readings. Since these sensors use an alternating current in the primary coil, hence producing an output voltage at the same frequency, they require more complex electronics than normal resistive tactile sensors as the alternating signal amplitude must be demodulated (226).

1.2.6 Others

Except for the transduction mechanisms mentioned above, other transduction principles have also been utilized to sense pressure. A resonant pressure sensor, with the structure of sandwiching a deformable dielectric layer between two inductive spirals, is capable of detecting pressure attributing to the resonant frequency shift under pressure (37). This kind of flexible pressure sensor initiated the wireless monitoring the health index of human for medical diagnosis and bioresearch. The transistortype pressure sensor is a good candidate for a highly-sensitive pressure sensor. Transistors are mainly studied for organic field-effect transistors, and their sensitivity is defined by the deformability of the gate dielectric layer under applied pressure, similar to capacitive-type pressure sensors (260). Lately, triboelectric pressure sensors based on the coupling of contact electrification and electrostatic induction has drawn plentiful attention, which generating electrical signal as a response to external stimulation without power supply (233).

1.3 Main Fabrication Techniques for Tactile Sensors

From an applicative perspective, we are interested in understanding how to make tactile sensing. As for manufacturing, 3D printing and deposition techniques are the most commonly used for tactile sensors building. A detailed description of these manufacturing methods follows and a summary of their pros and cons will be assessed, while determining how inkjet printing behaves in respect to manufacturing.

1.3.1 3D Printing

3D printing (also termed as additive manufacturing) is a resourceful procedure that performs manufacturing of physical items from a 3D computer-aided design (CAD) model in an additive (usually layer) approach. Numerous features can be addressed, including better utilization of materials, customized products on demand, development of multipart structures with easy fabrication and quick prototyping (75). Furthermore, advantages of this technology includes time saving, cost effective and economical manufacturing process. Using this technology, force sensors have been utilized in various areas, like robotics, biomedical environment, and meteorological applications (250). Figure 1.2 shows various steps in a 3D printing technique. In the first place, the product concept has been transformed into a 3D model using any popular CAD software, like CATIA or AUTO CAD. A standard tessellation language (STL) file is commonly termed as standard in each 3D printing method. It converts the continuous geometry in the CAD file into small triangles (242). It is sliced into thin cross-section layers using precise software. Then, the part is fabricated using one of the

3D printing technologies. With post-processing, the final product is prepared (224). Fused Deposition Modeling (FDM) is a popularly 3D printing method used in tactile sensor design , due to its features like simple, high speed and cost-effective manufacturing process (42; 174). Also, other techniques play essential role, including Selective Laser Sintering (SLS) (73; 261) and Stereolithography (SLA) (231). These methods can be broken down into high resolution methods (those a minimum feature size of 50 m) and low resolution methods (those with a minimum feature size of 0.5 mm) (21). FDM and SLS suffers from low resolution, while SLA has the highest quality in terms of resolution and surface (24; 30). Figure 1.3 shows the 3D printing techniques commonly used for tactile sensors design.

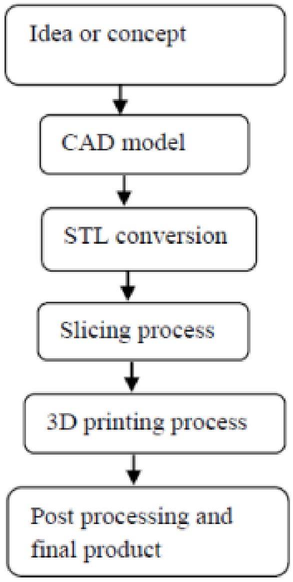

Figure 1.2 Various steps in a 3D printing technique (242).

1.3.2 Deposition Techniques

In the last decade, deposition techniques like drop casting, spin coating, spray coating and screen printing have emerged as manufacturing methods for tactile sensors in robotics applications (23; 39; 97; 229; 255). In particular, drop casting, spin coating and screen printing are widely used in applications requiring the deposition of elastomeric materials, as well as the fabrication of multilayered devices. Drop casting is a simple film-forming technique and it does not require specific equipment. The solution containing the desired material is cast on a substrate following by the evaporation of the solvent. However, it is difficult to obtain a uniform layer and to control its thickness. This technique is similar to

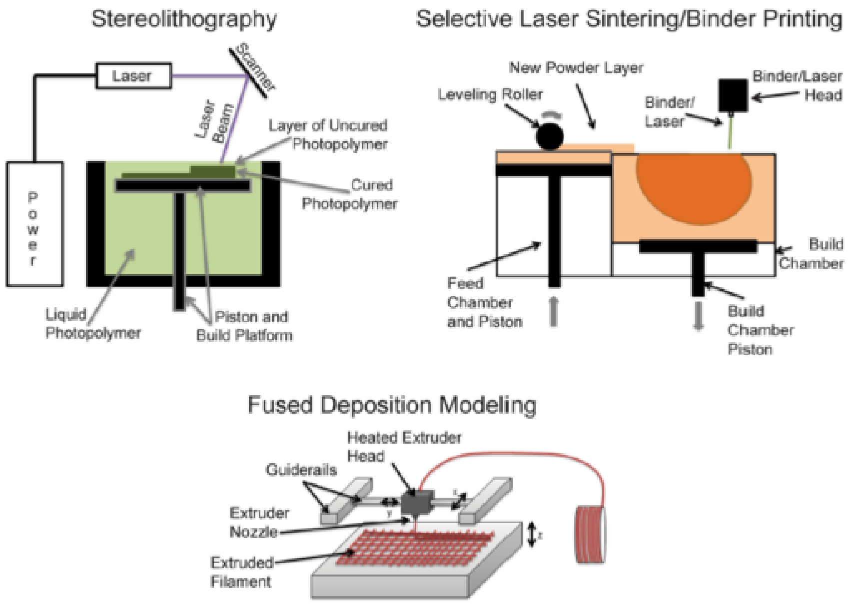

Figure 1.3 3D printing techniques for tactile sensors (21): Stereolithography, Selective Laser Sintering, Fused Deposition Modeling.

spin coating, which involves the deposition of a solution on a substrate and the spinning of this substrate at a chosen rotational speed. It allows for obtaining quickly homogeneous films with high reproducibility in thickness and morphology. However, it is a wasteful technique: most of the solution is ejected during spinning. Additionally, this can make it difficult to coat with a low-concentration solution. The main limitations of spin coating are that it is only effective for coating small substrates and is limited to batch processing and it is completely unsuitable for large-scale production. Spraycoating is based on sub-micrometric droplets ejection on a substrate. The aerosol is created by passing ink through a nozzle. The path traveled by the nozzle over the wafer is optimized to ensure that the coating is applied evenly to the substrate. The solutions used in spray coating usually feature a very low viscosity, which guarantees fine droplets formation. With this technique, the ink waste is not negligible. In a screen printing process, the solution of the active material is squeezed by a moving blade through a screen mask onto the substrate surface. This method is widely use in the manufacturing of tactile sensors due to its simple and rapid prototyping as well as the choice of different materials that can be used. However, it requires additional equipment, like masks or stencils, limiting its use for large-area production. Other limitations of this method are the difficulty to control thickness and uniformity of the material and the waste of the latter. Figure 1.4 shows the deposition techniques used in tactile sensors manufacturing.

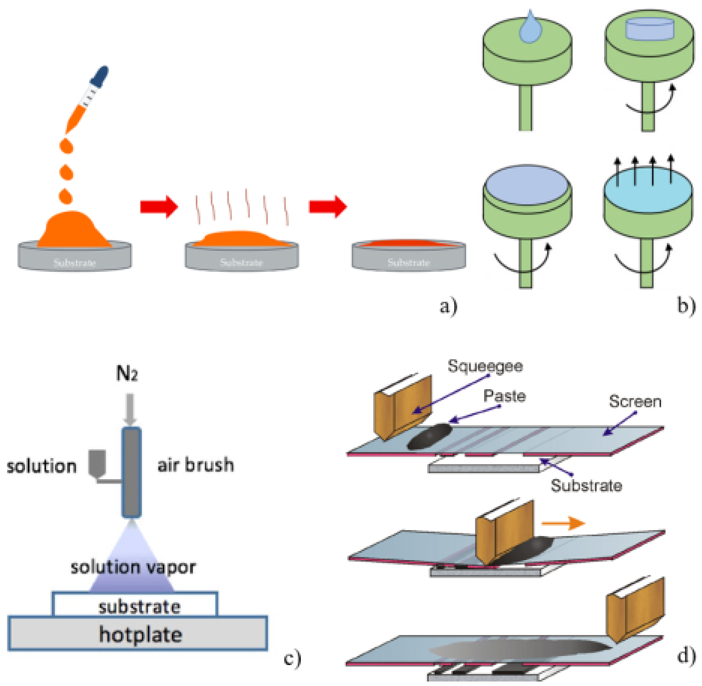

Figure 1.4 Other common fabrication methods for tactile sensors: a) Drop Casting (23), b) Spin Coating (255), c) Spray Coating (97), d) Screen Printing (229)

1.3.3 Advantages and disvantages of manufacturing techniques

Table 1.1 presents a comparison between the frequently used techniques for tactile sensors manufacturing, analysing advantages and disadvantages, to underline how inkjet printing can overcome some limits of these technologies, such as thickness control and homogeneus deposition of material, as well as a large scale production. Inkjet printing technology enables the fabrication of elastomer-based devices and simplifies the fabrication process of multilayered sensors, in contrast to the conventional processes, which often requires additional equipment, such as punching tools or stencils (167). Furthermore, the digital nature of inkjet printing enables the fabrication of elastic interconnects simply by modifying the patterning geometries (167). Despite many advantages of inkjet printing, even this fabrication method suffers from some disvantages, which will be desribed in the next chapter.

Table 1.1 Features of the fabrication methods frequently used for the manufacturing of tactile sensors

Fabrication Method	**Advantages**	**Disvantages**
3D PRINTING	• Customization and complex layout • Minimum material waste • 3D CAD model can be shared • Simple and cost effective	• Limited material selection • Post processing in required • Waste of support materials • Dimenional accuracy • Weak mechanical properties for polymers and compisites
DROP CASTING	• Very simple • Na material waste	• Limitation in large-area coverage • Hard to control thickness and uniformity
SPIN COATING	• Very simple • Thickness control down a few nm	• Material waste • Limitation in large-area coverage
SPRAY COATING	• Thickness control • Large-area coverage • Conformal coating	• No homogenity: the material is not applied homogeneously on the substrate
SCREEN PRINTING	• Simple and rapid • Different print of materials	• Additional equipment (mask or stencil) • Hard to control thickness and uniformity • Material waste
INKJET PRINTING	• Simulataneous printing with multiple materials • High resolution and smooth surface finish • Printing over large-area • Thickness control • Homogenity • No material waste • Simple to use • Used also in non-plana geometries	• Low part strenght compared to bulk materials • Substrate requirements • Nozzle clogging

Chapter 2

Inkjet Printing Technology

The inkjet printing technology has become significant in recent years, and it can be considered one of the the most innovative methodologies for the manufacturing of large area tactile sensors (6; 11; 199; 212; 223). Inkjet printing is part of the class of additive manufacturing technologies (21). The inkjet printing technique has all the advantages of the additive methodologies, in particular relating to the versatility and the cost-effective linked to a rational use of materials. In the inkjet printing process, a controlled print head deposits tiny droplets of ink on an underlying substrate (199). This technology has emerged as a new solution for designing flexible and wearable sensors for its versatility with respect to other common technologies (6; 140; 193; 207; 231; 267). In fact, CAD tools allow straightforward geometric modification of the sensor layout as well as a precise control of the printer parameters, significantly reducing the setup time and costs paving the path for the customization of these products (6; 95). This is important in all applications where sensors customization is needed, and this is certainly the case for robot applications. Furthermore, inkjet printing has a high versatlity since it can be appplied to different support materials allowing to print conductive patterns on different substrates made of both organic and inorganic materials, finally also reducing material waste (56; 102; 110; 207; 212; 243; 248). Inkjet printing often takes place at room temperatures (128; 151; 188; 198; 213; 237; 257), and non-contact patterning with minimized contamination is involved (6; 33). Finally, inkjet printing leads to a limited number of manufacturing steps reducing the setup costs and time, thus leading to fast production and making large area sensors fabrication highly cost effective. (199; 223; 257), (257). The state of art of tactile sensors has been discussed in the literature (116; 146; 218). This chapter aims to demonstrate the relevance of inkjet printing for the design and implementation of large area tactile sensors with respect to the current state of art (manufacturing techniques and technologies including parameters such as materials, layout, processing). The contribution of the thesis is to show how inkjet printing overcomes the main challenges arising during the design of tactile sensors and how this technology can boost the development of tactile sensors on large scale of production, leading to high *technology readiness level (TRL)* cost effective devices ready for the market. Furthermore, a view of the most relevant open problems that should be addressed to improve the effectiveness of these processes is provided. Section 2.1 describes the inkjet printing process, with its advantages and shortcomings, highlighting typical parameters with relevance to tactile sensors that can be achieved with this technology. Then, the main challenges associated with the inkjet printing process have been discussed in Section 2.2. Section 2.3 gives a summary of inkjet-based sensor design solutions, including an assessment of the different characteristics of the fundamental transduction principles, to show how inkjet printing allows to overcome some difficulties that arise in the development of tactile sensors for real robot applications. In Section 2.4 we assess the most appropriate design solutions for different application areas. Open problems are finally drowned. The state of the art of the thesis particularly focuses on the inkjet printing of large area tactile sensors for robotics applications, but all the treated topics can be extended to generic systems.

2.1 Inkjet printing modes of operation

The use of the inkjet printing technology allows a calibrate use of materials, making possible on one hand the versatility in the construction of components, and on the other hand a targeted use of materials with reduction of waste and, therefore, benefits in terms of costs and environment.

There are two modes of operation for inkjet printing: *drop-on-demand (DoD)* and *continuous inkjet printing (CIJ)* as shown in Figure 2.1. In most DoD printers, the droplets are induced by a piezoelectric actuator. In CIJ printers, a continuous electro-conductive stream of fluid is delivered through a nozzle because of piezoelectric actuator vibrations, regulating the breakup of the stream into individual uniform droplets with uniform spacing. In the DoD method, single drops of ink are released onto a wide range of substrates in response to a digital signal or waveform, allowing for the printing of both aqueous and UV curable inks. It allows for the control and calibration of the ejection of ink droplets from each nozzle. This method is widely used due to its high placement accuracy, controllability and efficient material usage, where no excess ink is wasted, as it is only dropped where and when needed. As a result, this method is frequently implemented in research and in industrial applications. Furthermore, it is adaptable to the printing of water-based inks containing conjugated polymers, as it uses lower temperatures. Piezoelectric inkjet printing relies on the mechanical action of a piezoelectric membrane to generate a pulse. Nozzle sizes are in the range of 20-30 mm, and droplets sizes are in the range of 10-20 pL. The diameter of an ink drop on a substrate is about twice the size of the released drop (18; 34; 117). Continuous inkjet technology differs from DoD in the way the ink is deposited from the cartridge. Specifically, CIJ produces a continuous stream of ink, where drops break up from the print head nozzle by applying harmonic modulation. The separation of the drops is determined by the modulation frequency and the speed of the jet. Continuous inkjet systems typically produce 80 to 100 mm droplets travelling at speeds of 20 m/s with drop frequencies that can exceed 250 kHz. In the most common implementation of CIJ printing, electrostatic charging and deflection are used to select and steer individual drops to define the final printed pattern. On the other hand, CIJ can operate with fluids of lower viscosity and at a higher drop velocity than DoD. However, CIJ printing requires a larger amount of fluid. This demonstrates the advantage of DoD systems over CIJ in the area of inkjet printed electronics, as it consumes less ink and accordingly cuts down the overall fabrication cost (33; 256).

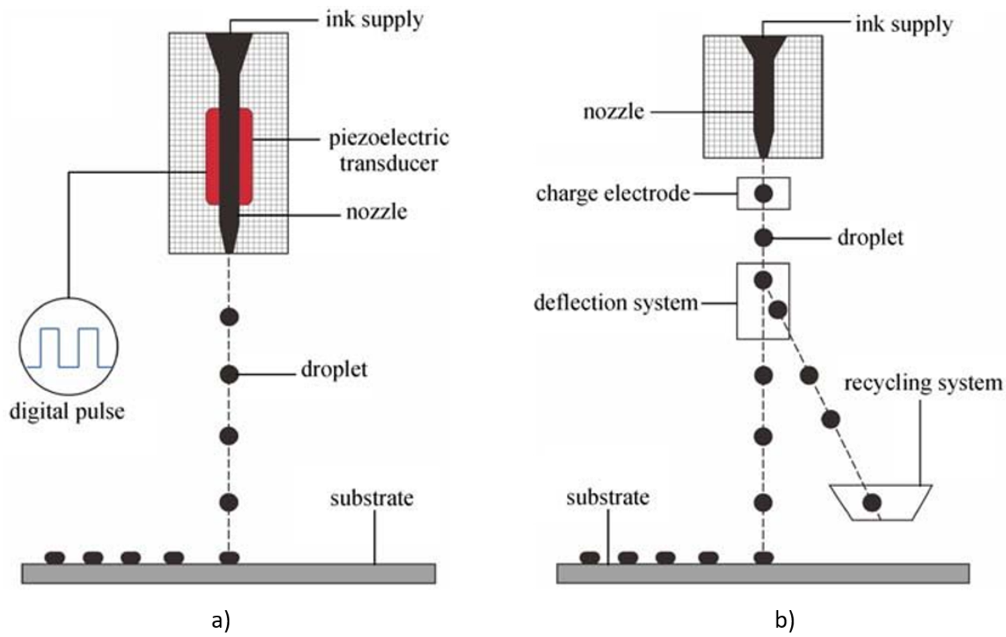

Figure 2.1 Schematic diagram of inkjet printing processes. a) DoD mode; b) Continuous mode .

2.1.1 Inkjet printing components

In any inkjet printing process, three main components are required: the inkjet printer, the ink and the substrate and they are shown in Figure 2.2. There are several commercially available inkjet printers which are widely used for research purposes. Among these, Dimatix Fujifilm printers (DMP-2831 and the newer DMP-2850) are the most commonly used types of inkjet printers for research (6). Industrial devices (from Fujifilm) are based on the same technology. Inkjet printing technologies are widely used in these years for the development of flexible electronics as they offer a fabrication alternative to lithography-based approaches (53; 245), introducing the use of new intrinsically stretchable inks (2; 4; 5; 12; 22; 34; 41; 43; 45; 46; 61; 72; 99; 102; 104; 113; 119; 121; 138; 142; 147; 148; 176; 182; 189; 191; 194; 201; 205; 209; 211; 215; 216; 222; 230; 258; 264), avoiding the challenge related to the brittleness of traditional materials used to manufacture tactile sensors (10; 17; 60; 137; 144; 145; 164; 172; 187; 197; 219; 259).
Furthermore, inkjet technology makes the system conformable by printing on different types of flexible substrates (6). Paper substrates are the most common flexible type of substrates, which are used in inkjet printing of electronics and sensors, as will be discussed in Section 5.2. Polymer substrates such as polyether imide, polycarbonate, polyarylate, polyamide, polyethylene and terephthalate are also types of commonly used flexible substrates (22; 118; 189). PDMS is frequently used as a stretchable substrate (44; 98; 217; 246). It is a silicon-containing elastomer, which is also widely used to construct microfluidic devices and lab-on-chip systems. On one hand, the aforementioned stretchable inks and flexible substrates allow to overcome the challenge related to the conformability of the tactile sensors. On the other hand, these two main components allow to produce printable sensors with printable stretchable wires as in the work of Albrecht et al. (9), which may find use in artificial skin for humanoids. The optimized wiring is one main advantage of the application of inkjet printing for tactile sensors, which leads to the printing of wires instead of physically turning them, for example, between the robot joints. Thus, inkjet printing introduces a difference between printed wires and non-printed ones. In the first case, the stretchability of wires permits a simpler routing, allowing a high level of integration to the entire system. In the second case, the problem of flying and non-stretchable cables arises, leading to the routing of wires problem.

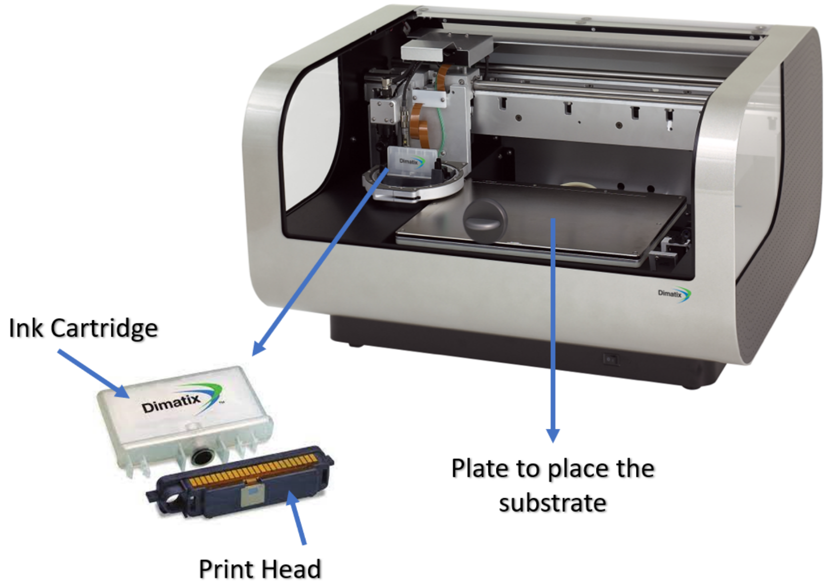

Figure 2.2 Main components in inkjet printing processes: inkjet printer, ink and substrate.

2.1.2 Relevant Parameters

The resolution of inkjet printing is an important parameter that mainly depends on the ink volume propelled by the inkjet-printing machine. The width of the printed tracks is limited by the resolution of the printer. For example, the resolution of Dimatix is 10–30 μm depending on the drop volume (199). The constituents of the ink, the substrate, the sintering process and the voltage waveform applied to the jetting nozzles affect the resolution and accuracy of the inkjet-printing process (199). The best resolution achieved using inkjet-printing technology is 2 μm and it is proposed in the works of (112) and (124).

2.2 Challenges of inkjet printed tactile sensors

This section analyses the major challenges related to the manufacturing of inkjet printed tactile sensors. The first problem regards the choice of the ink, looking at its proprieties such as viscosity, surface tension and contaminants or polymer chains. Other issues include the adhesion of the inks to the selected substrate, sintering processes after the printing and sensors mechanical durability.

When designing inks for inkjet printing, the properties of interest are primarily viscosity and surface tension (166). So, inks must have the required value of viscosity as not to clog the printer nozzles (33; 168; 266) and a required value of surface tension to permit the bonding

between the drop and the substrate (204). In case of too viscous materials, a dilution with a solvent is required, until the mixture will reach the right viscosity (166), (162). Here, the challenge is to choose the right solvent concentration to maximise the ink's material-content. An excess of solvent with respect to the main material can alter the properties of the latter. Furthemore, the need for a right viscosity upon the extrusion through the printhead can also limit the range of materials that the inkjet printing technique can use.
Once the appropriate dilution is found, the ink must pass through a filter before being inserted in the cartridge. Filtering is an important step to prevent nozzle clogging prior to printing, either from any contaminants, or from polymer chains or other ink components that are too large (166). Fluid particles must generally be 1/100 of the printer nozzle size (6). For example, the 10 pL cartridge of the commercial printer Fujfilm Dimatix Material Printer DMP-2850 has a nozzle of 21 μm; in this case the particle diameter must be 0.2 μm and so a filter with a pore size of 0.2 μm need to be used.
The second key issue is the adhesion of the ink to the selected substrate. In several works, the substrate surface is modified using plasma treatments to make it hydrophilic allowing the adhesion of ink particles (3; 19; 67; 88; 117; 134; 244; 254). The adhesion problems can also arise in the case of multiple depositions. This challenge is particularly sensitive in the case of PDMS-based inks (166). In this example, the problem is the adhesion of the silver nanoparticle (AG NP) ink on top of PDMS layers. The authors propose to use nitrogen plasma treatments for printing the conductive layers, enhancing its adhesion with the hydrophobic PDMS. Mikkonen et al. (165) studied and compare other methods to improve the adhesion between the ink and the substrate. These methods include other chemical modifications such as (3- mercaptopropyl)trimethoxysilane (MPTMS) and pyrolytic coatings. Another method to improve the adhesion is ink sintering, which also has a decisive role on ink conductivity properties (6). Sintering is the last step in an inkjet printing process, and it is essential for the evaporation of the solvent that might be present in the ink, and it is performed by applying heat to the printed pattern. On one hand, high sintering temperatures increase electric conductivity by dissolving more of the solvent and further fusing the nanoparticles of the conductor (6). On the other hand, high sintering temperatures may harm the substrate and change its properties (6). In fact, sintering processes make sure high conductivity but they can also reduce the lifetime of the substrates (199). A third key element in the development of inkjet printed tactile sensors is their mechanical durability (6). Clearly, a tactile sensor which can sustain prolonged bending or stretching, while maintaining its response characteristics is desirable. As a matter of fact, electrical conductivity of the sensors electrodes is the priority. Typically, sensors are tested for the number of bending/stretching cycles they can

undergo before cracking and/or slipping of the conductive lines (6). In the case of sintering process, the solvent in the deposited ink evaporates and the conductive lines, which have different thermal expansion coefficient with respect to the substrate, tend to crack, therefore affecting the electrical conductivity of the printed lines (74). However, various strategies have been adopted to reduce this effect. One possible strategy is to print thicker conductive tracks (even if thicker tracks may reduce bendability). Alternatively, using thinner substrates. Otherwise, using flexible inks and substrates (6). Furthermore, the strategy of sandwiching the conductive lines between two elastomer layers has shown a reduction in crack formation (166),(83). During sensors life cycle tests, slipping of the printed conductive lines with respect to the substrate can occur if the adhesion between them is insufficient (83). In this context, the challenge can be overcome using a right adhesion process (as discussed above).

2.3 Inkjet printed tactile sensors

For inkjet printed tactile sensors there are three types of transduction technology: piezoresistive, capacitive and piezoelectric and, depending on the application, some are more suitable than others (50; 135), as will be discussed later.
A summary of inkjet-based sensor design solutions is described in the following, including an assessment of the different characteristics of the various manufacturing solutions.

2.3.1 Piezoresistive

Using inkjet printing technology, silver, single-wall carbon nanotubes (SwCNT) and graphene are conductive materials used in many works (64; 71; 138; 145; 191). The contribution of inkjet printing for the manufacturing of these kind of sensors is to introduce a cheaper alternative aiming to minimize the complexity without compromising the quality and sensing performance for the target application. Significant advantages on these aspects are discussed in the work of Lo et al. (145). Here, an inkjet printed resistive pressure sensor that offers high sensitivity and can be fabricated using a very simple process is reported. The device is comprises a conductive silver nanoparticle (AgNP) layer directly printed onto a polydimethylsiloxane (PDMS) substrate and encapsulated by a Very High Bond (VHB) tape. The pressure is measured by changing electrical resistance caused by pressure-induced strain in the printed AgNP thin film. From the geometry point of view, Li et al. (138) proposed a novel ring-shaped piezoresistive pressure. Carbon nanotube (CNT)-polyimide (PI) nanocomposites with different CNT concentrations are prepared in a liquid mixture as the fabrication material. The ring-shaped nanocomposite thin film device is deposited on a circular polyimide diaphragm by inkjet printing fabrication method. The drop-on-demand fabrication process of the inkjet printer enables the fabrication of nanocomposite thin film in various geometries and shapes to achieve better structural compatibility with the sensor port and over-all measurement accuracy. Thanks to the last one sensor features, the sensors offer some advantages as an easy fabrication process, excellent flexibility and high sensitivity. Figure 2.3 shows the piezoresistive tactile sensors manufactured in (145) and (138).

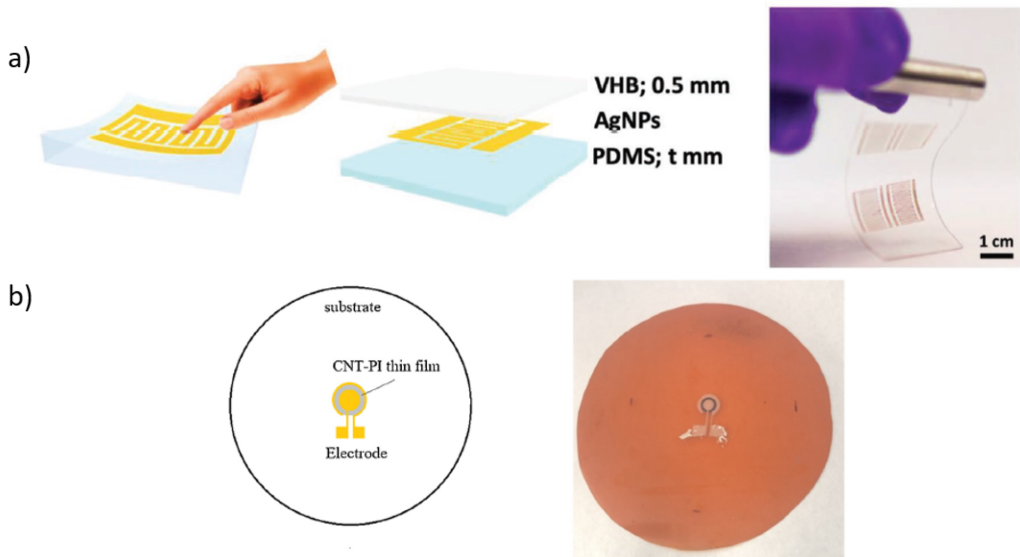

Figure 2.3 Schematic illustrations of printed piezoresistive sensors: a) (145), b) (138).

2.3.2 Capacitive

Inkjet printing technology facilitates the utilization of a variety of flexible substrates for various designs (199). Polyethylene terephthalate (PET) is widely used as a flexible substrate for inkjet printed capacitive sensors (10; 12; 148; 187). Furthermore, printed electronics of paper allows to implement flexible sensors and it has been used to manufactured printed capacitive sensors in (41; 142; 258). The paper substrate has many advantageous features, e.g. it is inexpensive, eco-friendly, lightweight, expandable, foldable in three dimensions and available everywhere (40; 89; 111; 141; 251). Basak et al. (17) and Zhang et al. (266) developed their printed capacitive sensors on thermoplastic polyurethane (TPU) and aluminum substrates, respectively. Mikkonen et al. (164) proposed a novel approach using a water-soluble polyvinyl alcohol (PVA) layer as the substrate. In this work, they report a

simple method for fabricating fully printed, elastomeric capacitive sensors with high flexibility and great sensitivity at a wide pressure range. A significant advantage of this work is the development of a straightforward method for inkjet printing of PDMS. They fabricated conductive mesh electrodes by inkjet printing silver nanoparticles on PVA, while a dielectric layer, consisting of a PVA mesh layer embedded in an inkjet printed PDMS layer, was placed between the mesh electrodes to form a capacitive tactile pressure sensor.
Figure 2.4 shows some substrates used to manufacture capacitive sensors, while Figure 2.5 shows the capacitive tactile sensor manufactured in (164).

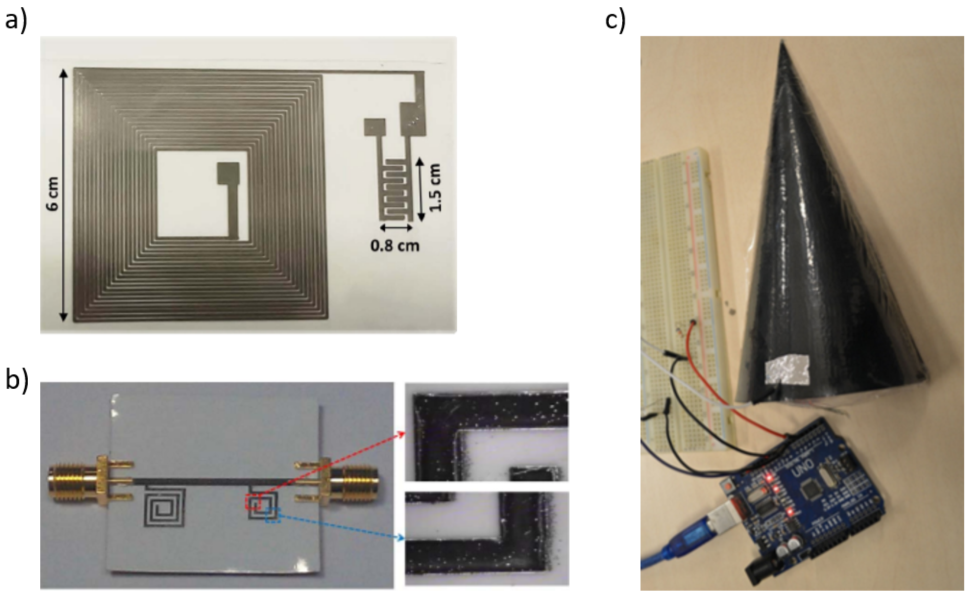

Figure 2.4 Inkjet printed capacitive sensors layout on a) PET substrate (12), b) Photopaper (41), c) TPU substrate (17).

2.3.3 Piezoelectric

Among the existing piezoelectric materials, piezoelectric polymers are the most suitable for tactile sensors printing because of their superior flexibility and high transparency. These materials are being highly investigated because of their high mechanical stability and compatibility with solution-based printing technologies (236). Polyvinylidene fluoride-triflouroethyleje, also known as P(VDF-trFE), is of particular interest, since it is a piezoelectric material commonly used to manufacture 3D printed (185; 203) and inkjet printed tactile sensors (60; 172; 225). Two of its applications in the inkjet printing field are shown in Figure 2.6.

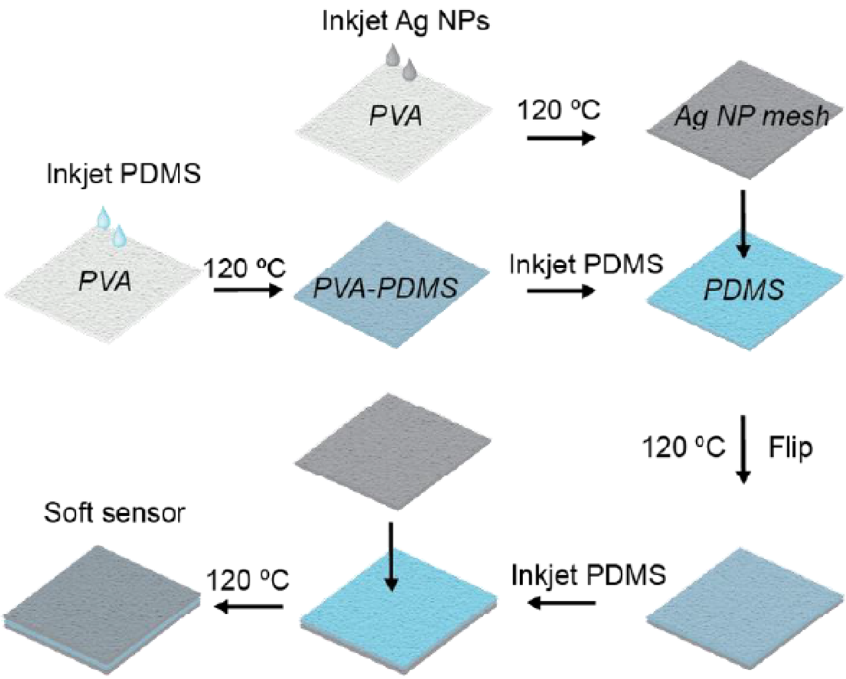

Figure 2.5 Schematic illustration of sensor manufacturing process in (164).

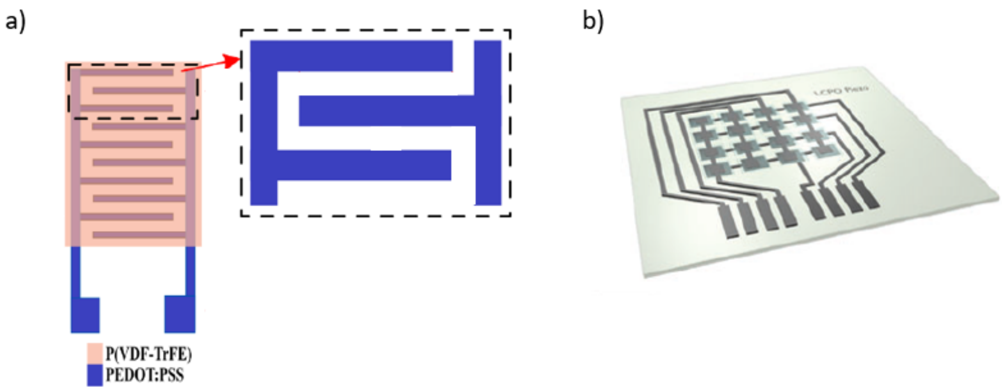

Figure 2.6 Schematic illustration of printed piezoelectric sensors: a) (172); b) (225)

2.3.4 Other transduction methods

Different solutions based on inkjet printing technique have been recently presented in (70) and (200) and they are shown in Figure 2.7. The work of Fu et al. (70) reports an all inkjet printing approach for fabricating flexible bimodal sensors (able to measure two parameters) and large-area sensing arrays, that can simultaneously sense bending strain and pressure. The sensor unit is composed of a bottom electrode on polyethylene naphthalate (PEN) and a top electrode on paper and silver nanoparticles (AgNPs) suspension was used as the conductive ink. The device has excellent performance with low pressure-detection of 2 Pa and high stability over more than 5700 cycles for pressure sensor. The device can recognize the radius of curvature of human activities and objects, and can detect the pressure distribution and the curvature of irregular surfaces. In the work of Salim et al. (200) an inkjet printed kirigami inspired split ring resonator (SRR) strain sensor is proposed, able to adapt to curved surfaces, easy to fabricate and cheap. Kirigami is an oriental technique of carving and folding of paper to obtain three-dimensional shapes starting from a single sheet, without removing pieces. So, in (200), two sheets of paper were used as the dielectric for compatibility with the kirigami technique, as shown in Figure 2.7b, and a conductive pattern was inkjet printed on the top paper using silver nanoparticle ink, whereas the ground plane on the bottom paper was inkjet printed using stretchable inks.

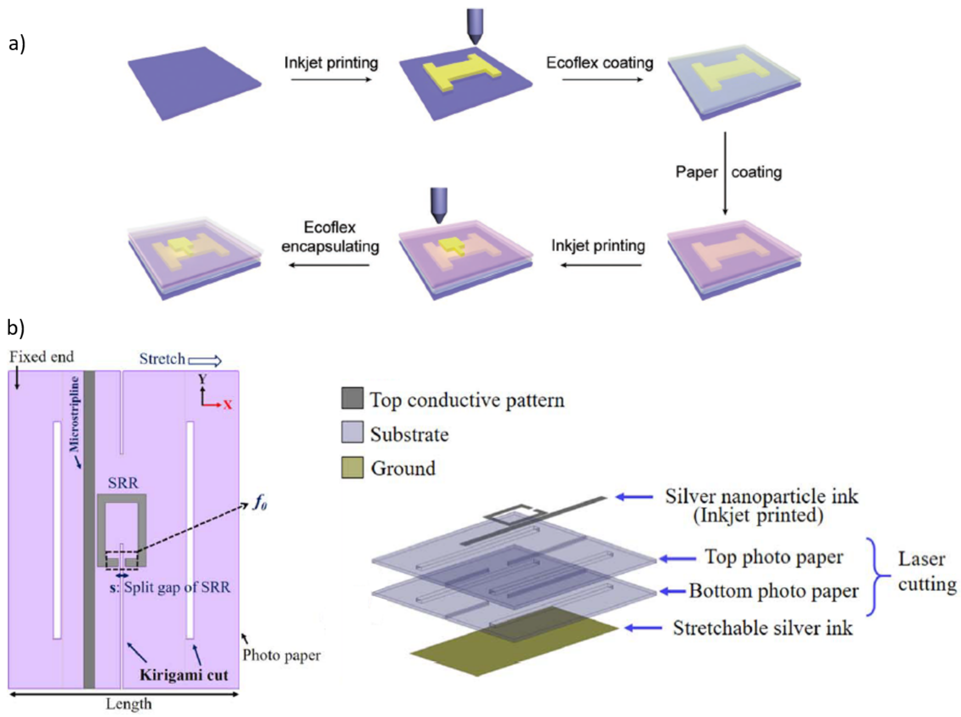

Figure 2.7 Schematic illustrations of sensors manufacturing processes in (70; 200): a) bimodal sensor and circuit diagram in (70), b) sensing principle and layout for the proposed inkjet printed kirigami inspired split ring resonator (SRR) strain sensor at zero strain and corresponding resonance frequency (f_0) (200).

2.3.5 Features of the proposed manufacturing solutions

Analyzing the characteristics of the various manufacturing solutions, it is possible to understand how the inkjet printing technology can overcome the system-level integration challenges arising during tactile sensors design. Firstly, the variety of flexible inks and substrate for various designs makes the sensors conformable to cover arbitrary curved robot body parts. Since the substrates are important for conformability, measurement principles and applications, the common ones presented in this chapter and their physical properties are listed in Table 2.1. Furthermore, the inkjet printing technology can be a good manufacturing solution as it permits a simple sensors layout design on specific surfaces. Then, in the inkjet printing process, the geometric placement techniques of sensors can be used during the design phase, once it is possible to create custom devices at a significantly lower cost than existing technologies. The possibility of designing custom-made sensors with accurate taxel placement may reduce the need of major geometric calibration procedures, reducing the setup time and costs of the sensor. The expected repeatability of the inkjet printing techniques is also likely to reduce the extend of the calibration of the response of each tactile element. Finally, as mentioned in Section 4, the inkjet printing technology allows to place sensors far away from the processing unit in artificial skins for robot, introducing the possibility to print conductive wires on stratchable materials at very low-cost (9). In Figure 2.8 a comparison between inkjet printed wiring and conventional wiring is presented. The performances of the most relevant works are summarized in Table 2.2.

a)

b)

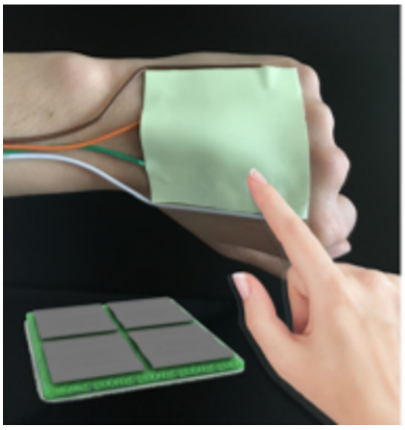

Figure 2.8 Comparison between a) inkjet printed wiring (9) and b) conventional wiring (263)

Table 2.1 Substrates and their physical properties presented in this thesis.

Substrate	Thickness [μm]	Transparency [%]	Density [g/cm^3]	Young Modulus [GPa]	Ref.#
PAPER	25-250	-	0.6 - 1.0	0.5 - 3.5	(41; 64; 142; 258)
POLYMIDE	12-125	-	1.4	2.5	(22; 138)
PET	16-100	90	1.38	2.8	(10; 12; 148; 187; 191)
PEN	12-250	87	1.4	3.0	(70; 118; 189; 225)
PDMS	5-1500	92	0.965	0.57 - 3.7	(9; 44; 98; 145; 184; 200; 217; 235; 246)

Table 2.2 Performances of the most relevant works presented in this thesis.

Principle	Sensitivity	Detection Range	Repeatability	Ref.#
Piezoresistive	0.48 kPa^{-1}	15 kPa	High (1000 cycles)	(145)
	-	151 kPa	Good	(138)
Cacapitive	4 MPa^{-1}	50 kPa	High (2000 cycles)	(164)
Piezoelectric	3.9 ± 0.5 pC/N	-	Good	(172)
Others	-	1000 kPa	High (4500 cycles)	(70)
	4.2 x $10^7 Hz/\%$	-	Good	(200)

2.4 Inkjet Printed Tactile Sensors Applications

In the previous sections we have described the general features of inkjet printed tactile sensors principles. From this standpoint, it possible to asses the most appropriate design solutions for different application areas. Tactile sensors have been used in different domains, including bioengineering (especially for areas such as rehabilitation, soft robotics, wearable electronics, surgical robotics) and industrial environments. In this section we will focus on the reported usage of inkjet printed tactile sensors in these sectors, that are finally shown in Figure 2.9. The inkjet printing technology has an immediate advantage for large area applications (as for bioengineering and industrial domains).

A future development for this technology can be investigated for applications regarding the realization of miniaturized sensors. The latter is still an open problem for this type of technology, and it will be discussed in the next section.

2.4.1 Tactile sensing for rehabilitation

Rehabilitation is one of the main fields of application for tactile sensing. In particular, robot-assisted rehabilitation has been widely used for repetitive and interactive treatments, such as upper limbs orientation and recovery (183). Among the various technologies, smart tactile gloves have been largely used, especially in stroke rehabilitation (183). Inkjet printing is an emerging technique for the patterning of sensors and conducting traces onto gloves or textiles (92; 106; 108; 206; 240). Tactile sensors can also be printed onto the glove to measure the pressure exerted by the fingers. Ervasti et al. (64), propose a stretchable inkjet printed piezoresistive tactile sensor with high sensitivity to bending for finger joints flexion measurements.

2.4.2 Tactile sensing for soft robotics

Soft robotics is a subfield of robotics that concerns the design, control, and fabrication of robots composed of compliant materials, instead of rigid links. The applications of soft robots is gaining a growing relevance, as they are flexible and adaptable to operate in complex environments. Tactile sensors are one of the most important components for soft robotics for their role in the perception of the physical interaction with the environment (265). Inkjet printing technology emerged in this domain for its potential to manufacture highly integrated and custumized sensors, as well as for the possibility of designing small devices. The development of tactile sensors for soft robots evolves with the investigation and development of inkjet printed electronics solutions for deformable and stretchable materials (64; 82; 150).

2.4.3 Tactile sensing for wearable devices

Wearabe devices sensorized with tactile sensors have been proposed in the literature (252). Nowadays, several monitoring devices face drawbacks such as rigid equipment, low accuracy and high expenses. Inkjet printing technology leads to tactile sensors with a high level of wearability in terms of bendability and flexibility, enhancing their interfaces with the contact objects. Therefore, printed tactile sensors are capable of conformably covering arbitrary curved surfaces over their stiff counterparts without incurring into damage (252). By making electronic devices flexible, it is possible to significantly enhance their healthcare applications in the emerging Internet of Things (IoT) (16). Furthermore, wearable electronic skin (e-skin) devices with skin-like properties can adhere conformally to the skin and interface with the human body to mimic the human somatosensory system and enable convenient and non-invasive tracking of physical and biochemical signals (64; 92; 132; 149; 249; 253). The most promising tactile sensing applications are gait detection and analysis (156) and motion monitoring (235). Furthermore, as remarked in (204), printed tactile sensors can play a major role in applications as expression recognition, diagnosing conditions like Parkinson's, sign language translation and body gesture . As mentioned in the previous sections, Albrecht et al. (9) proved the development of inkjet printed stretchable wires, used to connect sensors with the remote processing unit, integrated in smart clothes, or, more in general, for artificial skin also for robots. This innovative manufacturing solution is usefull for tactile sensors in sportswear, compression underwear, and in robotic applications (9).

2.4.4 Tactile sensing for surgical robotics

Surgery is a developing area where tactile sensing is of central importance. Minimally invasive surgery (MIS) is now routinely used as the preferred choice for many operations (131). Although the benefits of MIS technology have been proven, the limitations of two-dimensional visualization, lack of haptic feedback and long learning times are their limiting factors (227). In this context, tactile sensing is used to study the interactions between the confined tissue environments and the instruments based on contact information and haptic feedbacks (86; 114; 163; 186; 191; 221). Force sensing capability in an instrument helps to improve the instrument-body interaction and it can reduce damages in order to ensure effective manipulation. So, for surgical and medical devices, sensors need to be compact, low power consuming and less bulky with simple associated electronics (62). The inkjet printing technology could brings improvements in the development of these devices leading to soft and flexible sensors which can also ensure better compatibility with human tissue. The first example is given by Ponraj et al. (191), who describes the design, fabrication, and application of a soft inkjet printed piezoresistive tactile sensor used for safe human–tissue interactions. The sensor can be integrated with surgical devices providing forces feedback. A key contribution of the paper is to prove inkjet printing as a cheap solution for the sensorization of surigcal equipments.

2.4.5 Tactile sensing for industrial applications

Within the industry 4.0 paradigm, advanced robotic technologies are a key element to enable the safe human-robot interaction. Robots and manipulators are expected to safely adapt their behavior with respect to obstacles and humans (208). Human operators become a fundamental part of robot's operating environment, since they represent external unpredictable agents to comply with. So, new technologies are required to implement and promote safe and proficient human-robot interaction. Recently, 3D and inkjet printing for tactile sensing have been used in this context (12; 65; 184). The capability to develop inkjet printed sensors on large area, opens the possibility of fully sensing robots that perceive their surroundings in much greater detail, ensuring safer interactions between humans and robots.

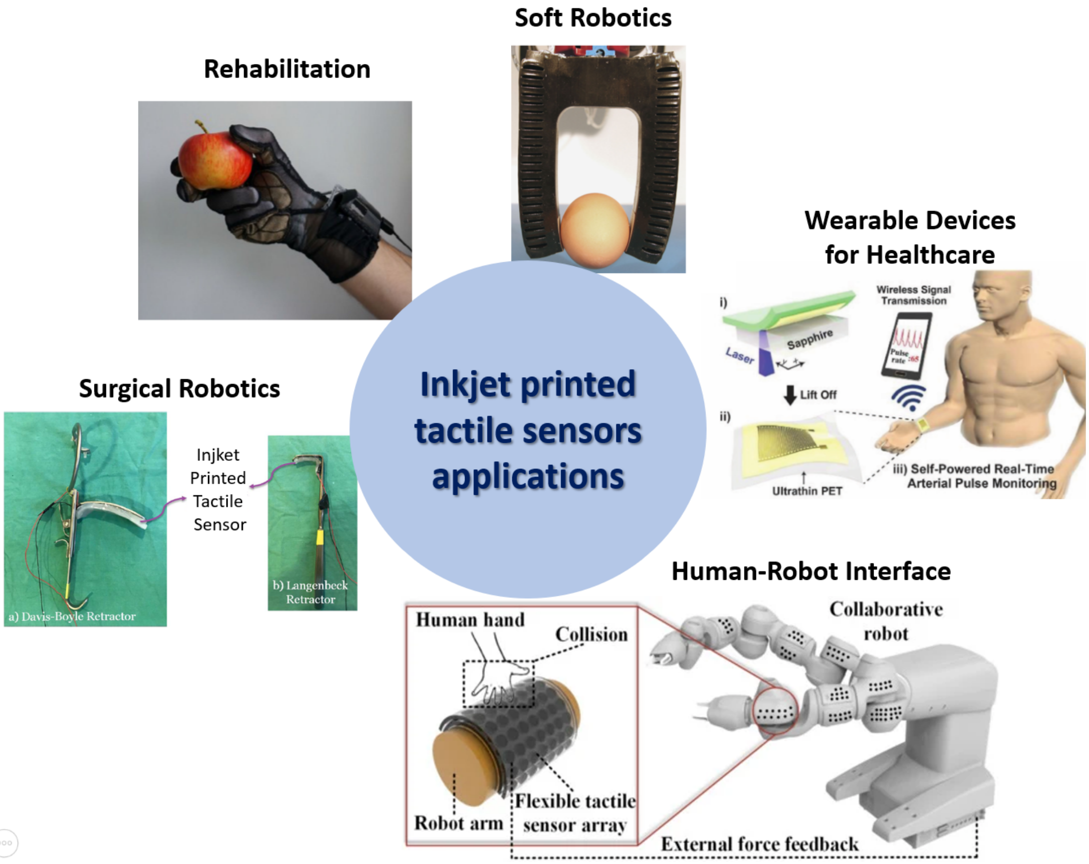

Figure 2.9 Diagram of inkjet printed tactile sensors relevant applications: rehabilitation (92), soft robotics (150), wearable devices (249), surgical robotics (191), human-robot interface (184).

2.5 Open Problems

This chapter aims to provide an overview of how inkjet printing can boost the development of tactile sensors on a large scale of production, leading to high *technology readiness level (TRL)* cost effective devices ready for the market. As discussed in Chapter 1, the fundamental requirements for the design of large area tactile sensors are conformability, distribution and placement, spatial calibration and routing of wires. The difficulties to obtain these conditions have been addressed with the inkjet printing technology. Although inkjet printing can be considered one of the most promising technologies in tactile sensors scenario, some open questions have not been addressed in the literature with this technology yet . In particular, open problems for the development of complex tactile sensors are referred to the vias fabrication. Also, a relevant problem is referred to the robust bonding of chips on the sensor substrate, also related to the flexibility requirements of the skin. Moreover, the ageing of the materials used, in particular of the inks, which might limit the operational and/or shelf life of the devices. Finally, a major challenge would be the possibility of a direct printing of sensors on the target surfaces by exploiting the state of the art of robotic technologies. The problem of vias fabrication is critical, especially in multilayered tactile devices, in which functional devices from different layers need to be connected together by vertical interconnects (195). The other challenge is to obtain the integration of the chip with the substrate, guaranteeing the mechanical stability of the system, reliability and robustness, avoiding noise in the acquired signals. Even if, sometimes, sensors built with traditional technologies have the electronics mounted on the device, the problem regards the bonding on inkjet printed tactile sensors, whose robustness can be lower than those of a traditional devices. Some relevant upgrades have been proposed in (107). Furthermore, one of the major problems that affects the tactile sensors' functioning is the aging of the materials, which change their sensitivity over time. The challenge is the study of new materials that are not affected by aging and that they can be printed by inkjet printing. Finally, the direct inkjet printing of sensors on the target surface is still a challenge, and it may requires other forms of additive manufacturing (MID). The possibility of direct printing allows to understand how exactly the sensor is positioned on the robot body, avoiding spatial calibration procedures. Inspired by the idea of the 6-axis additive manufacturing (35; 239), the inkjet printing technology could find a future application in the production of miniaturized devices, allowing the creation of patterns for transducers even on small and non-planar surfaces. Table 2.3 systematizes in detail all the aforementioned open problems.

Table 2.3 Open problems description.

Open Problems	*Description*
Vertical vias fabrication	The fabrication of vias is a critical problem, especially in multilayered tactile devices, in which functional devices from different layers need to be connected together by vertical interconnects.
Bonding of chips on the sensor substrate	Since tactile sensors are devices subjected to significant mechanical stresses due to contacts, the problem of bonding and of sensor integration with the electronics is a problem from the durability and robustness point of view. This problem regards in particular the inkjet printed tactile sensors, whose robustness can be lower than those of a traditional devices.
Ageing of materials	The ageing of the material used is a problem that has to be considered, as it leads to a decrease in sensor lifetime and sensitivity.
Direct printing of sensors on the target surface	The direct inkjet printing of sensors on the target surface is still a challenge, and it may requires other forms of additive manufacturing. The possibility of direct printing allows to understand how exactly the sensor is positioned on the robot body, avoiding spatial calibration procedures.

Chapter 3

Mathematical model and experimental characterization of vertically stacked capacitive tactile sensors

Robots have gathered a lot of attention in the last two decades, and they have been playing a bigger part in the industrial scene and in everyday life. Using the human as a model, advanced technology and great progresses in mimicking sensory capabilities have been demonstrated (78; 234). Tactile information, such as the magnitude and direction of a contact force, temperature, humidity, and texture, can be obtained by robots equipped with tactile sensors, which is crucial for secure grasps, path planning and obstacle avoidance in unstructured environments (91). Additionally, reliable touch sensors are required for both object manipulation activities and safe human–machine interaction (69). Capacitive sensing is one of the most common principles used in robotic tactile sensing. The capacitance of a parallel plate capacitor is expressed as $C = \frac{\varepsilon_0 \varepsilon_r A}{d}$, where A is the overlapping area of the two electrodes, ε_0 is the permittivity of vacuum, ε_r is the relative permittivity of the dielectric layer, and d is the distance between the electrodes (thickness). Researchers are interested in capacitive sensors because of their great sensitivity, resolution, costs and read out electronics.

For a good response, capacitive sensors require a wide dynamic range, defined as the ratio between the maximum and the minimum value that the sensor can detect. The dynamic range can be increased by maximizing the sensor capacitance (C) and it is strictly correlated to the sensitivity (S) of the transducer, expressed as the ratio between the variation in capacitance for a given variation of contact pressure. The capacitance C can be increased by decreasing the sensor thickness and/or by increasing the sensor area. Unfortunately, both the approaches bring to some drawbacks. In particular, the decreasing of the sensor thickness is limited by

the technology used to manufacture the sensor. Furthermore, the increasing of the sensor area can lead to space problems on small surfaces. There are works in literature which proposed methods to enhance the dynamic range of capacitive tactile sensors (76; 105; 169; 247; 262). An interesting approach is the exploitation of the vertical direction. Results from the works of (31; 36; 38; 90; 122) show that this design for capacitive sensors reduces the projective area taken on the xy-plane for enhanced spatial resolution and sensitivity and it can be used for extreme miniaturizations. Hao et al (94) developed and characterized a capacitive tactile sensor that simultaneously supports high detection sensitivity and high spatial resolution with a hollow dielectric structure, by vertically stacking two capacitors. Taking advantages of these approaches, the aim of this work is to maximize the dynamic range of capacitive tactile sensors and their sensitivity by exploiting the vertical direction and creating stacks of more than two capacitors. If the previous mentioned works propose a specific solution, the goal of this thesis is to develop a model that allows to choose the design parameters and to evaluate different stacking options to reach the desired sensitivity. This work provides the following contributions: 1) the development of a mathematical model for tactile capacitive sensors, in order to find a configuration to increase their sensitivity with respect to the common single capacitors; 2) the validation of the mathematical model with finite element simulations, by studying the sensors responses; 3) a straightforward method for manufacturing and characterizing vertically stacked capacitive tactile sensors. The chapter is organised as follows.
Section 3.1 presents a mathematical model for capacitive sensors. The aim is to demonstrate that the sensitivity of a single capacity is lower with respect to a stack of capacitors. The model allows to give the guidelines for the design of new layouts in order to increase the perfomances of these kind of sensors. Section 3.2 presents finite element simulations for validating the proposed mathematical model and for studying the mechanical behaviour of the dielectric material, also introducing non-linear simulations to compare the results with the experiments. Section 3.3 presents the manufacturing and the characterization procedures used to built the capacitors.

3.1 Mathematical Model of a Capacitive Tactile Sensor

As discussed above, in order to increase the dynamic range and the sensitivity of the response, the idea discussed here is of building stack of capacitances in parallel. The sensitivity of capacitance measurement is dependent of thick values of the capacitance. For a given thickness the first goal is to evaluate how thick the layers composing the stack must be to optimize sensor response, respecting design and manufacturing constraints. The second purpose of the demonstration is to indicate how many capacitors have to be stacked in order to maximize the resulting sensitivity.

3.1.1 Capacitive sensors principle

As it appears from Fig. 3.1, the variation of the pressure applied on the sensor due to the force F uniformly distributed on the transducer area A can be written as:

$$\Delta P = -\frac{F}{A} \tag{3.1}$$

where the pressure variation $\Delta P = P - P_0$ is supposed to be uniform on the whole sensor area. P is the applied pressure and P_0 is any possible equilibrium pressure (e.g, pre-loading pressure, or atmospheric pressure in the case of pressure compensated sensors etc.). We start to share how an applied pressure is uniformly distributed on the sensor surface, and we can compare the deformation of the dielectric material of the capacitive sensor with the deformation of the *equivalent spring*, using the following formula:

$$F = k \cdot \Delta t, \Delta t < 0 \tag{3.2}$$

Where k is the elastic constant of the *equivalent spring* representing the linearized effect of the applied force in terms of the sensor deformation. $\Delta t = t - t_0$ is the displacement, t is the resulting thickness of the dielectric due to the pressure applied on the transducer and t_0 is the initial thickness

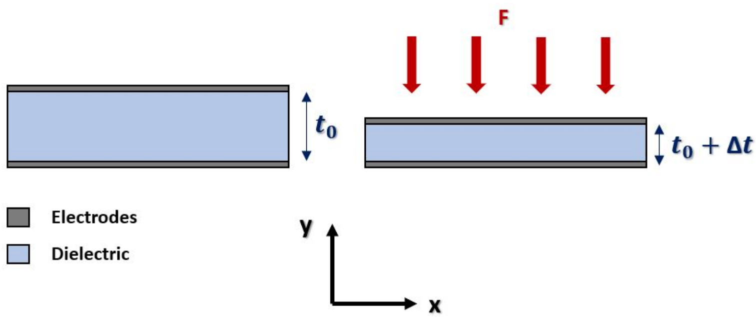

Figure 3.1 Schematic diagram of the working principle of a capacitive tactile sensor.

Using the standard stiffness engineering model (81; 125), we have that:

$$k = \frac{E \cdot A}{t_0} \tag{3.3}$$

where E is the Young's Modulus of the material.
By substituting the value of F computed from equation 1 in to equation 2 and using the definition of k of the equation 3 we obtain the following equality:

$$-A \cdot \Delta P = \frac{E \cdot A}{t_0} \cdot \Delta t \tag{3.4}$$

Which can also rewritten as:

$$\frac{\Delta t}{t_0} = -\frac{\Delta P}{E} \tag{3.5}$$

assuming a linear stress-strain relationship for the material used to build the sensor. Let us now consider the nominal value of the sensor capacitance in the absence of contact pressure. The value is C_0 and it is expressed as:

$$C_0 = \gamma \frac{A}{t_0} \tag{3.6}$$

$\gamma = \varepsilon \varepsilon_r$, where ε and ε_r are the vacuum electric permeability and the dielectric constant of the material used, respectively. Once a pressure is applied on the sensor, the resulting capacitance become:

$$C = \gamma \frac{A}{t_0 + \Delta t} \tag{3.7}$$

under the assumption that the transducer area does not change under the effect of a contact pressure. The difference between C and C0 can than be written as:

$$\begin{aligned} \Delta C = C - C_0 = \gamma \frac{A}{t_0 + \Delta t} - \gamma \frac{A}{t_0} = \\ = \gamma A \left(\frac{1}{t_0 + \Delta t} - \frac{1}{t_0} \right) = \gamma A \left[\frac{-\Delta t}{t_0 \left(t_0 + \Delta t \right)} \right] = \\ = \frac{\gamma A}{t_0} \left[\frac{-\Delta t}{t_0 + \Delta t} \right] = -C_0 \left[\frac{\Delta t}{t_0 + \Delta t} \right] \end{aligned} \tag{3.8}$$

By using the equation 5, we can write the equation 8 as follow:

$$\Delta C = C_0 \frac{t_0 \frac{\Delta P}{E}}{t_0 - t_0 \frac{\Delta P}{E}} = C_0 \frac{t_0 \Delta P}{t_0 E - t_0 \Delta P} = C_0 \frac{\Delta P}{E - \Delta P} \tag{3.9}$$

3.1.2 Introduction to the stacked capacitances: the 2 layers stack

From now on we analyze the dielectric thickness requirement, to achieve the first objective mentioned above, and let's consider a capacitive sensor configured as parallel capacitances (stack), composed of two layers of dielectric material, as in Fig. 3.2.

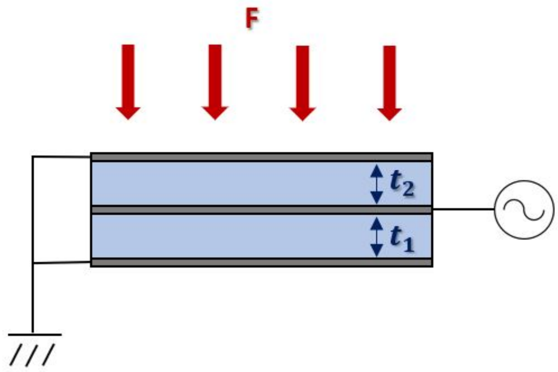

Figure 3.2 Schematic diagram of a capacitive sensor configured as parallel capacitances. The thickness variation of the electrodes is always negligible compared to the dielectric deformation.

For capacitive sensors, in general the dielectric greatly affects the responce of the device (153). In this paper we only take into account the effect of the dielectric in terms of its deformation. From the equation 9, can define the total variation of the stack as the sum of the variation of the two capacitors.

$$\begin{aligned} \Delta C = C_{1_0}\frac{\Delta P}{E-\Delta P} + C_{2_0}\frac{\Delta P}{E-\Delta P} = \\ = \left(C_{1_0}+C_{2_0}\right)\frac{\Delta P}{E-\Delta P} = C_0\frac{\Delta P}{E-\Delta P} \end{aligned} \tag{3.10}$$

where $C_0 = C_{1_0} + C_{2_0}$ is now the total initial capacity of the stack. Suppose we want to design a stacked sensor with these characteristics such that the total thickness of the sensor (design parameter) is defined as equal to t_{tot}. In this case, the thicknesses of the two capacities t_1 and t_2 become the design parameters. With these considerations, we can write C_0 as :

$$C_0 = \gamma A\left[\frac{1}{t_1}+\frac{1}{t_2}\right] = \gamma A\frac{t_1+t_2}{t_1 t_2} = \gamma A\frac{t_{\text{tot}}}{t_1\left(t_{tot}-t_1\right)} \tag{3.11}$$

So, for a given capacitor thickness, the goal is to decide how much t_1 and t_2 should be.

$$\frac{t_1}{t_{tot}} + \frac{t_2}{t_{tot}} = 1 \tag{3.12}$$

By defining:

$$\frac{t_1}{t_{tot}} = x, \frac{t_2}{t_{\text{tot}}} = 1 - x \tag{3.13}$$

we can write the equation 11 using equations 12 and 13:

$$C_0 = \gamma A \frac{1}{x(1-x)} \tag{3.14}$$

The sensitivity S is defined as the ratio between the variation of capacitance ΔC and the variation of the exerted pressure ΔP (i.e., the stress):

$$S = \frac{\Delta C}{\Delta P} \tag{3.15}$$

The sensitivity is proportional to ΔC and by equation 10 to C_0. Therefore, for a given ΔP, C_0 must be maximized.
Fig. 3.3 shows the trend of C_0 with respect to the layer thickness, expressed with the variable x (minimum possible thickness for the dielectric).

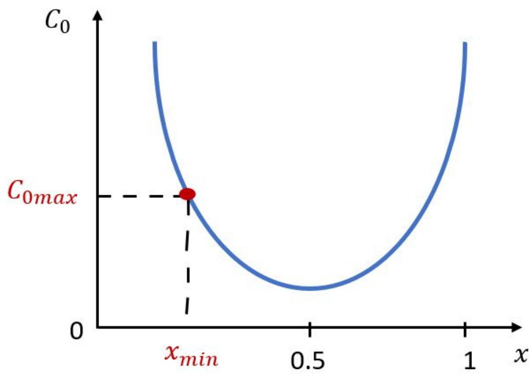

Figure 3.3 Plot showing the initial capacity C_0 with respect to the layer thickness.

The formulation of the computation of the maximum of C_0 must be constrained since the minimum value of x is indeed a physical constraint which might depend on the technology

used for the manufacturing of the sensor and on the characteristics of the material involved in the design.
From this result we can say that the decreasing of the layer thicknesses improves the output and so the sensitivity of the capacitive sensor.

3.1.3 Introduction to the stacked capacitances: capacitance from 3 to N layers

In order to generalize to the case of a N layer stack (N-stack), let us consider as an example the case of a 3-stack. Using the same notation of Section 3.1.2 we define as x_1, x_2 and x_3 the normalized thicknesses of the three layers t_1, t_2 and t_3 with respect to the total expected sensor thickness t_{tot}. Then the following optimized problem must be solved:

$$\begin{gathered} \max C_1 + C_2 + C_3 \\ \text{s.t.} \\ x_1 + x_2 + x_3 = 1 \\ x_i > x_{\min}, \forall i \end{gathered} \tag{3.16}$$

In order to find a maximum of the above cost function, consider a feasible choice for x_1, x_2 and x_3 and assume (without loose of generality) x_1 fixed. Then following the rationale used in Section 3.1.2 it is straight forward to verify that:

$$\begin{gathered} x_2 = \min \\ x_3 = (1 - x_1) - x_{\min} \end{gathered} \tag{3.17}$$

maximises $C_2 + C_3$. Since C_2 cannot be increased further, x_2 can be fixed and the above rationale can be repeated for x_1 and x_3 so that it can be:

$$\begin{cases} x_2 = x_{\min} \\ x_1 = x_{\min} \\ x_3 = 1 - 2x_{\min} \end{cases} \tag{3.18}$$

We can represent these layers as in the Figure 3.4.

Eventually loads to a feasible solution maximize the capacitance of the 3-stack. It is also quite easy to check that for a given transducer thickness t_{tot}, the capacitance of a 3-stack is greater than a 2-stack one. The dimension above suggests that for a given thickness t_{tot}, the layers should have the following distribution:

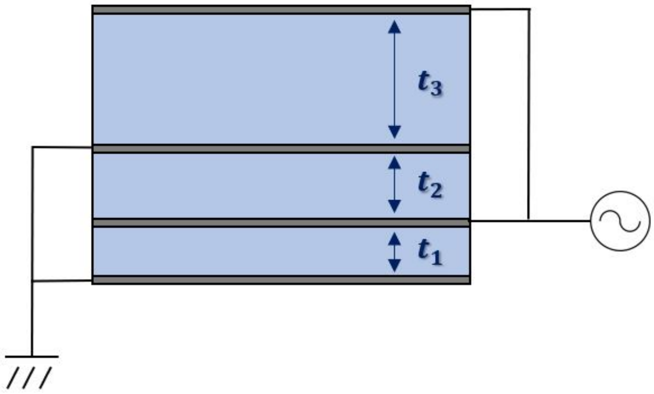

Figure 3.4 Thicknesses of the layers forming the capacitive sensor.

$$\begin{cases} x_1 = x_{\min} \\ x_{N-1} = x_{\min} \\ x_N = 1 - (N-1)x_{\min} \end{cases} \tag{3.19}$$

The formal proof is in Appendix.

3.2 Finite Element Simulations

In this section we use finite element simulations to validate the mathematical model presented in the previous section and to explain the mechanical behaviour of the dielectric material, also modeling the non-linear effect featuring the real system. On one hand, the linear simulated model is useful to validate the models discussed in Section 3.1; on the other hand, the non-linear simulated model is important to compare the finite element results with the experimental ones presented in Section 3.3. First, we define the sensors model, which is essential to simulate the sensor response. Then, we compute the sensors finite element responses with their corresponding sensitivity and we compare the results between a single capacitor and stacks of capacitors to demonstrate that a stack performs better than a single capacity.

3.2.1 FEM Sensor model

Practical guidelines for the implementations of capacitive tactile sensors have been presented in (155). The geometry and the material properties used for the simulated models have followed those guidelines and are related to existing tactile sensors implementation (154).

The simulated transducer is a single circular taxel with a diameter d = 4 mm. Tests on Section 3.2.2, which are used to validate the mathematical demonstration, include models with the same thickness t_0 = 1 mm. Tests on Section 3.2.3, which are used to study the mechanical behaviour of the dielectric material, include models with different thicknesses, which increase every time we add a capacitity in parallel to the stack. In this case, each capacity has a thickness t = 100 μm. The choice of the dielectric and conductive layer materials is consistent with the materials used for the experimental tests described in the following Section. In particular, the dielectric is made of Polydimethylsiloxane (PDMS) and Silver ink is used for the conductive capacitor plates and electrodes. The mechanical characteristics of the conductive layers are assumed negligible and not modelled in the FEM simulations. For the non-linear mechanical analysis we used a neo-Hookean constitutive model for the PDMS. Table 3.1 summarizes the most relevant material properties of the dielectric material used, which are:

- The Young's modulus, defined as $E = \frac{\sigma}{\varepsilon}$, where σ and ε are the material's stress and strain respectively (220), is used to compute the elastomer strain under an exerted pressure.
- The Poisson's ratio (ν) is a measure of the Poisson effect originating from the elastomer expansion along the direction normal to pressure application.
- The dielectric permittivity (ε_r), which impacts on capacitance variations (155) and so on the sensor sensitivity.

3.2.2 Simulations results: validation of the methematical model

COMSOL Multiphysics has been used to implement the models and performance simulations, and simulation results have been further analyzed with Matlab. For the simulations two classes of contacts have been selected, following (155; 158). The first class is referred to as *gentle touch* and is characterized by contact pressures in the 0–10 KPa range, whereas the second class, *manipulation-like touch*, refers to pressures in the 10–100 KPa range.
Looking at the consideration of the Section 3.1, we want to validate through FEM i) the optimal layer distribution and ii) the maximization of the performances by increasing the number of layers. For sake of simplicity, in all models the sensitivity has been calculated as the angular coefficient of the linear fitted curve, which can cover all the ranges, with a maximum pressure of 100 kPa, from gentle touch to manipulation-like touch.

Table 3.1 Most relevant dielectric material properties.

Young's Modulus **(E)**	200 [kPa]
Poisson Ratio (ν)	0.49
Dielectric Permittivity (ε_r)	2.75
Shear modulus for neo-Hookean model (μ)	42 [kPa]

Optimal layer distribution

Let us now consider two models, which represent a stack with the same total thickness t_0 = 1mm composed of 4 layers. In the first case the layers have the same thickness, in the second case the layers are distributed according to the analysis of the previous section, assuming a minimum thickness of 100 μm. Figure 3.5 and Figure 3.6 show the two stack configurations in the case of uniform pressure applied on the top layer of 100 kPa. Figure 3.7 shows the finite element response of the first configuration, while Figure 3.8 shows the finite element response of the second configuration. For the validation, the models have been considered linear. By comparing the two finite element results, the second case has a 7 % increase in sensitivity with respect to the first case. This further validate the first part of the mathematical demonstration, on which we propose the optimal layer distribution to increase the sensor response.

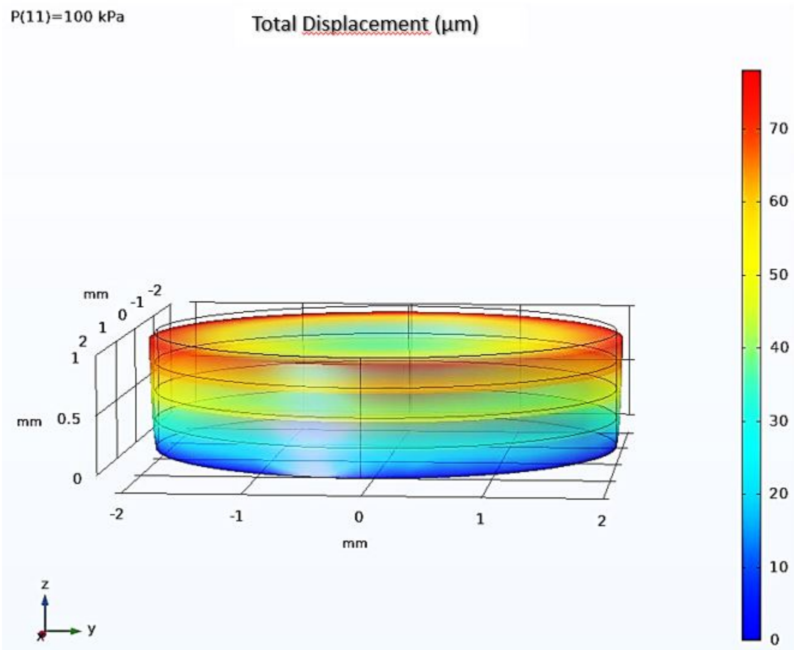

Figure 3.5 Simulation for a 4 stack capacitor with t_{tot} = 1mm and $t_1 = t_2 = t_3 = t_4 = 250\ \mu$m. The Figure refers to the case of a uniform pressure of 100 kPa.

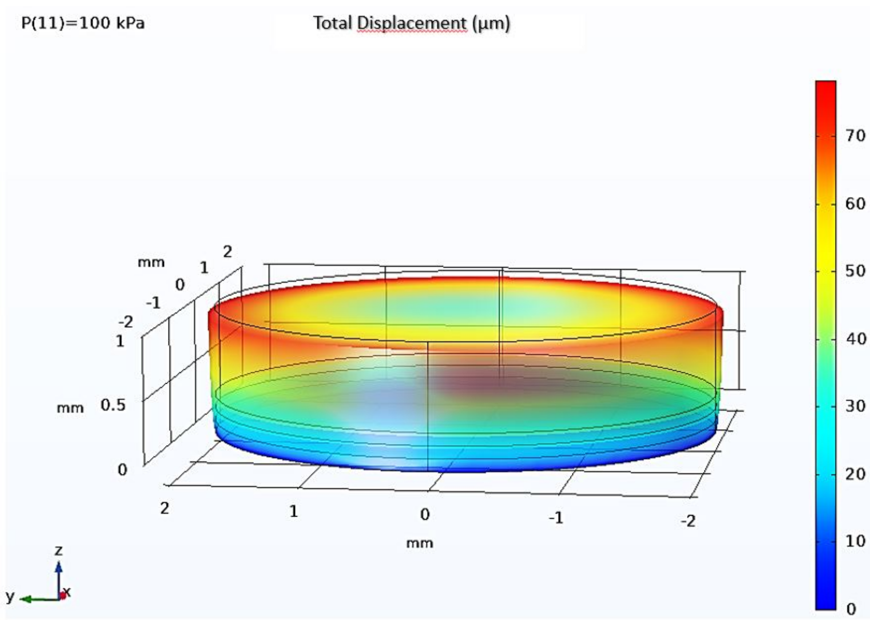

Figure 3.6 Simulation for the 4 stack capacitor with t_{tot} = 1mm and $t_1 = t_2 = t_3 = 100\ \mu$m and $t_4 = 700\ \mu$m. The Figure refers to the case of a uniform pressure of 100 kPa.

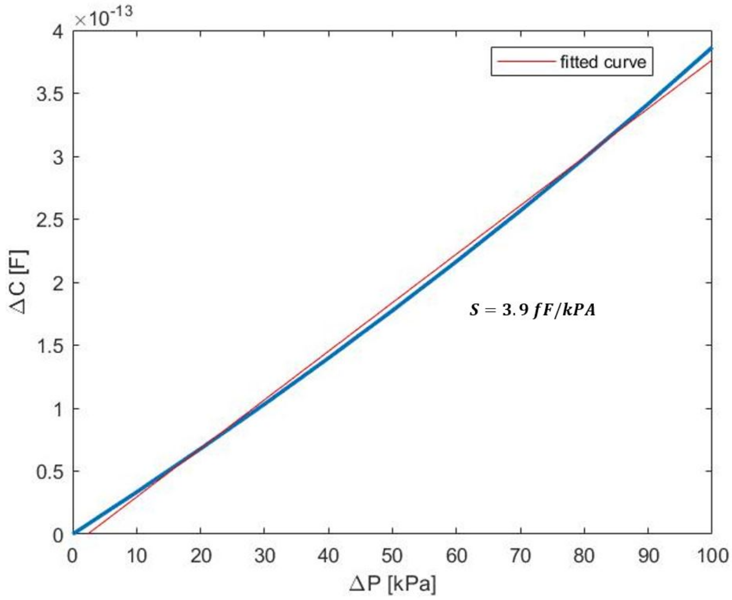

Figure 3.7 Computed change of capancitance ΔC for a change of applied pressure ΔP for the case of Figure 3.5. The fitted curve is reported for the calculation of the sensitivity.

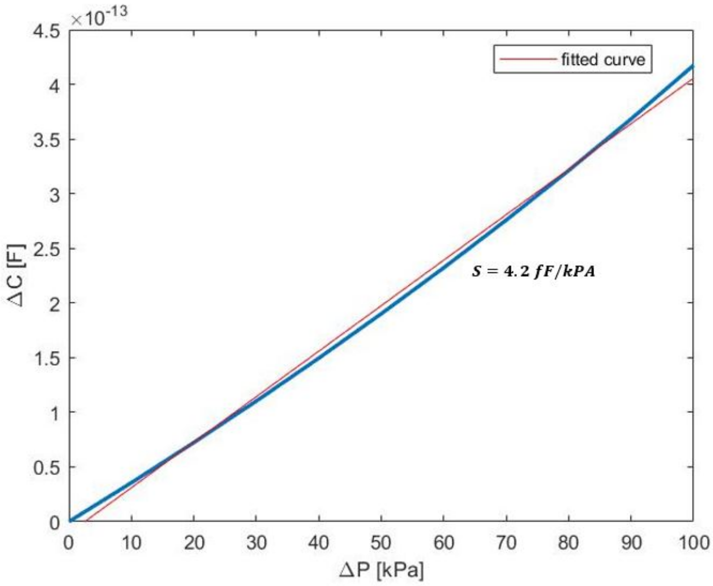

Figure 3.8 Computed change of capancitance ΔC for a change of applied pressure ΔP for the case of Figure 3.6. The fitted curve is reported for the calculation of the sensitivity.

Maximization of the performances by increasing the number of layers

Let us now consider other two models, which represent a stack composed of 4 layers and a stack composed of 6 layers, with the same total thickness t_0 = 1mm and both with the optimized layer configuration. For the 4 stack capacitor, we consider the best configuration of the previous section, and so we refer to Figure 3.6 for the model and to Figure 3.8 for the response. Figure 3.9 shows the 6 layer stack and Figure 3.10 shows the finite element response of the 6 stack model. Also in this case, for the validation we consider linear models. By comparing the two finite element results, the 6 layer stack has a greater sensitivity with respect to the 4 layer stack. This comparison tell us that by increasing the number of layers in optimal configuration by 50 %, a sensitivity variation of 130 % is produced.

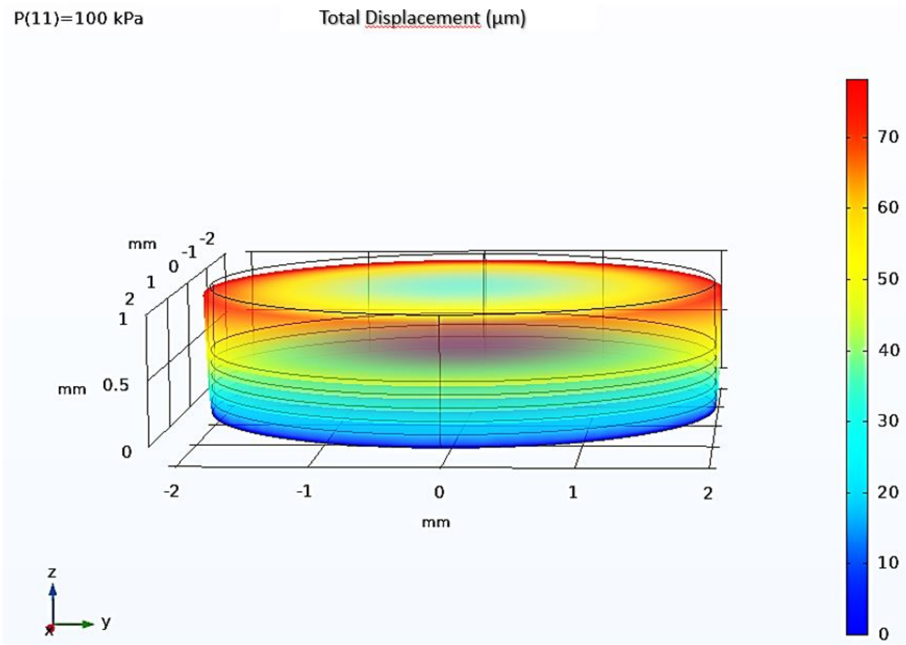

Figure 3.9 Simulation for the 6 layer stack with t_{tot} = 1mm and $t_1 = t_2 = t_3 = t_4 = t_5 = 100$ μm and $t_6 = 500$ μm. The Figure refers to the case of a uniform pressure of 100 kPa.

In order to show the effectiveness of the optimal configuration, we also compared the case of 4 layers of equal thickness (see Figure 3.5) with the case of 6 layers of equal thickness (see Figure 3.11). The results of these two non-optimal configurations are shown in Figure 3.7 and Figure 3.12. In this case, a sensitivity variation of 120 % is produced.

Through all these tests and comparisons, we have validated the entire mathematical demonstration, and we can affirm that, for improving the performance of capacitive sensors, the aim is to manufacture sensors composed of several stacks of capacitances; moreover, each layers have to be designed according to the optimal distribution explained above.

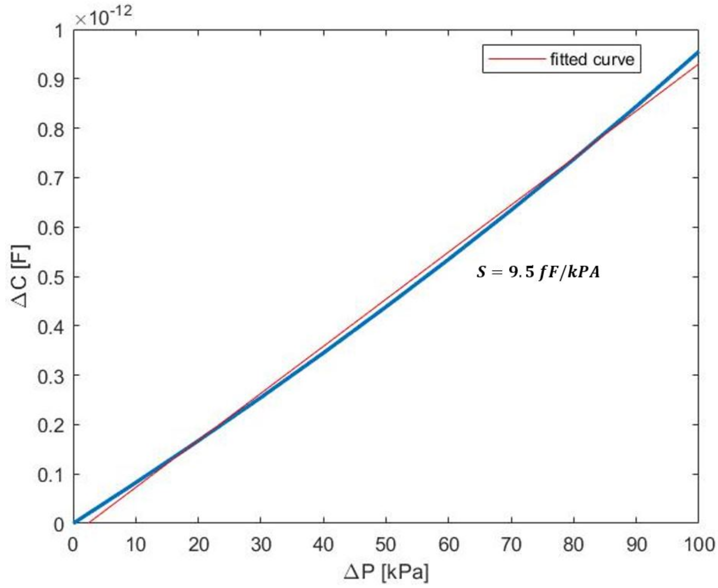

Figure 3.10 Computed change of capancitance ΔC for a change of applied pressure ΔP for the case of Figure 3.9. The fitted curve is reported for the calculation of the sensitivity.

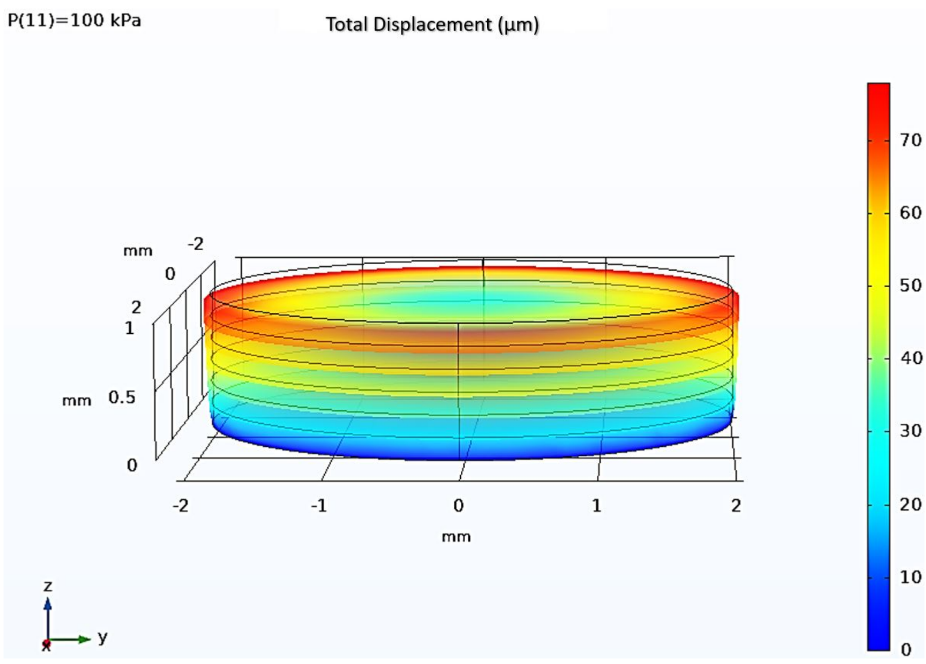

Figure 3.11 Simulation for the 6 layer stack with t_{tot} = 1 mm and $t_1 = t_2 = t_3 = t_4 = t_5 = t_6 =$ 100 μm. The Figure refers to the case of a uniform pressure of 100 kPa.

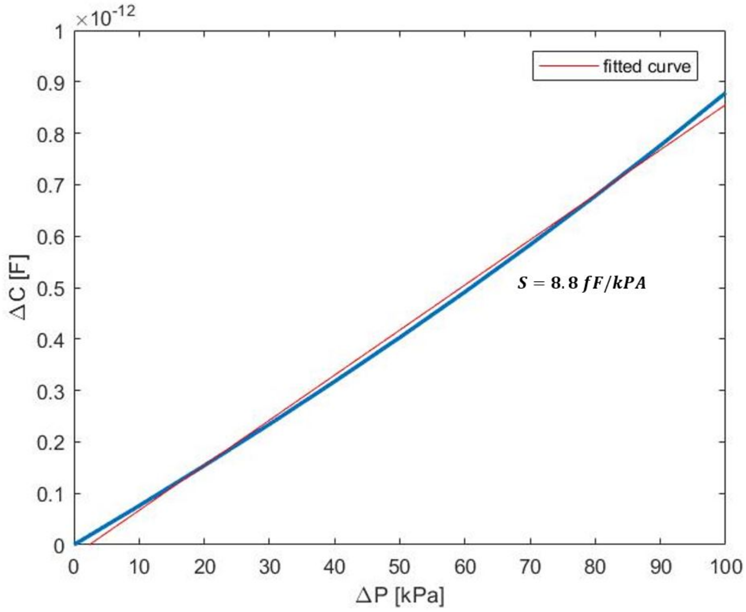

Figure 3.12 Computed change of capancitance ΔC for a change of applied pressure ΔP for the case of Figure 3.11. The fitted curve is reported for the calculation of the sensitivity.

3.2.3 Simulations results: a study on the mechanical behaviour of the dielectric material

In the previous paragraphs, the analysis aims to demonstrate that more optimized stacked capacitors have good performances. We now focus on the most technologically tractable case, in which layers have all equal thicknesses. So, we work with non-optimal configurations from the layout point of view. In this case, all the elements necessary to make the results comparable with the experimental analysis have been introduced into the FEM. In particular, in addition to the PDMS as a dielectric, kapton was also added in the simulations, as in the experiments the sensors present both materials to form the dielectric. For the models, a single capacitor, a 2 stack capacitor and a 3 stack capacitor have been considered. The first simulation test refers to the analysis of the response of a 1 stack and 2 stack, and the second simulation test refers to the analysis of the response of a 2 stack and 3 stack, in order to understand how the dielectric is compliant under the action of a uniform pressure applied on the surface area. Figures 3.13, 3.14, 3.15 show the mechanical responses of 1 stack, 2 stack and 3 stack, respectively, in terms of dielectric total displacement under the maximum pressure applied. The initial values of the single capacity (C_{0_1}), of the 2 stack (C_{0_2}) and of the 3 stacks (C_{0_3}) are 3.65 pF, 7.29 pF and 10.9 pF, respectively.

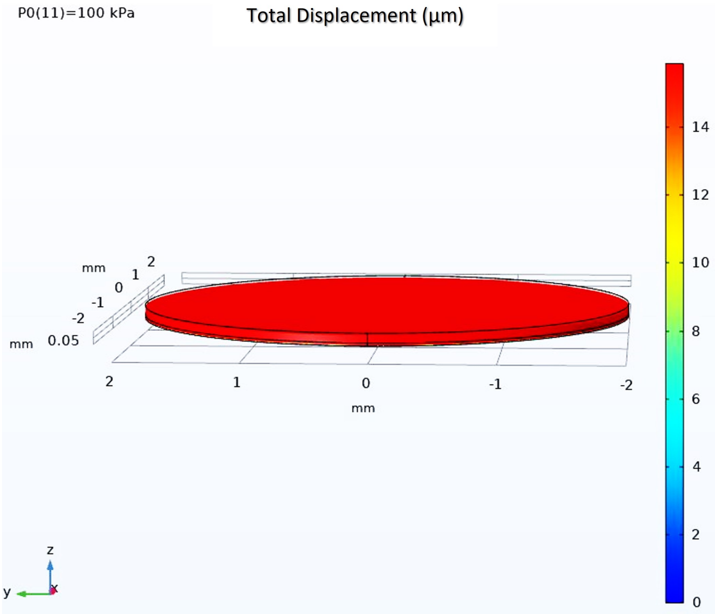

Figure 3.13 Behaviour of the 1 stack capacitor in terms of dielectric total displacement under a range of pressures applied.

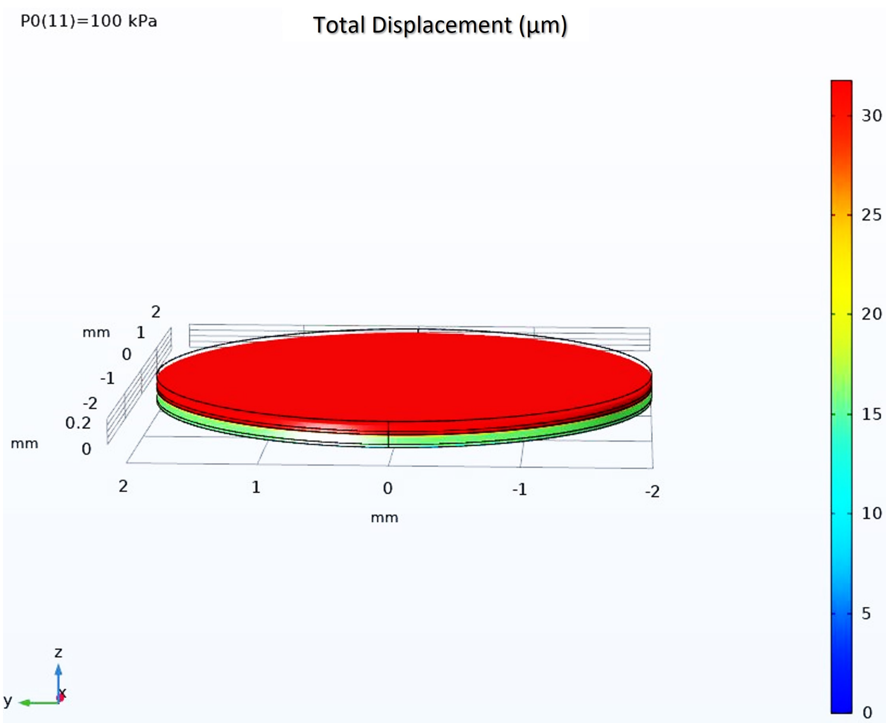

Figure 3.14 Behaviour of the 2 stack capacitor in terms of dielectric total displacement under a range of pressures applied.

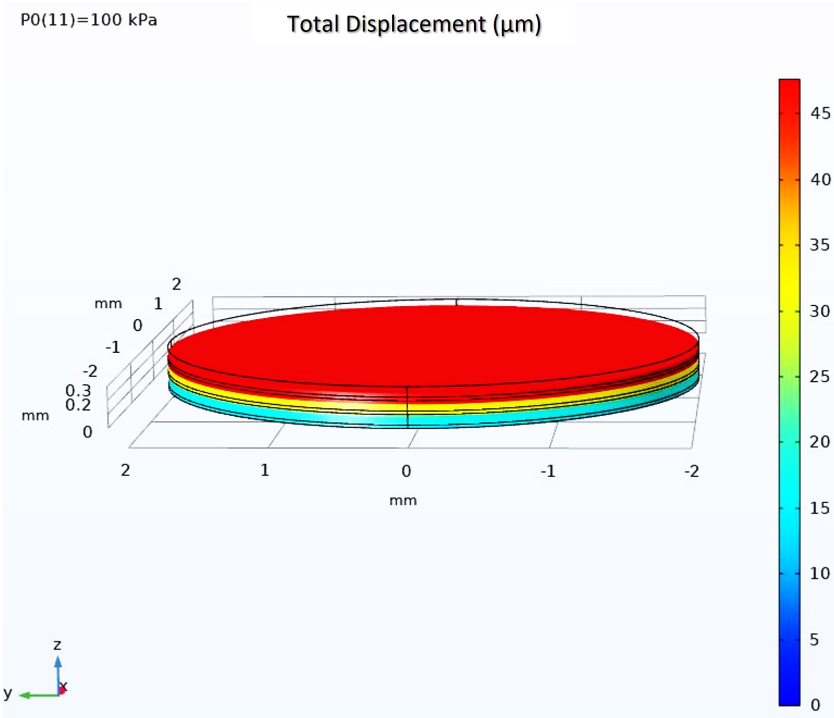

Figure 3.15 Behaviour of the 3 stack capacitor in terms of dielectric total displacement under a range of pressures applied.

Figure 4.13 shows the ideal sensors output and their corresponding sensitivity in the linear case. More detailed information are given in Figures 3.17, 3.18 and 3.19 which show the ideal sensors output and their corresponding sensitivity in the non-linear case. This is a more real representation of the sensors response, and for this reason we will consider these values as a reference to compare them with the experimental results. Results from the neo-Hookean model show that the sensitivity has an increase of the 90 % passing from a single capacitor (S = 8.9 fF/kPa) to 2 stack (S = 16.9 fF/kPa), and an increase of 48 % passing from a 2 stack to a 3 stack (S = 25 fF/kPa). The sensitivity has an increase of 180 % if we pass from a single capacitor to a 3 stack capacitor. Also in this case, the sensitivity will increase every time we add a capacity in parallel to the stack.

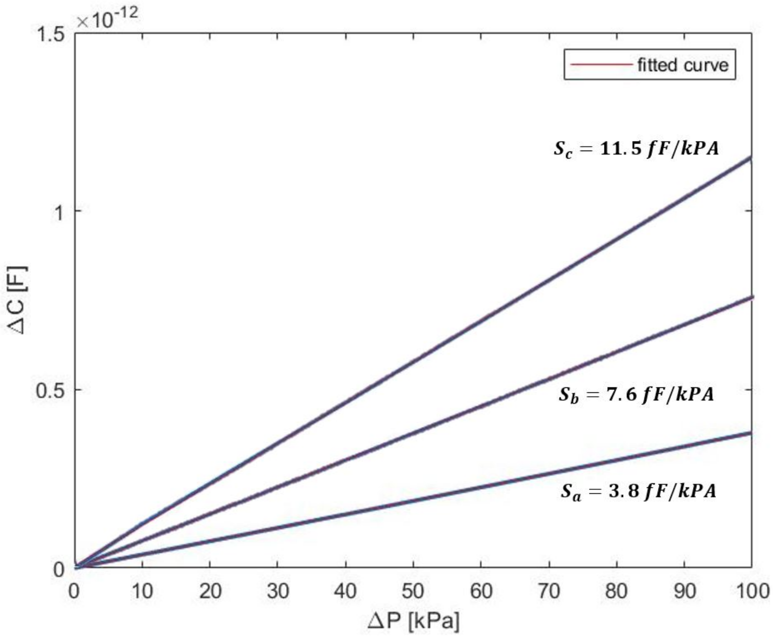

Figure 3.16 Finite element response with the corresponding sensitivity in the case of a) 1 stack, b) 2 stack capacitor and c) 3 stack capacitor, assuming a linear model for the dielectric material.

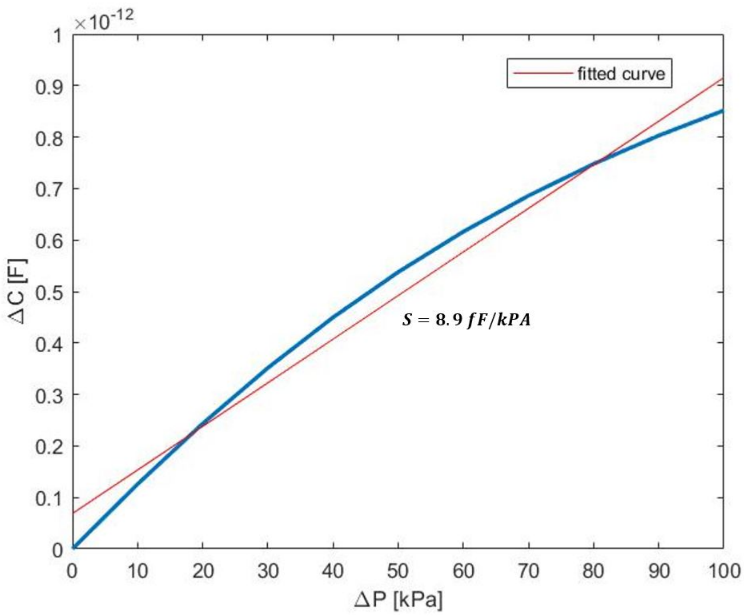

Figure 3.17 Finite element response with the corresponding sensitivity in the case of 1 stack capacitor, using neo-Hookean non-linear elastic constitutive model for the dielectric material. The fitted curve is reported for the calculation of the sensitivity.

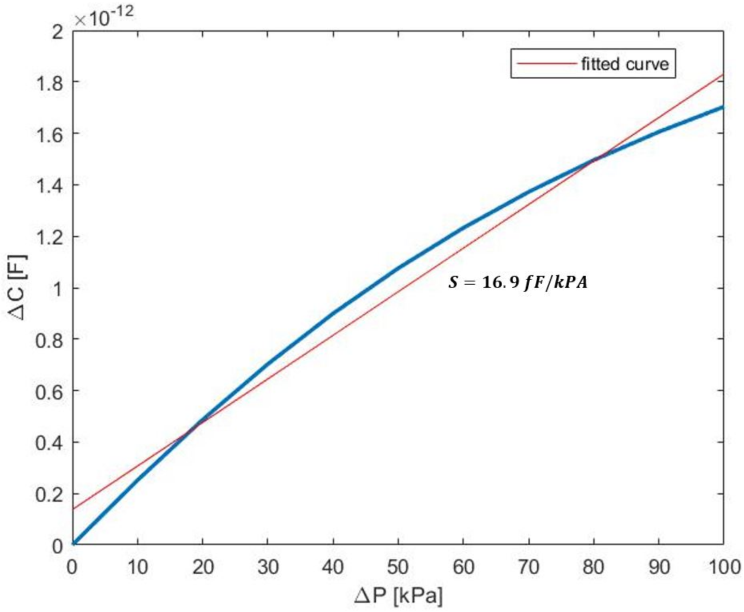

Figure 3.18 Finite element response with the corresponding sensitivity in the case of the 2 stack capacitor, using neo-Hookean non-linear elastic constitutive model for the dielectric material. The fitted curve is reported for the calculation of the sensitivity.

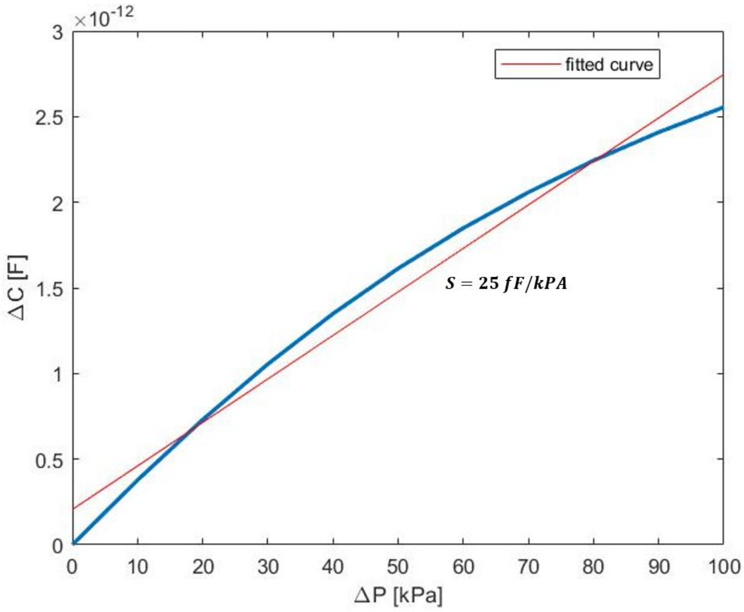

Figure 3.19 Finite element response with the corresponding sensitivity in the case of the 3 stack capacitor, using neo-Hookean non-linear elastic constitutive model for the dielectric material. The fitted curve is reported for the calculation of the sensitivity.

3.2.4 Simulations on the sensors response by increasing the number of capacitors in parallel

The realization of a greater number of layers involves process difficulties and greater encumbrances. In this thesis, the simulations and the experimental tests have been conducted up to three layers of dielectric. For larger layers, we conducted simulations that give us information on what to expect by increasing the number of parallel capacitors (all the sensors features remain the same of Section 3.2.3). Figure 3.20 shows the non-linear response of a 5 stack and a 10 stack capacitors. The predictions tell us that by continuing to increase the number of stacks, there are improvements on the variation of the sensor capacity, which is therefore more sensitive.

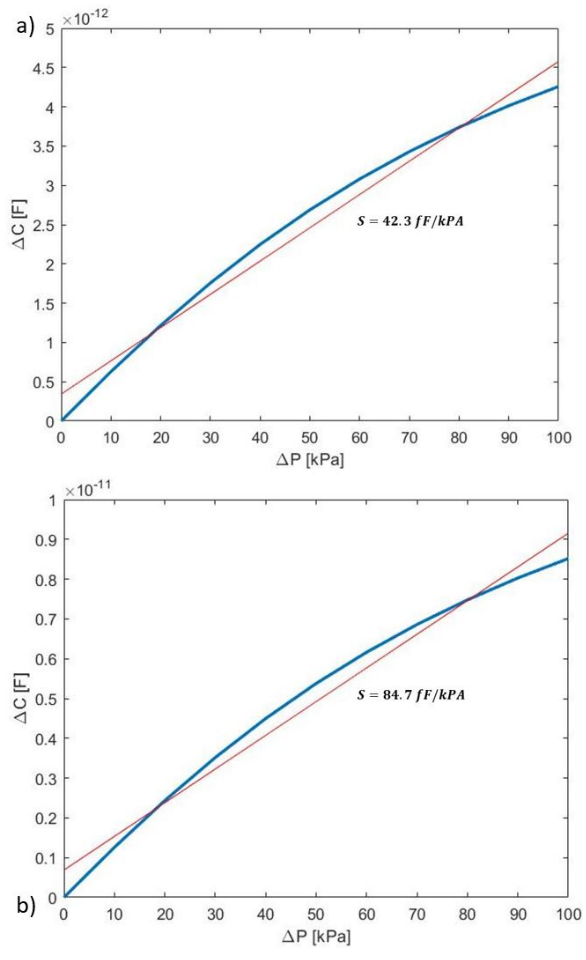

Figure 3.20 Prediction on the sensor response in the case of a) 5 stack capacitor; b) 10 stack capacitor. The fitted curve is reported for the calculation of the sensitivity.

3.3 Experimental Manufacturing and Characterization

In this section we first show the manufacturing procedures used to make a single capacitor and stacks of capacitors (all with a diameter of 4 mm, as for the simulation models). Then, we present the characterization procedure used to compute the parameters required to validate the finite element simulations of Section 3.2.3. The manufacturing process is based on the use of two techniques: inkjet printing and spin coating. The peculiarity of this approach is that it can be potentially used to obtain stacks of several capacitors in parallel and the procedure can be customized to optimize the sensors covering on different surfaces. In this work, three kinds of sensors have been manufactured and their performances have been analyzed. The characteristics of a 1 stack capacitor, the output of a 2 stack capacitor and the output of a 3 stack capacitor have been computed and the results have been compared with those obtained from the simulations.

3.3.1 Tactile sensor composed of a single capacity

Dielectric Preparation

Sylgard 184 (Dow Corning) is used as the dielectric material. The PDMS base and the curing agent is mixed in a 10:1 ratio (base to catalyst) in all experiments and steered for 2 min. Then, the PDMS is placed in vacuum desiccators for degassing (10–13 minutes). Than, a thin layer of PDMS has been deposited on the capacitor substrate by spin coating. As discussed in (166), a thickness of 25 μm guarantees an excellent electrical insulation between the conductive layers. The PDMS thickness mainly depends on spin speed and duration (129; 133). In this work, this thickness has been obtained by depositing in sequence 2 layers of PDM, each obtained through a spin coating with a speed of 2000 rpm and a duration of 5 min. With these parameters, each layer has a thickness of $\sim$ 12 μm and so the total dielectric thickness is $\sim$ 24 μm.
The dielectric preparation is the same also for the case of the stacked capacitors described later.

Device Fabrication

The capacitor substrate consists of a suitably cleaned kapton sheet (75 μm thick). Two layers of Silver Nanoparticle ink (Ag NP ink, SunTronic® EMD5730) have been inkjet printed directly on the substrate with the commercial inkjet printer Dimatix DMP-2850 Fujifilm.

The printed substrate is briefly placed on an hot plate to evaporate the solvent, until the silver color of the ink emerge. After that, the curing is terminated in an oven at 150 °C for 30 min. Subsequently, the PDMS is spin coated (as discussed in the above paragraph "Dielectric Preparation") on top of the conductive layer and oven cured at 120 °C for 25 min allowing the solvent to evaporate and cross-link the PDMS. At the same time, another identical conductive pattern is inkjet printed on a second kapton substrate and, after the curing phase, is placed on top of the dielectric material, placed on the first substrate, to form a single capacity. Figure 3.21 shows the sensor fabrication process and Figure 3.22 shows the vertical section of the structure.

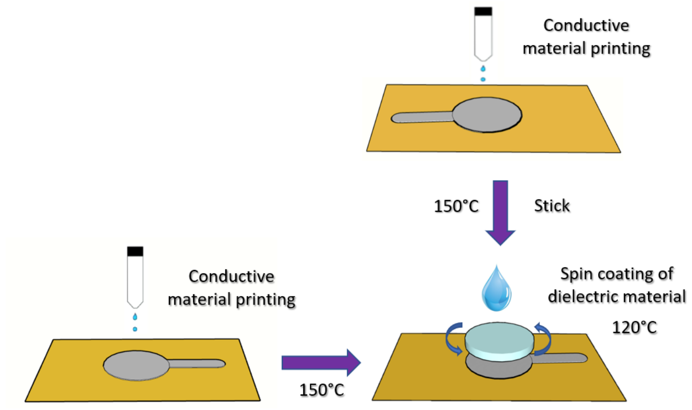

Figure 3.21 Schematic illustration of the sensor fabrication process.

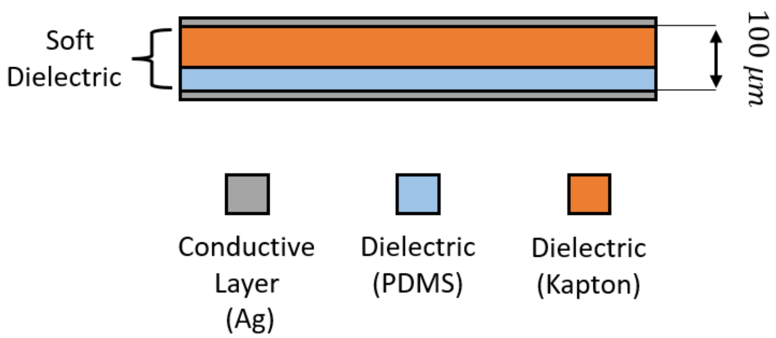

Figure 3.22 Vertical section of the structure.

3.3.2 Tactile sensor composed of a stack of capacitances

Device Fabrication

Starting from the manufacturing of the single capacity, stacks of N capacitors can be built by following the schematic illustration of the sensor fabrication process in Figure 3.23. This method allows to stack one capacity on top of the other, forming a stack of capacitors in parallel. Each capacitor is manufactured with the aforementioned fabrication process (see section 2.3.1). As from the Figure 4, in order to obtain a set of capacitors in parallel, all the odd layers must be electrically connected together as well as all the even armatures. To the same, the printed pattern of each armature is formed by a circle and an extruded electrode which will be used to interconnect the remaining layers. From the final tranducer, the sensor is composed of $2N$ right electrodes and $2N-1$ left electrodes. All the right electrodes are electrically connected with each other with a conductive resin (MG Chemicals 842UR) and the same thing for the left electrodes. For a good electrical connection between the armatures, the layers are stacked one on the other and each of them is rotate of few grades with respect to the lower, in order to avoid short circuits. This layout allows the electrical connection vertically. The use of conductive glues has been chosen to solve a problem regarding the vias fabrication in tactile sensors, in which functional devices from different layers need to be connected by vertical interconnects (14; 196). Through other common fabrication methods, some works addressed the problem by manually creating vertical feedthrough (creating holes and metallizing them), during or even after the device fabrication (30; 80). This process is normally conducted in rigid double layer devices. More difficulties arise in the case of multi-layered sensors (more than two layers). The drilling must be done with a perfect cut to ensure that the subsequent metallization contacts all the conductive layers involved. In this way, the vias making for multi-layered sensors is supposed to be easier also because the via itself is not drilled but built like a conductive pillar. Figure 3.24 shows the vertical section of the 3 stack capacitor.

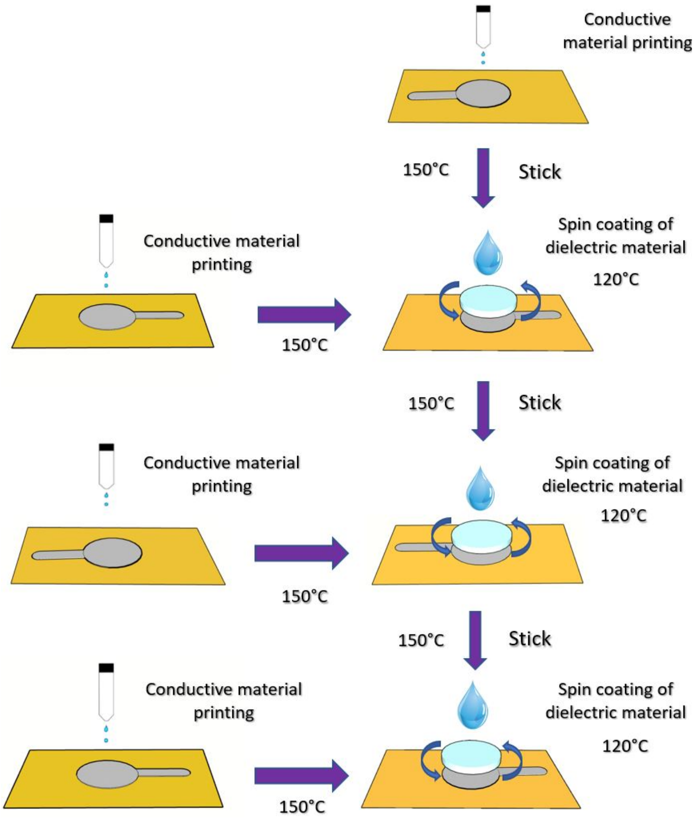

Figure 3.23 Schematic illustration of the sensor fabrication process for 3 dielectric layers.

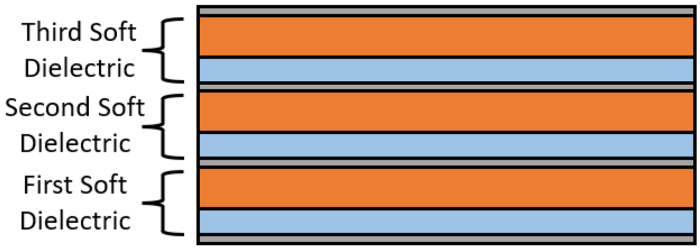

Figure 3.24 Vertical section of the structure for 3 dielectric layers.

3.3.3 Characterization: pressure-capacitance measurements

To evaluate the pressure range and the sensitivity of the manufactured capacitive sensors, the electrodes of the sensor were connected to the alligator clips of an LCR meter (GW Instek LCR-6100). We used a mechanical hand-made test-rig, shown in Figure 3.25, consisting of a vertical steel rod with a plastic cylindrical tip sustained by a linear bearing embedded in the supporting frame. The pressure applied on the capacitor is changed by adjusting the load by applying different weights on the upper supporting structure. For each experiment, the rod is placed on top of the capacitor and loads are placed until a predetermined pressure (force

divided by the rod surface area) is reached by stacking loads in sequence. Pressures ranging from 10 kPa to 100 kPa were tested, using 14 loads with the same weight. Each load was maintained for 10 s (recording 30 measurements) and then the next load was applied. All the measurements were repeated at least four times. While different loads were being applied, the capacitance of the sensor was measured using the LCR meter with a bias voltage of 1 V at a 1 kH frequency. In this way we extracted the capacitance change ΔC of the sensor and its sensitivity S.
The manufactured 3 stacked sensor is shown in Figure 3.26.

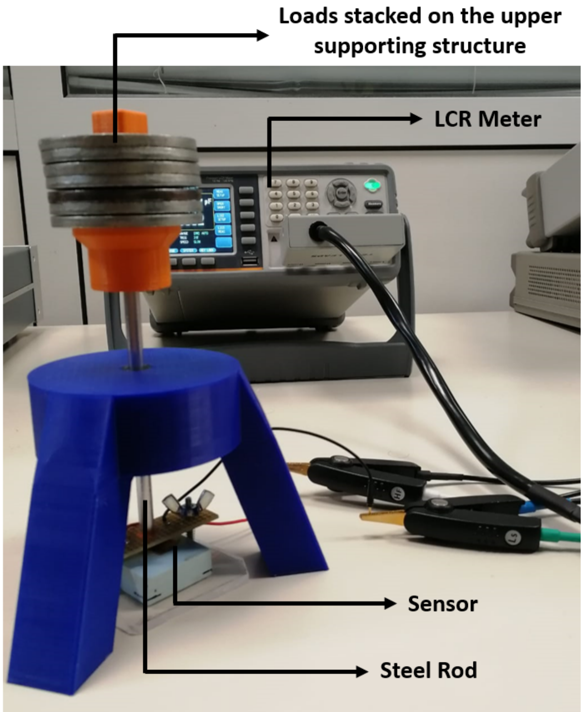

Figure 3.25 Experimental setup for measuring the change in capacitance in response to applied pressure.

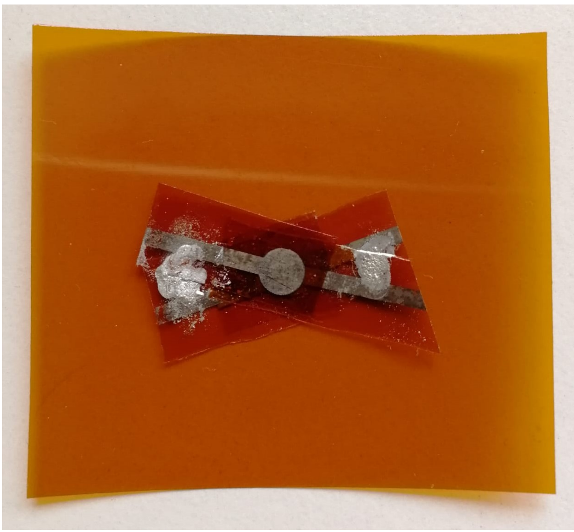

Figure 3.26 Manufactured 3 stacked capacitive sensor.

3.3.4 Results

In this section we studied the pressure response of the 1 stack capacitor, 2 stack capacitor and 3 stack capacitor, measuring their corresponding ΔC while the sensors were pressed. Figures 3.27 a, 3.28 a and 3.29 a plot the means and standard deviations, while Figures 3.27 b, 3.28 b and 3.29 b show the change in capacitance with respect to the applied pressure for each sensor type. The total ΔC on the total ΔP is higher by increasing the number of stacks. Passing from 1 stack to 2 stack capacitor, we have a sensitivity increase of 300 %. Passing from 2 stack to 3 stack capacitor, the increase is of 50 %. These results are confirmed looking at Section 3.2.3.

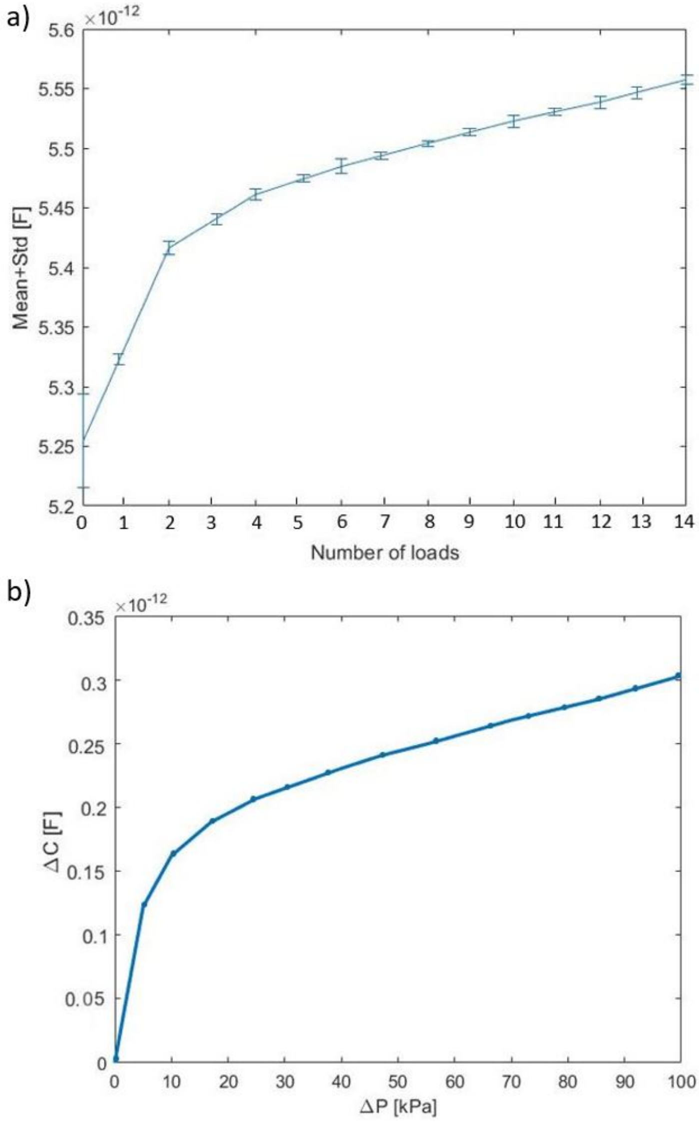

Figure 3.27 Experimental sensor output in the case of the 1 stack capacitor. a) Means and standard deviations of the output values; b) output in terms of ΔC with the corresponding sensitivity.

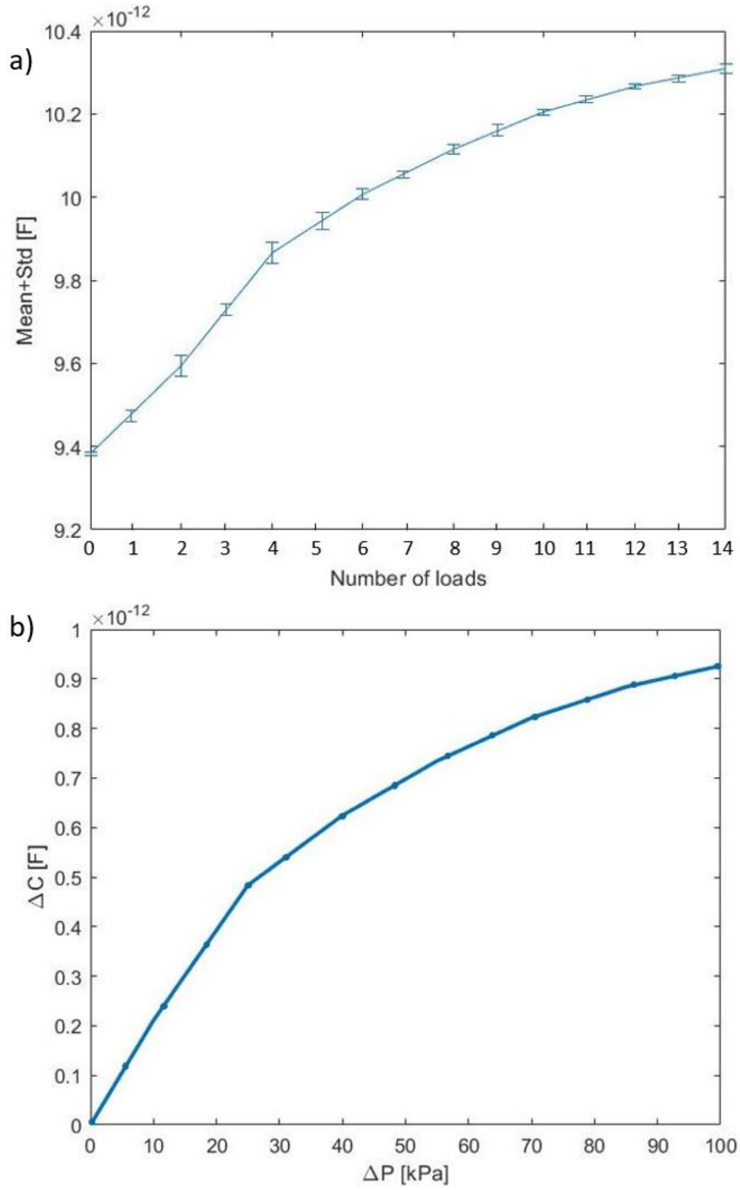

Figure 3.28 Experimental sensor output in the case of the 2 stack capacitor. a) Means and standard deviations of the output values; b) output in terms of ΔC with the corresponding sensitivity.

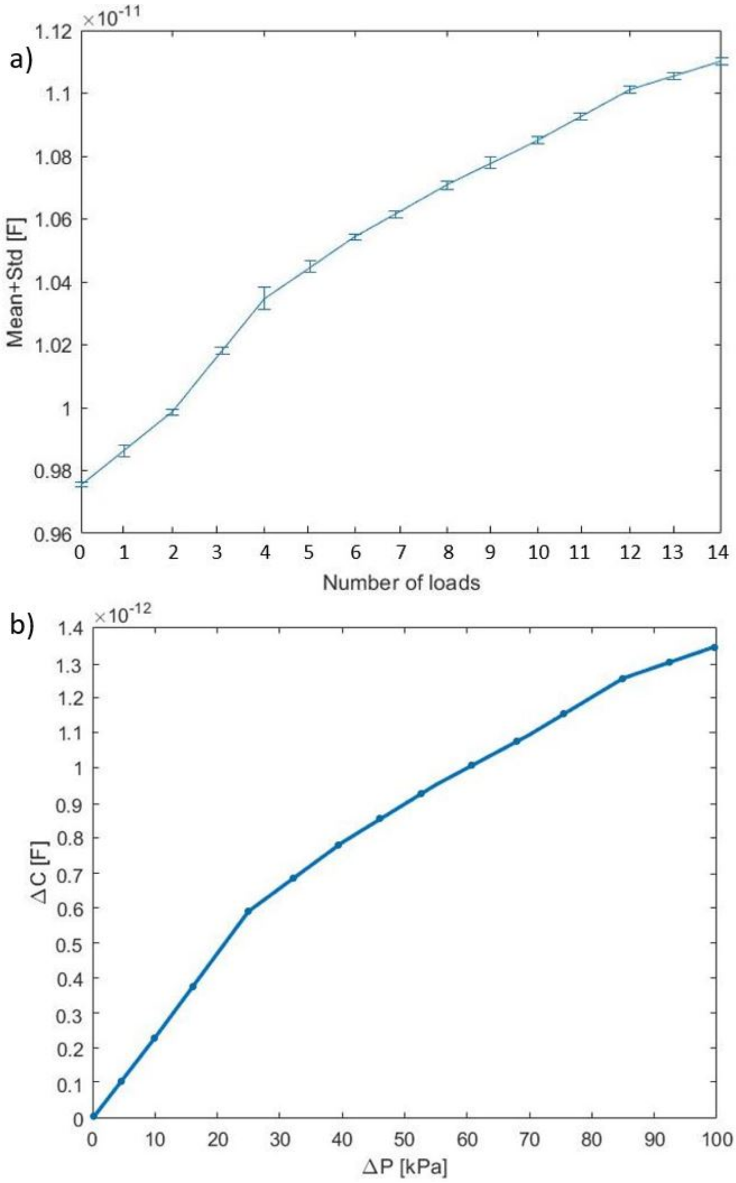

Figure 3.29 Experimental sensor output in the case of the 3 stack capacitor. a) Means and standard deviations of the output values; b) output in terms of ΔC with the corresponding sensitivity.

Chapter 4

Electronics design

Tactile sensors are based on capacitance sensing: a variation on the dielectric's thickness affects the distance between the electrodes, inducing a variation on the capacity. Capacitance to digital converters (CDC) measure sensor's capacity variation and convert it into digital bits. The basic working principle and a possible example are shown in Figure 4.1 and Figure 4.2. Therefore, CDC is the optimal solution to develop an electronic skin to collect data from the environment, transform and process them for the robot to behave in an autonomous way (e.g, work safely in collaborative tasks with humans). During the years, indeed, CDC was deployed in combination with a microcontroller unit to transmit and elaborate converted data. A recent study demonstrates that the old architecture can be replaced with a new one by employing only a microcontroller unit with capacitance to digital conversion capability. This has benefits on the costs, occupied area and technological implementation, making the robot skin more flexible and efficient (101). The microcontroller used for this thesis is the programmable Cypress PSoC4100S Plus, and tested on its evaluation board. The goal is to create an event-based algorithm with such device and test it in order to corroborate new architecture's benefits and design a possible integration with the inkjet printed sensors.
Section 4.1 provides the hardware and software requirements for the electronics design. Section 4.2 explains how the output capacitances are measured and converted, while Section 4.3 explains the logic behind the developed algorithm. Section 4.4 describes the tests done with the Cypress sensors and Section 4.5 shows the first obtained integration between the electronics and the inkjet printed tactile sensors, and the design of an optimized architecture which can confer much robustness and flexibility to the new improved skin.

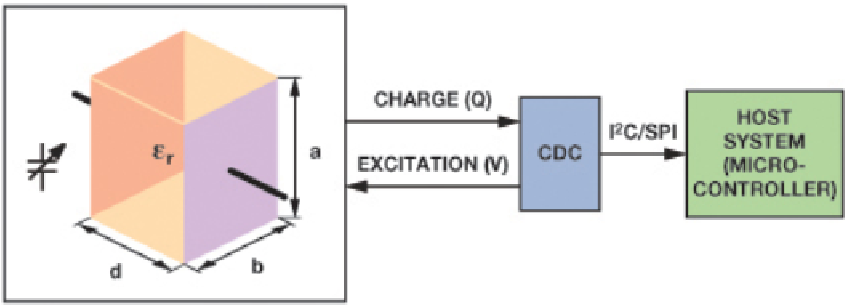

Figure 4.1 Measuring a parallel-plate capacitor's capacitance.

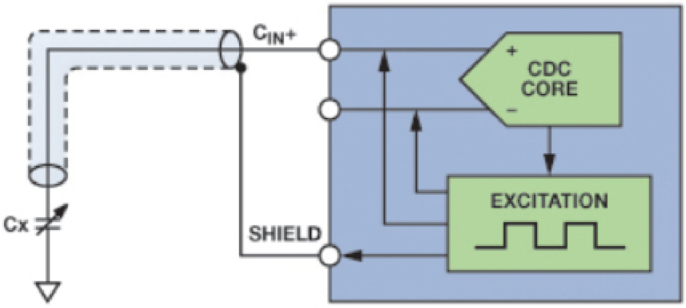

Figure 4.2 Example of how CDC work in a single ended grounded sensor.

4.1 Requirements

4.1.1 Hardware components: Cypress Electronics

The micro controller PSoC4100S Plus is a device of the type 32-bit ARM Cortex M0 with a clock rate of 48 MHz. The micro controller also has a part of the architecture in which find functional blocks that allow data to be processed in parallel. This allows data acquisition at the same time as transmission data from the previous reading cycle. For integration into a system that contains multiple components, it is possible to use the various standard communication protocols such as, for example, SPI, I2C and CAN. The standard protocol used in this application was UART with a maximum transmission speed of 57600 baud rate. The PSoC4100S is designed for applications that include capacitive sensors. For this reason it offers a wide range of programmable parameters dynamically for data acquisition optimization. Among the most important parameters must surely be mentioned:

- the number of conversion bits, a value that can vary from 7 to 16.
- gain, which allows an ideal calibration.

Moreover, it is possible to apply a digital filtering to the captured data of integrated hardware blocks, not used for this project. To eliminate as much noise as possible, the PSoC4100S has a shield that surrounds both the lists and the sensor. The shield and sensors are excited with a square wave at 250 HZ. This feature wasn't tested in this thesis. To ensure an acquisition with minimal noise, the microcontroller makes small calibration corrections automatically. Figure 4.3 shows the PSoC4100S Plus evaluation board used for the project.

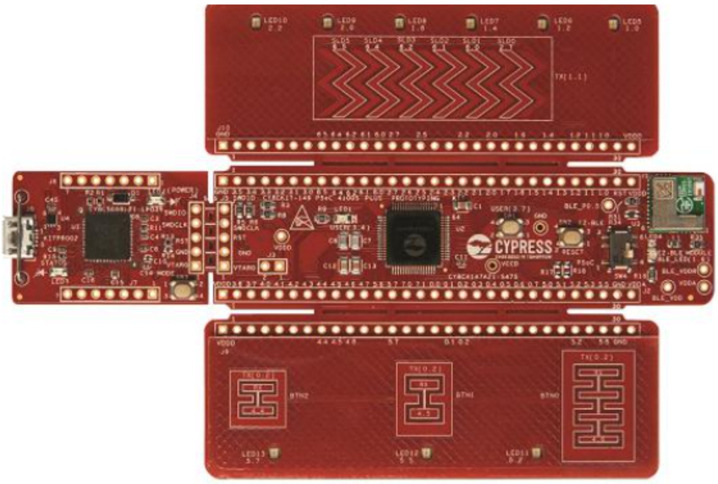

Figure 4.3 PSoC4100S Plus evaluation board.

4.1.2 Software Tools

PSoC Creator

The program PSoC Creator 4.2 has been used for programming the microcontroller Cypress PSoC4100S Plus. This IDE (Integrated Design Environment) is the best development environment for the microcontroller used both with regard to software development, compilation and debugging that for logical design hardware in which it is integrated. Starting from a logical scheme, the IDE automatically includes libraries provided by Cypress, specially designed for processors, in the firmware project. PSoC Creator also allows to debug in real time, connecting the hardware part. The microcontroller and consequently the PsoC Creator were chosen based on the good performance they have provided in previously developed systems in the laboratory. Figure 4.4 shows the PSoC programming interface, while Figure 4.5 shows the blocks used for programming.

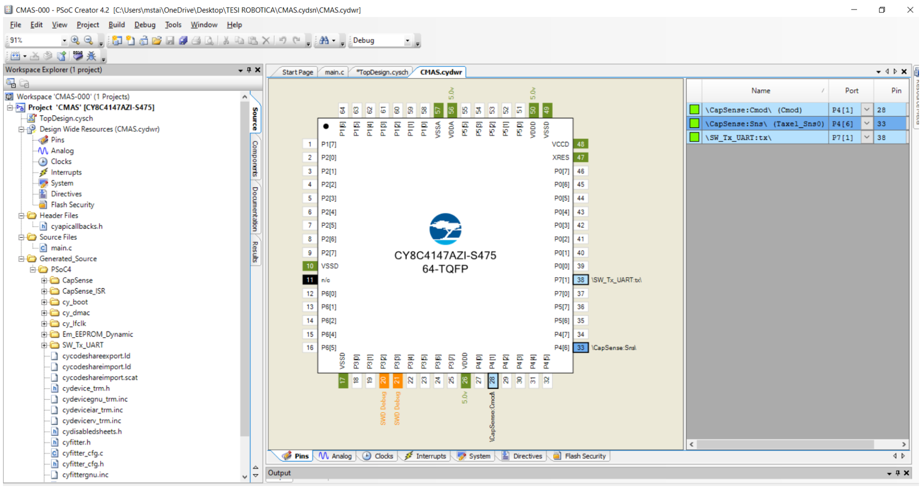

Figure 4.4 PSoC Creator 4.2 programming interface.

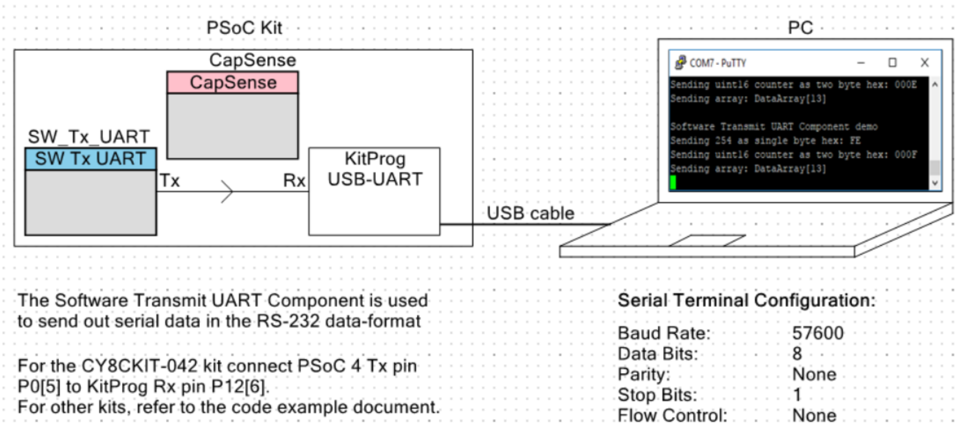

Figure 4.5 PSoC Creator 4.2 components interface.

Tera Term

Tera Term (alternatively TeraTerm) is an open-source, free, software implemented, terminal emulator (communications) program. It emulates different types of computer terminals, from DEC VT100 to DEC VT382. It supports telnet, SSH 1 and 2 and serial port connections. The tool is used to interface with the microcontroller and read the data collected from it, and a view of the interface is shown in Figure 4.6.

Eagle

EAGLE is and electronic design automation (EDA) software that lets printed circuit board (PCB) designers seamlessly connect schematic diagrams, component placement, PCB rout-

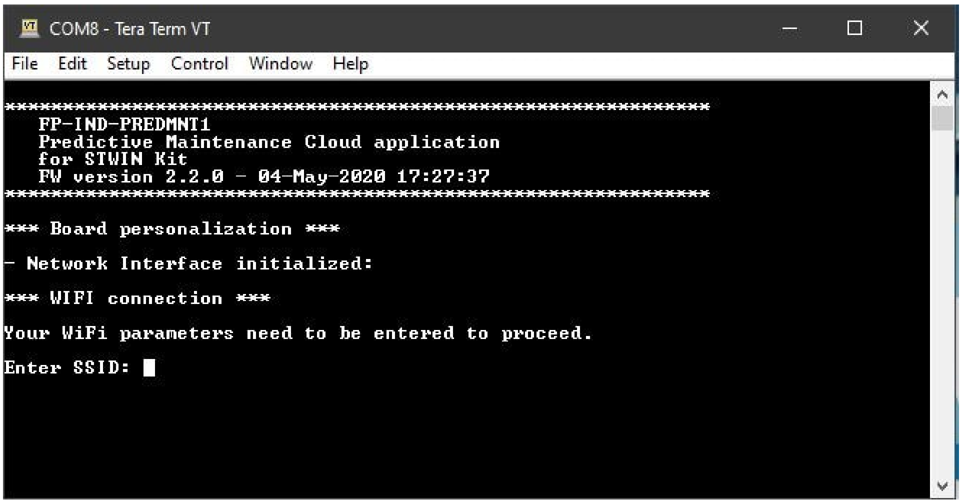

Figure 4.6 Example of the Tera Term interface.

ing, and comprehensive library content. This software tool has been used to design an optimized real integration between the electronics and the manufactured sensors, which could confer much robustness and flexibility to the new improved skin.

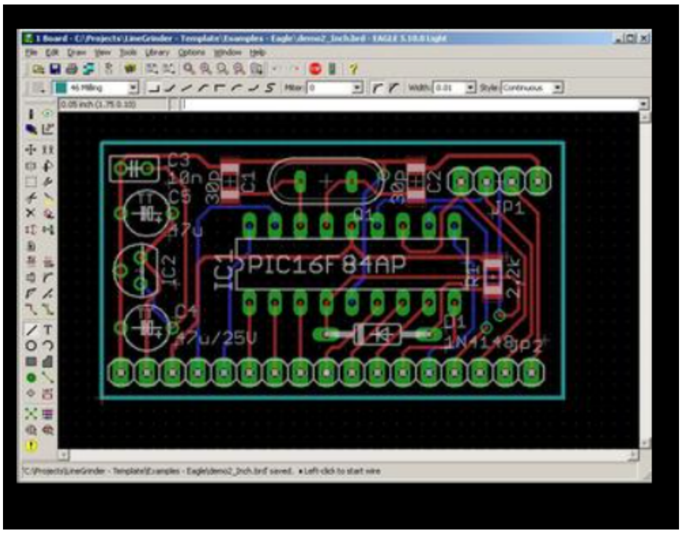

Figure 4.7 Example of the EAGLE interface.

4.2 CAPSENSE™ Technology

The reason to select Cypress PSoC4100S Plus as the main electronic component for capacitance to digital conversion, data transmission and manipulation lies on its CapSense module. CapSense is a touch-sensing technology that works by measuring the capacitance of each I/O pin on the CapSense controller that is designated as a sensor. Capacitance can be measured between two points using either self-capacitance or mutual capacitance. In this case self-capacitance is preferred because is best suited for single-touch sensors. Moreover for either measurements exists the respective sensing method: CapSense Sigma Delta (CSD) for self-capacitance and CapSense Crosspoint (CSX) for the mutual one. Coherently with the precedent choice, CSD is the touch sensing method to look into. Figure 4.8 shows a simplified block diagram of the CSD method.

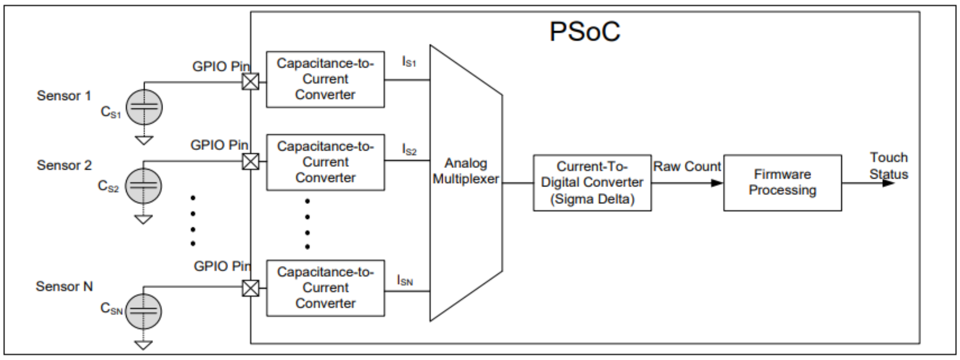

Figure 4.8 Simplified diagram of CAPSENSE™ sigma delta method

In CSD, each GPIO has a switched-capacitance circuit that converts the sensor capacitance into an equivalent current. An analog multiplexer then selects one of the currents and feeds it into the current to digital converter. The current to digital converter is similar to a sigma delta ADC. The output count of the current to digital converter, known as raw count, is a digital value that is proportional to the self-capacitance between the electrodes. The relationship between raw count and sensor capacitance:

$$rawcount = G_c C_s \tag{4.1}$$

Where G_c is the capacitance to digital conversion gain of CSD, and C_s is the self-capacitance of the electrode. When a finger touches the sensor, the C_s increases from C_p to $C_p + C_f$, and the raw count increases. By comparing the change in raw count to a predetermined threshold, logic in firmware decides whether the sensor is active (finger is present). Figure 4.9 depicts a plot of raw count over time.

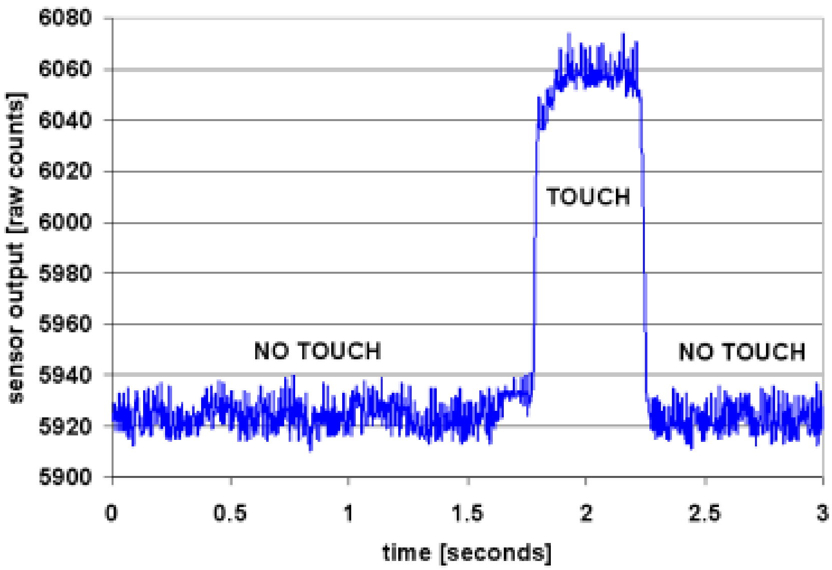

Figure 4.9 Raw count versus time

4.3 Firmware

The firmware is done with PSoC Creator 4.2, previously described. The aim is to develop an algorithm that notifies when a touch event is happening or not. The program works in two phases: first calibrates the sensor and then acquires data to detect if a touch event has occurred or not sending the output through UART at an host PC. Figure 4.10 outlines the logic behind the code.

4.3.1 Calibration Phase

For capacity conversion, the microcontroller works in two steps: first stage is carried out a conversion capacity - current and in the second phase is carried out an analog current conversion - digital. For conversion it is possible to set a gain that allows you to influence directly the dynamics. During the calibration phase this gain is set in such a way the recorded data exploits the maximum possible dynamics and the effect of noise minimize. At the beginning of the calibration the gain is set and only later a compensation parameter, which allows to increase the slope of the conversion function. Figure 4.11 shows graphically the concept.

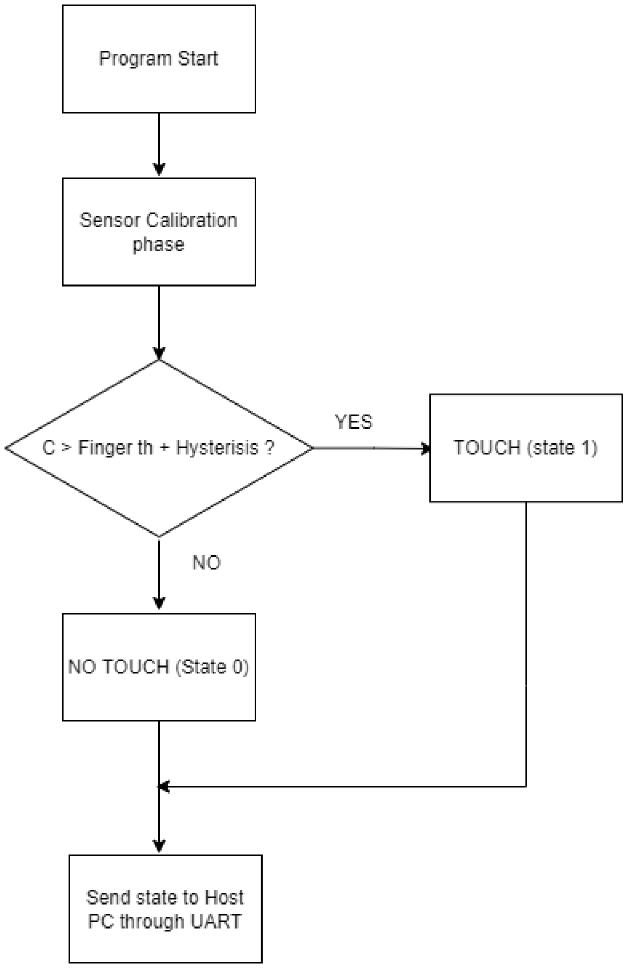

Figure 4.10 Algorithm's Block Diagram

To find the correct value for the gain, the following formulas have been used:

$$rawcount = G_{csd}C_s - (2^n - 1)\frac{I_{COMP}}{I_{MOD}} \quad (4.2)$$

$$G_{csd} = (2^n - 1)\frac{V_{REF}F_{SW}}{I_{MOD}} \quad (4.3)$$

Where:

V_{REF} = Comparator reference voltage

F_{SW} = Sense clock frequency

I_{MOD} = Modulator IDAC current

N = Resolution of the sigma to delta converter

I_{COMP} = Compensation IDAC current

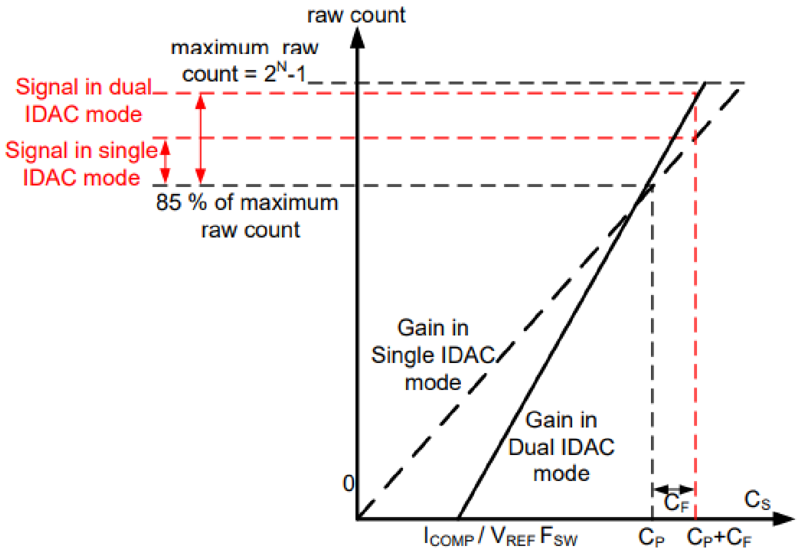

Figure 4.11 Recommended tuning in dual IDAC mode.

The G_{csd} gain is set via the I_{MOD} current generated by the modulation IDAC. The other parameters are set according to the desired resolution and the time of conversion. For the thesis' purpose 16 resolution bits are chosen and scan time equal to 1ms for the sensor. Moreover the I_{MOD} and I_{COMP} are auto calibrated since the CapSense module get autonomously the best ratio between noise and signal (SNR). Figure 4.12 resumes the hardware parameters set.

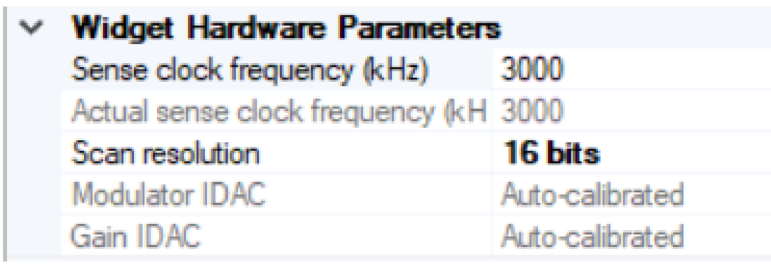

Widget Hardware Parameters	
Sense clock frequency (kHz)	3000
Actual sense clock frequency (kH	3000
Scan resolution	**16 bits**
Modulator IDAC	Auto-calibrated
Gain IDAC	Auto-calibrated

Figure 4.12 Widget Hardware parameters

Next step in calibration regards setting the thresholds parameters which determine the conditions to control the state. These values correspond to a percentage of the measured signal. This is done manually in the code by setting a scan time of 1 ms after initialized the CapSense module since it needs to get the sensor's capacitance and set the proper Modulator and Gain IDAC. Hereafter the pseudocode of the calibration phase:

```
int main(){
 Initialization of variables and components
        ...
 /*Scan all widgets before process them*/
 CapSense_ScanAllWidgets();

 for(;;){
  if (CapSense is not busy){
   /*Process all widgets*/
   CapSense_ProcessAllWidgets()

   /*Establish a communication with the tuner
   to take more accurate measurements*/
   CapSense_RunTuner();

   /*Get the capacitance of the sensor*/
   cap = CapSense_GetSensorCapacitance();

   /*START CALIBRATION*/

   if (Sensor is active and flag == true){
    for(i, i<1000, i++){
     /*Take raw counts values in 1ms*/
     diff_count[i] = CapSense_TAXEL_SNS0_DIFF_VALUE;
    }

     /*Get the max signal to set thresholds*/
     diff_calibrate = GetMax(1000,diff_count);

     /*Set the finger threshold for
     the touch event (80% of the signal)*/
     finger_th = diff_calibrate * 0.8;
     CapSense_SetParam(CapSense_TAXEL_FINGER_TH_VALUE, finger_th);

     /*Set the noise threshold (40% of the signal)*/
     noise_th = diff_calibrate * 0.4;
     CapSense_SetParam(CapSense_TAXEL_NOISE_TH_VALUE, noise_th);

     /*Set the hysteresis (10% of the signal)*/
     hysterisis = diff_calibrate * 0.1;
     CapSense_SetParam(CapSense_TAXEL_HYSTERESIS_VALUE,hysterisis);
     flag = false;
```

```
    }
     /*END CALIBRATION*/
        ...
}
```

Listing 4.1 Calibration phase

To get the max value of raw count a simple function *GetMax(int n,uint32 x[n])* is created.

```
/*function to get the max number in an array*/
uint32 GetMax(int n,uint32 x[n]){
    uint32 max=x[0];
    for(int i=0; i<=n-1; i=i+1) {
      if( x[i]>max ) {
        max=x[i];
      }
    }
    return max;
}
```

Listing 4.2 GetMax() function

4.3.2 Control and Transmission Phase

Once thresholds are set, a simple finite state machine algorithm determines if a touch occurs or not. A touch event is detected when measured capacitance is bigger than the finger thresholds + hysteresis. Here the related bunch of code:

```
    /*get the real time signal*/
    diff = CapSense_TAXEL_SNS0_DIFF_VALUE;

    /*Get the touch event (0 No, 1 Yes)*/
    if(diff<=(finger_th+hysterisis)){
        state = 0;
    }

    else{
        state = 1;
        }
```

Listing 4.3 Control phase

Finally information about the state and the measured capacitance are sent to an host PC through UART at 57600 baud rate by using Software Transmit UART module giving the possibility to monitor the situation, process and elaborate the data.
Here the piece of code:

```
/*convert uint in string to put in UART*/
sprintf(state_uart, "%lu", state);
sprintf(cap_uart, "%lu", cap);

/*sending state and capacitance with CSV format*/
SW_Tx_UART_PutString(state_uart);
SW_Tx_UART_PutString(",");
SW_Tx_UART_PutString(cap_uart);
```

Listing 4.4 Transmission phase

4.4 Tests on Cypress sensors

As interface to see the output data the software Tera Term is used. Figure 4.13 shows the output data from the board's sensors. This confirms that the algorithm works in the proper way by knowing when a touch event is made or not with also measuring the correct capacitance with an accuracy of 15%. In addition to demonstrate that the microcontroller has efficient performances tests on noise and dynamics are done, mainly on board's sensor. The noise measured in the absence of pressure on the sensors is practically non-existent. This was also found in cases where the recommended minimum distances were violated. This is due to the fact that the shielding surrounding the sensors can eliminate all undesirable effects. Tests are done with different bit resolution and different size buttons when pressure is constantly applied. In particular it is considered three rectangular pads with various area (1 mm^2, 1.5 mm^2 and 3 mm^2). The sample are chosen rectangular because of the board fabrication. It is noticed that within a range of 9-13 bit resolution, the noise grows from 3 to 7 bit, producing an SNR which goes from 40 to 103, higher than the sufficient one for a good transmission which is 5. On the other hand if bit resolution arise the noise is negligible with respect to the signal response, but is around 40 bit. However the size of the pads doesn't affect much noise, on the three sample the difference is only of 1 bit between the smallest and the bigger one. Table 4.1 sums up all the considerations. Also Figures 4.14 and 4.15 show the dynamics of a calibrated sensor and the measure of the noise and signal under pressure, respectively.

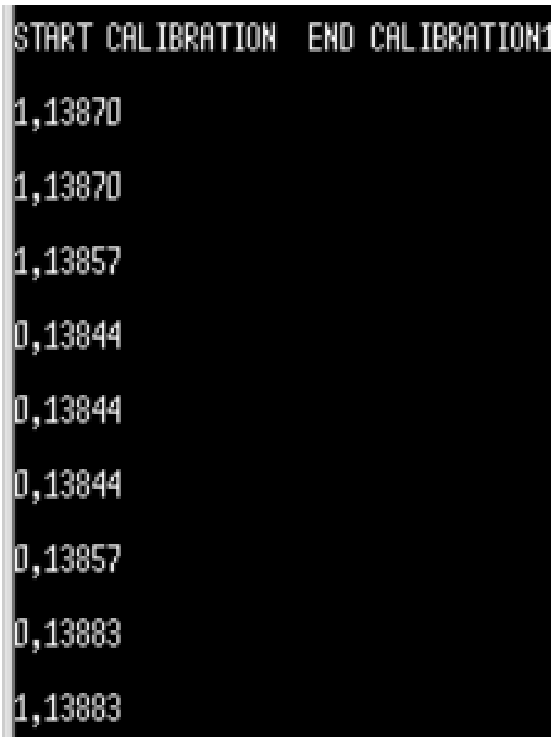

Figure 4.13 Output data: state and capacitance expressed in fF from board's sensors.

Table 4.1 Results of the tests.

Button size and bit resolution	Noise	Signal	SNR
1 mm^2 and 9 bit	3 counts	56 counts	18.71
1.5 mm^2 and 9 bit	3 counts	57 counts	19.05
3 mm^2 and 9 bit	4 counts	79 counts	19.76
1 mm^2 and 10 bit	3 counts	121 counts	40.37
1.5 mm^2 and 10 bit	3 counts	122 counts	41.06
3 mm^2 and 10 bit	4 counts	164 counts	41.16
1 mm^2 and 13 bit	7counts	723 counts	103.28
1.5 mm^2 and 13 bit	7 counts	724 counts	103.42
3 mm^2 and 13 bit	8 counts	827 counts	103.37
1 mm^2 and 15 bit	42 counts	5229 counts	124.51
1.5 mm^2 and 15 bit	42 counts	5230 counts	124.53
3 mm^2 and 15 bit	43 counts	5354 counts	124.51
1 mm^2 and 16 bit	48 counts	6022 counts	125.46
1.5 mm^2 and 16 bit	48 counts	6023 counts	125.48
3 mm^2 and 16 bit	49 counts	6148 counts	125.47

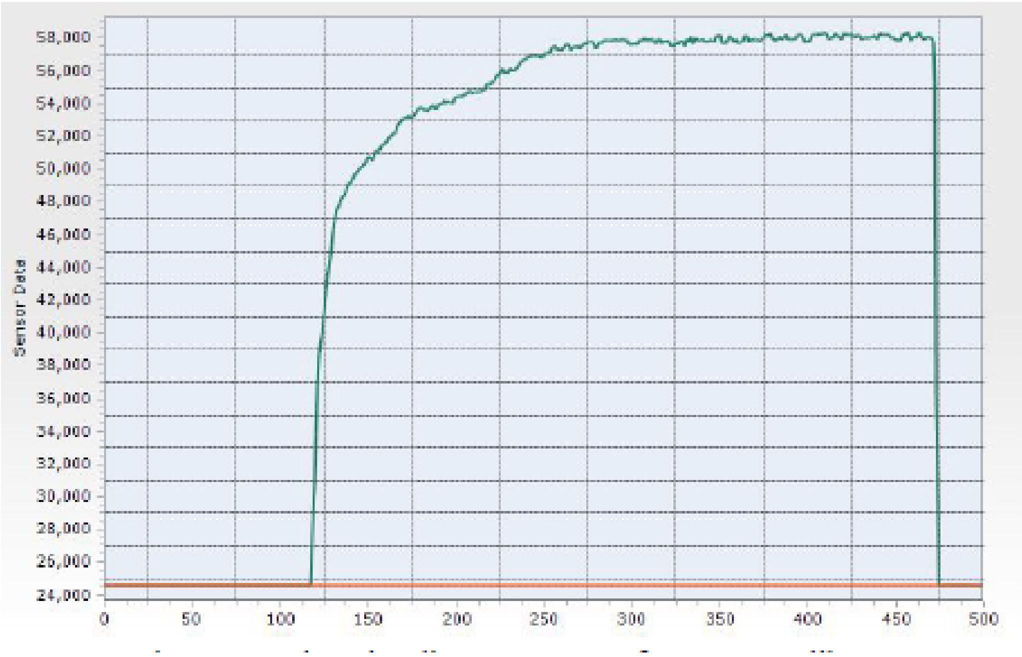

Figure 4.14 Dynamics of a calibrated sensor.

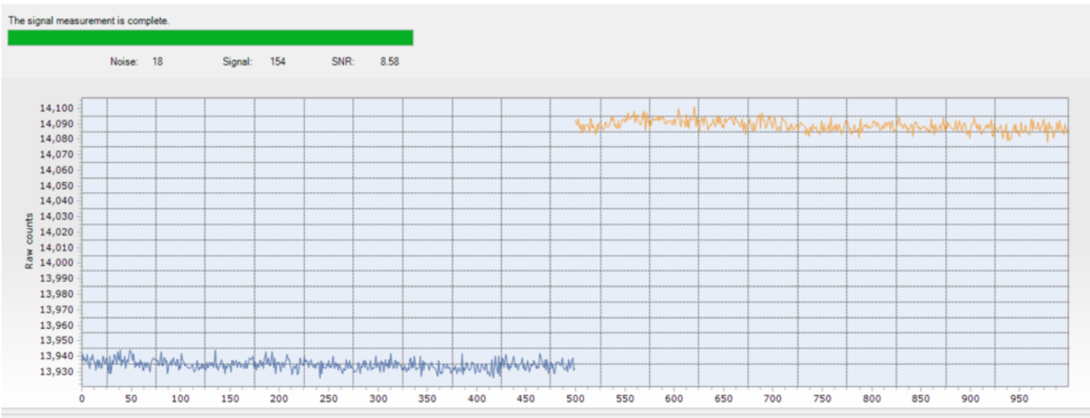

Figure 4.15 Example of test to measure noise, signal and SNR of an external sensor to see if the program has worked properly.

Therefore, the new architecture that provides the employment of the single microcontroller for both CDC and transmission is a robust, flexible and efficient solution to realize a new improved robot skin.

4.5 First integration and prototype design

The final step is to design a real robot skin integrating the tested electronics and the manufactured sensors. The first approach was to connect the inkjet printed sensor to the microcontroller by attaching two wires at the dedicated pins, one for the GND and the other in P4[7], the GPIO corresponding to CapSense controller. The setup is depicted in Figure 4.16.

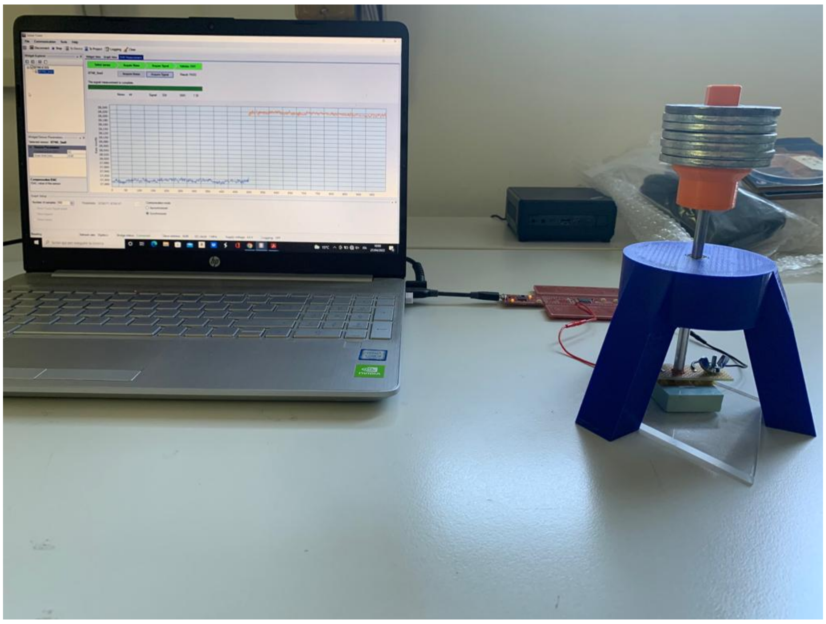

Figure 4.16 First integration of the sensor linked with the microcontroller in a testing phase.

This first implementation is geometrical bulky and not suitable for covering robot's part surfaces which could be also curved. Nevertheless, this raw embedded solution gives further validations about PSoC4100S Plus' capability, measuring the correct capacitance with low noise (see Figure 4.17).

Thus, next stage includes the design of a possible real deployment on a robot. As object of study, a Baxter's arm is taken into account and it is shown in Figure 4.18.

After measuring the surface area of the robot's arm, it is decided to consider the realization of 2 flexible PCBs' blueprint with 24 inkjet printed capacitive sensor in combination with 2 PSoC 4100S Plus microcontrollers. Two microcontrollers have been chosen instead of one to increase the number of sensors covering the surface. Figure 4.19 shows the logical idea of a possible real implementation where capacitance are converted into digital bits by the PSoC and then sent to the host.

```
Sending Capacitance: 39424 fF

Sending Capacitance: 39427 fF

Sending Capacitance: 39374 fF

Sending Capacitance: 39427 fF

Sending Capacitance: 39427 fF

Sending Capacitance: 39427 fF
```

Figure 4.17 Output of TeraTerm with the measured capacitance; for this test an algorithm that measures only the capacity has been used.

Since 2 flexible PCB needs to be connected, board-to-board connectors and ZIF connection are applied. Moreover a reference capacitance C_{MOD} for the conversion is required. To design the circuit schematic (shown in figure 4.20) and the prototype (shown in Figure 4.21), the EAGLE software tool has been used.

As it can be seen by Figure 4.21, the shape of PCBs is strongly constrained by the shape of the 3D body's sample. Vias are the interconnection method between the PCBs and the tactile sensors. A kapton sheet with the inkjet printed taxels is attached on the PCBs. In correspondence of the vias, holes are created to electrically link by means of conductive adhesive the sensors with the microcontroller. Due to the failed supply of components, it was not possible to physically realize the boards and to test the entire prototype on the real robot. However the goal of the thesis is achieved by design a possible embedded solution for the new robot skin which is flexible and low cost.

Figure 4.18 Figure on the left represents Baxter's arm with old electronic skin; on the right the same arm without electronic skin. The red part is the aim of the prototype.

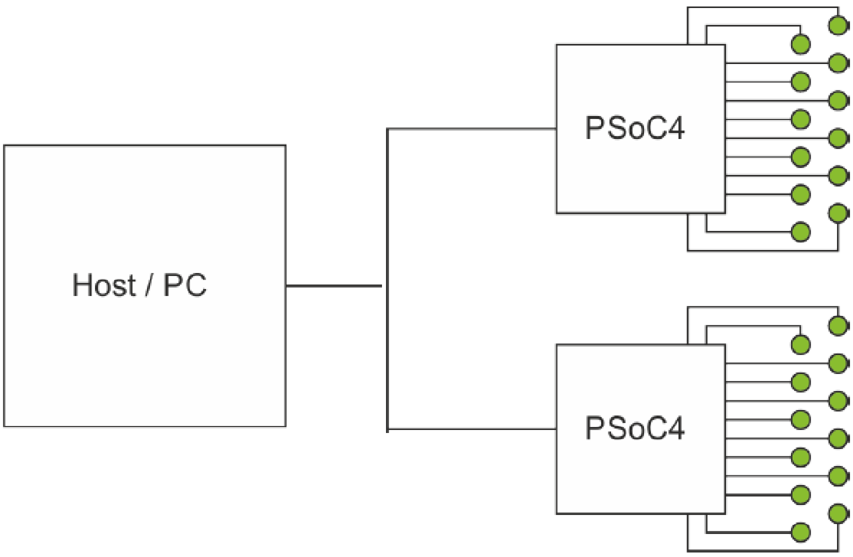

Figure 4.19 Block diagram of the process.

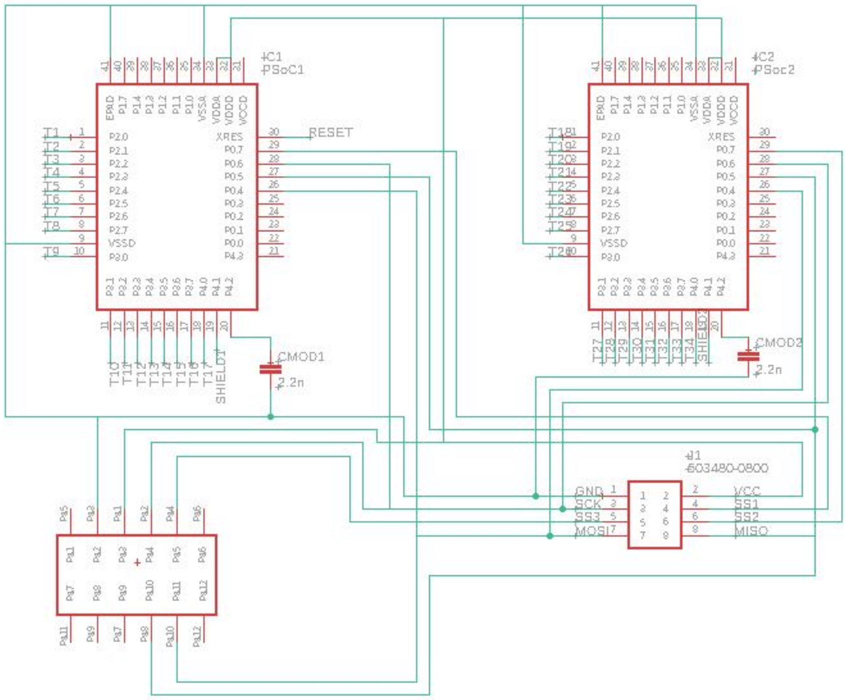

Figure 4.20 Schematic of the electronic circuit.

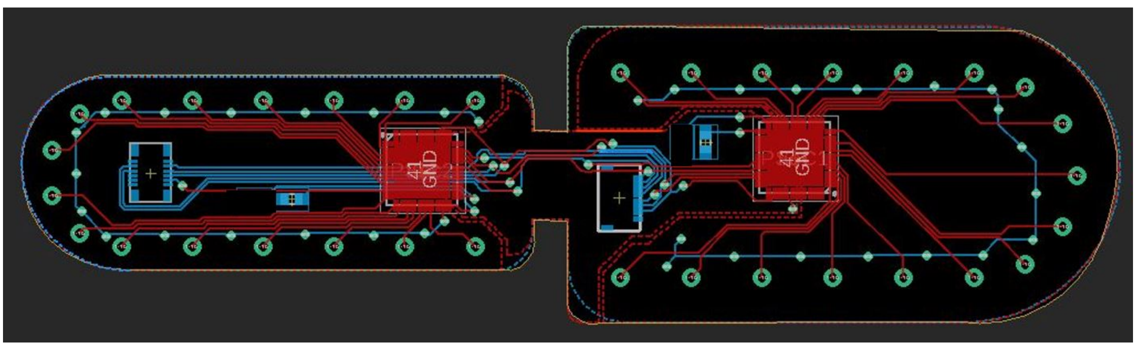

Figure 4.21 Design of the PCBs.

Chapter 5

Conclusions

This thesis proposes the design of capacitive tactile sensors which can be installed on robot bodies, with the aim of maximizing their dynamic range and sensitivity, also founding a manufacturing solution that allows to optimize the sensor placement especially on curved surfaces, with the embedded electronics.

The first contribution of this work aims to discuss the inkjet printing technique as a fabrication method for the development of large-area tactile sensors. The work firstly focuses on the manufacturing techniques and various system-level sensor design aspects related to the inkjet manufacturing processes. The goal is to assess how printed electronics simplify the fabrication process of tactile sensors with respect to conventional fabrication methods and how these contribute to overcome the difficulties arising in the development of tactile sensors for real robot applications. To this aim, a comparative analysis among different inkjet printing technologies and processes is performed, including a quantitative analysis of the design parameters, such as the costs, processing times, sensor layout, and general system-level constraints. The goal is to provide a complete map of the state of the art of inkjet printing, focusing on the most effective topics for the implementation of large-area tactile sensors and a view of the most relevant open problems that should be addressed to improve the effectiveness of these processes.

The second contribution provides a method to maximise the dynamic range and the sensitivity of capacitive tactile sensors by exploiting the vertical direction and creating stacks of capacitors. Firstly, by introducing our mathematical model for capacitive tactile sensors, the solution is motivated by a simplified model leading to an optimal configuration of the layers composing the stack, in order to maximise the sensor response. Then, the characteristics of the simplified model have been validated with finite element simulations and finally the effectiveness of stacked capacitors in a sub-optimal configuration has been tested by using inkjet printing and spin coating as fabrication techniques. The procedure for building capacitors has been proposed although it is certainly not effective for a scale production. The experimental solution presented in this work has to be intended only as a reference to other solutions, and the production and realization must be evaluated and tested starting from the works presented in the literature. The technical problems for implementing stacked capacitors in an efficient way are well known and refer to the need to develop conductive circuits on multiple layers, using printed electronics solutions.

Finally, the new electronic architecture composed of a single microcontroller (PSoC4100S Plus) brings a low-cost solution and allows to increase the number of sensor from which gather data and process them, meaning that a large contact area of the robot can be covered by the sensors and its electronic components. Also the microcontroller provides robust and low-noise operations. The final result is the design of an embedded system that combines the manufactured part with electronics creating an optimal blueprint for a future real implementation.

References

[MID] "molded interconnected devices (mids)". Available on line.

[2] Abadi, Z., Mottaghitalab, V., Bidoki, M., and Benvidi, A. (2014). Flexible biosensor using inkjet printing of silver nanoparticles. *Sensor Review*.

[3] Abu-Khalaf, J. M., Al-Ghussain, L., Al-Halhouli, A., et al. (2018). Fabrication of stretchable circuits on polydimethylsiloxane (pdms) pre-stretched substrates by inkjet printing silver nanoparticles. *Materials*, 11(12):2377.

[4] Abutarboush, H. F. and Shamim, A. (2012). based inkjet-printed tri-band u-slot monopole antenna for wireless applications. *IEEE Antennas and Wireless Propagation Letters*, 11:1234–1237.

[5] Al-Chami, H. and Cretu, E. (2009). Inkjet printing of microsensors. In *2009 IEEE 15th International Mixed-Signals, Sensors, and Systems Test Workshop*, pages 1–6. IEEE.

[6] Al-Halhouli, A., Qitouqa, H., Alashqar, A., and Abu-Khalaf, J. (2018). Inkjet printing for the fabrication of flexible/stretchable wearable electronic devices and sensors. *Sensor Review*.

[7] Albini, A., Denei, S., and Cannata, G. (2017). Human hand recognition from robotic skin measurements in human-robot physical interactions. In *2017 IEEE/RSJ International Conference on Intelligent Robots and Systems (IROS)*, pages 4348–4353.

[8] Albini, A., Grella, F., Maiolino, P., and Cannata, G. (2021). Exploiting distributed tactile sensors to drive a robot arm through obstacles. *IEEE Robotics and Automation Letters*, 6(3):4361–4368.

[9] Albrecht, A., Bobinger, M., Salmerón, J. F., Becherer, M., Cheng, G., Lugli, P., and Rivadeneyra, A. (2018). Over-stretching tolerant conductors on rubber films by inkjet-printing silver nanoparticles for wearables. *Polymers*, 10(12):1413.

[10] Albrecht, A., Trautmann, M., Becherer, M., Lugli, P., and Rivadeneyra, A. (2019). Shear-force sensors on flexible substrates using inkjet printing. *Journal of Sensors*, 2019.

[11] Ando, B. and Baglio, S. (2011). Inkjet-printed sensors: A useful approach for low cost, rapid prototyping [instrumentation notes]. *IEEE Instrumentation & Measurement Magazine*, 14(5):36–40.

[12] Andò, B., Baglio, S., Marletta, V., and Pistorio, A. (2014). A contactless inkjet printed passive touch sensor. In *2014 IEEE International Instrumentation and Measurement Technology Conference (I2MTC) Proceedings*, pages 1638–1642. IEEE.

[13] Anghinolfi, D., Cannata, G., Mastrogiovanni, F., Nattero, C., and Paolucci, M. (2013). On the problem of the automated design of large-scale robot skin. *IEEE Transactions on Automation Science and Engineering*, 10(4):1087–1100.

[14] Baldini, G., Albini, A., Maiolino, P., and Cannata, G. (2022). An atlas for the inkjet printing of large-area tactile sensors. *Sensors*, 22(6):2332.

[15] Bao, R., Wang, C., Dong, L., Yu, R., Zhao, K., Wang, Z. L., and Pan, C. (2015). Flexible and controllable piezo-phototronic pressure mapping sensor matrix by zno nw/p-polymer led array. *Advanced Functional Materials*, 25(19):2884–2891.

[16] Bariya, M., Nyein, H. Y. Y., and Javey, A. (2018). Wearable sweat sensors. *Nature Electronics*, 1(3):160–171.

[17] Basak, I., Nowicki, G., Ruttens, B., Desta, D., Prooth, J., Jose, M., Nagels, S., Boyen, H.-G., D'Haen, J., Buntinx, M., et al. (2020). Inkjet printing of pedot: Pss based conductive patterns for 3d forming applications. *Polymers*, 12(12):2915.

[18] Basiricò, L., Cosseddu, P., Fraboni, B., and Bonfiglio, A. (2011). Inkjet printing of transparent, flexible, organic transistors. *Thin Solid Films*, 520(4):1291–1294.

[19] Belsey, K., Parry, A., Rumens, C., Ziai, M., Yeates, S., Batchelor, J., and Holder, S. (2017). Switchable disposable passive rfid vapour sensors from inkjet printed electronic components integrated with pdms as a stimulus responsive material. *Journal of Materials Chemistry C*, 5(12):3167–3175.

[20] Bhattacharjee, T., Rehg, J. M., and Kemp, C. C. (2012). Haptic classification and recognition of objects using a tactile sensing forearm. In *2012 IEEE/RSJ International Conference on Intelligent Robots and Systems*, pages 4090–4097. IEEE.

[21] Bhushan, B. and Caspers, M. (2017). An overview of additive manufacturing (3d printing) for microfabrication. *Microsystem Technologies*, 23(4):1117–1124.

[22] Borghetti, M., Serpelloni, M., Sardini, E., and Pandini, S. (2016). Mechanical behavior of strain sensors based on pedot: Pss and silver nanoparticles inks deposited on polymer substrate by inkjet printing. *Sensors and Actuators A: Physical*, 243:71–80.

[23] Bormashenko, E., Bormashenko, Y., and Frenkel, M. (2019). Formation of hierarchical porous films with breath-figures self-assembly performed on oil-lubricated substrates. *Materials*, 12(18):3051.

[24] Boschetto, A. and Bottini, L. (2014). Accuracy prediction in fused deposition modeling. *The international journal of advanced manufacturing technology*, 73(5-8):913–928.

[25] Calandra, R., Ivaldi, S., Deisenroth, M. P., et al. (2015). Learning torque control in presence of contacts using tactile sensing from robot skin. In *2015 IEEE-RAS 15th International Conference on Humanoid Robots (Humanoids)*, pages 690–695. IEEE.

[26] Cannata, G., Dahiya, R. S., Maggiali, M., Mastrogiovanni, F., Metta, G., and Valle, M. (2010a). Modular skin for humanoid robot systems. In *4th Int. Conf. on Cognitive Systems*.

[27] Cannata, G., Denei, S., and Mastrogiovanni, F. (2010b). Towards automated self-calibration of robot skin. In *2010 IEEE International Conference on Robotics and Automation*, pages 4849–4854. IEEE.

[28] Cannata, G. and Maggiali, M. (2005). An embedded tactile and force sensor for robotic manipulation and grasping. In *5th IEEE-RAS International Conference on Humanoid Robots, 2005.*, pages 80–85. IEEE.

[29] Cannata, G., Maggiali, M., Metta, G., and Sandini, G. (2008). An embedded artificial skin for humanoid robots. In *2008 IEEE International conference on multisensor fusion and integration for intelligent systems*, pages 434–438. IEEE.

[30] Cao, Z., Yuan, Y., He, G., Peterson, R., and Najafi, K. (2013a). Fabrication of multi-layer vertically stacked fused silica microsystems. In *2013 Transducers & Eurosensors XXVII: The 17th International Conference on Solid-State Sensors, Actuators and Microsystems (TRANSDUCERS & EUROSENSORS XXVII)*, pages 810–813. IEEE.

[31] Cao, Z., Yuan, Y., He, G., Peterson, R., and Najafi, K. (2013b). Fabrication of multi-layer vertically stacked fused silica microsystems. In *2013 Transducers & Eurosensors XXVII: The 17th International Conference on Solid-State Sensors, Actuators and Microsystems (TRANSDUCERS & EUROSENSORS XXVII)*, pages 810–813. IEEE.

[32] Carrozza, M. C., Dario, P., Vecchi, F., Roccella, S., Zecca, M., and Sebastiani, F. (2003). The cyberhand: on the design of a cybernetic prosthetic hand intended to be interfaced to the peripheral nervous system. In *Proceedings 2003 IEEE/RSJ International Conference on Intelligent Robots and Systems (IROS 2003)(Cat. No. 03CH37453)*, volume 3, pages 2642–2647. IEEE.

[33] Castrejon-Pita, J. R., Baxter, W., Morgan, J., Temple, S., Martin, G., and Hutchings, I. M. (2013). Future, opportunities and challenges of inkjet technologies. *Atomization and sprays*, 23(6).

[34] Cha, K. J., Kim, T., Park, S. J., and Kim, D. S. (2014). Simple and cost-effective fabrication of solid biodegradable polymer microneedle arrays with adjustable aspect ratio for transdermal drug delivery using acupuncture microneedles. *Journal of Micromechanics and Microengineering*, 24(11):115015.

[35] Chalvin, M., Campocasso, S., Hugel, V., and Baizeau, T. (2020). Layer-by-layer generation of optimized joint trajectory for multi-axis robotized additive manufacturing of parts of revolution. *Robotics and Computer-Integrated Manufacturing*, 65:101960.

[36] Chandra, M., Ke, S.-Y., Chen, R., and Lo, C.-Y. (2017). Vertically stacked capacitive tactile sensor with more than quadrupled spatial resolution enhancement from planar arrangement. *Sensors and Actuators A: Physical*, 263:386–390.

[37] Chen, L. Y., Tee, B. C.-K., Chortos, A. L., Schwartz, G., Tse, V., J Lipomi, D., Wong, H.-S. P., McConnell, M. V., and Bao, Z. (2014). Continuous wireless pressure monitoring and mapping with ultra-small passive sensors for health monitoring and critical care. *Nature communications*, 5(1):1–10.

[38] Chen, Y.-W., Chandra, M., and Lo, C.-Y. (2021). Calibrations on shear angle detections in vertically stacked capacitive tactile sensors. *IEEE Sensors Journal*, 21(23):26269–26276.

[39] Chi, C., Sun, X., Xue, N., Li, T., and Liu, C. (2018). Recent progress in technologies for tactile sensors. *Sensors*, 18(4):948.

[40] Choi, K.-H., Yoo, J., Lee, C. K., and Lee, S.-Y. (2016a). All-inkjet-printed, solid-state flexible supercapacitors on paper. *Energy & Environmental Science*, 9(9):2812–2821.

[41] Choi, S., Eom, S., Tentzeris, M. M., and Lim, S. (2016b). Inkjet-printed electromagnet-based touchpad using spiral resonators. *Journal of Microelectromechanical Systems*, 25(5):947–953.

[42] Choudhary, H., Vaithiyanathan, D., and Kumar, H. (2021). A review on 3d printed force sensors. In *IOP Conference Series: Materials Science and Engineering*, volume 1104, page 012013. IOP Publishing.

[43] Chung, S., Jang, M., Ji, S.-B., Im, H., Seong, N., Ha, J., Kwon, S.-K., Kim, Y.-H., Yang, H., and Hong, Y. (2013). Flexible high-performance all-inkjet-printed inverters: Organo-compatible and stable interface engineering. *Advanced Materials*, 25(34):4773–4777.

[44] Chung, S., Kim, S. O., Kwon, S.-K., Lee, C., and Hong, Y. (2011a). All-inkjet-printed organic thin-film transistor inverter on flexible plastic substrate. *IEEE electron device letters*, 32(8):1134–1136.

[45] Chung, S., Lee, J., Song, H., Kim, S., Jeong, J., and Hong, Y. (2011b). Inkjet-printed stretchable silver electrode on wave structured elastomeric substrate. *Applied Physics Letters*, 98(15):153110.

[46] Cook, B. S. and Shamim, A. (2012). Inkjet printing of novel wideband and high gain antennas on low-cost paper substrate. *IEEE Transactions on Antennas and Propagation*, 60(9):4148–4156.

[47] Dahiya, R. (2019). E-skin: from humanoids to humans [point of view]. *Proceedings of the IEEE*, 107(2):247–252.

[48] Dahiya, R., Yogeswaran, N., Liu, F., Manjakkal, L., Burdet, E., Hayward, V., and Jörntell, H. (2019). Large-area soft e-skin: The challenges beyond sensor designs. *Proceedings of the IEEE*, 107(10):2016–2033.

[49] Dahiya, R. S., Metta, G., Valle, M., and Sandini, G. (2009). Tactile sensing—from humans to humanoids. *IEEE transactions on robotics*, 26(1):1–20.

[50] Dahiya, R. S., Mittendorfer, P., Valle, M., Cheng, G., and Lumelsky, V. J. (2013). Directions toward effective utilization of tactile skin: A review. *IEEE Sensors Journal*, 13(11):4121–4138.

[51] Dahiya, R. S. and Valle, M. (2012). *Robotic tactile sensing: technologies and system*. Springer Science & Business Media.

[52] Dahiya, R. S. and Valle, M. (2013). *Touch Sensing—Why and Where?*, pages 3–12. Springer Netherlands, Dordrecht.

[53] Dang, W., Vinciguerra, V., Lorenzelli, L., and Dahiya, R. (2017). Printable stretchable interconnects. *Flexible and Printed Electronics*, 2(1):013003.

[54] De Luca, A. and Ferrajoli, L. (2008). Exploiting robot redundancy in collision detection and reaction. In *2008 IEEE/RSJ international conference on intelligent robots and systems*, pages 3299–3305. IEEE.

[55] De Luca, A. and Mattone, R. (2005). Sensorless robot collision detection and hybrid force/motion control. In *Proceedings of the 2005 IEEE international conference on robotics and automation*, pages 999–1004. IEEE.

[56] Dearden, A. L., Smith, P. J., Shin, D.-Y., Reis, N., Derby, B., and O'Brien, P. (2005). A low curing temperature silver ink for use in ink-jet printing and subsequent production of conductive tracks. *Macromolecular Rapid Communications*, 26(4):315–318.

[57] Del Prete, A., Denei, S., Natale, L., Mastrogiovanni, F., Nori, F., Cannata, G., and Metta, G. (2011). Skin spatial calibration using force/torque measurements. In *2011 IEEE/RSJ International Conference on Intelligent Robots and Systems*, pages 3694–3700. IEEE.

[58] Del Prete, A., Nori, F., Metta, G., and Natale, L. (2012). Control of contact forces: The role of tactile feedback for contact localization. In *2012 IEEE/RSJ International Conference on Intelligent Robots and Systems*, pages 4048–4053. IEEE.

[59] Denei, S., Mastrogiovanni, F., and Cannata, G. (2015). Towards the creation of tactile maps for robots and their use in robot contact motion control. *Robotics and Autonomous Systems*, 63:293–308.

[60] Deng, Z., Rosales, B., Choi, L., Mooers, S., and Johnson, B. C. (2020). 3d-printed and wireless piezoelectric tactile sensors. In *Electroactive Polymer Actuators and Devices (EAPAD) XXII*, volume 11375, page 113752A. International Society for Optics and Photonics.

[61] Dong, H., Zhang, L., Wu, T., Song, H., Luo, J., Huang, F., and Zuo, C. (2021). Flexible pressure sensor with high sensitivity and fast response for electronic skin using near-field electrohydrodynamic direct writing. *Organic Electronics*, 89:106044.

[62] Eltaib, M. and Hewit, J. (2003). Tactile sensing technology for minimal access surgery—-a review. *Mechatronics*, 13(10):1163–1177.

[63] Ernst, M. O. and Banks, M. S. (2002). Humans integrate visual and haptic information in a statistically optimal fashion. *Nature*, 415(6870):429–433.

[64] Ervasti, H., Jarvinen, T., Pitkanen, O., Bozo, E., Hiitola-Keinanen, J., Huttunen, O.-H., Hiltunen, J., and Kordas, K. (2021). Inkjet-deposited single-wall carbon nanotube micropatterns on stretchable pdms-ag substrate–electrode structures for piezoresistive strain sensing. *ACS Applied Materials & Interfaces*.

[65] Faller, L.-M., Stetco, C., and Zangl, H. (2019). Design of a novel gripper system with 3d-and inkjet-printed multimodal sensors for automated grasping of a forestry robot. In *2019 IEEE/RSJ International Conference on Intelligent Robots and Systems (IROS)*, pages 5620–5627. IEEE.

[66] Fearing, R. S. (1990). Tactile sensing mechanisms. *The International Journal of Robotics Research*, 9(3):3–23.

[67] Francioso, L., De Pascali, C., Bartali, R., Morganti, E., Lorenzelli, L., Siciliano, P., and Laidani, N. (2013). Pdms/kapton interface plasma treatment effects on the polymeric package for a wearable thermoelectric generator. *ACS applied materials & interfaces*, 5(14):6586–6590.

[68] Frank, T., Doering, L., Heinrich, G., Thronicke, N., Löbner, C., Völlmeke, S., Steinke, A., and Reich, S. (2014). Silicon cantilevers with piezo-resistive measuring bridge for tactile line measurement. *Microsystem technologies*, 20(4):927–931.

[69] Fritzsche, M., Elkmann, N., and Schulenburg, E. (2011). Tactile sensing: A key technology for safe physical human robot interaction. In *Proceedings of the 6th International Conference on Human-robot Interaction*, pages 139–140.

[70] Fu, S., Tao, J., Wu, W., Sun, J., Li, F., Li, J., Huo, Z., Xia, Z., Bao, R., and Pan, C. (2019). Fabrication of large-area bimodal sensors by all-inkjet-printing. *Advanced Materials Technologies*, 4(4):1800703.

[71] Fu, Y.-M., Chou, M.-C., Cheng, Y.-T., Secor, E. B., and Hersam, M. C. (2017). An inkjet printed piezoresistive back-to-back graphene tactile sensor for endosurgical palpation applications. In *2017 IEEE 30th International Conference on Micro Electro Mechanical Systems (MEMS)*, pages 612–615. IEEE.

[72] Fuller, S. B., Wilhelm, E. J., and Jacobson, J. M. (2002). Ink-jet printed nanoparticle microelectromechanical systems. *Journal of Microelectromechanical systems*, 11(1):54–60.

[73] Gan, X., Wang, J., Wang, Z., Zheng, Z., Lavorgna, M., Ronca, A., Fei, G., and Xia, H. (2019). Simultaneous realization of conductive segregation network microstructure and minimal surface porous macrostructure by sls 3d printing. *Materials & Design*, 178:107874.

[74] Gao, M., Li, L., and Song, Y. (2017). Inkjet printing wearable electronic devices. *Journal of Materials Chemistry C*, 5(12):2971–2993.

[75] Gao, W., Zhang, Y., Ramanujan, D., Ramani, K., Chen, Y., Williams, C. B., Wang, C. C., Shin, Y. C., Zhang, S., and Zavattieri, P. D. (2015). The status, challenges, and future of additive manufacturing in engineering. *Computer-Aided Design*, 69:65–89.

[76] Gao, Y.-H., Jen, Y.-H., Chen, R., Aw, K., Yamane, D., and Lo, C.-Y. (2019). Five-fold sensitivity enhancement in a capacitive tactile sensor by reducing material and structural rigidity. *Sensors and Actuators A: Physical*, 293:167–177.

[77] Geravand, M., Flacco, F., and De Luca, A. (2013). Human-robot physical interaction and collaboration using an industrial robot with a closed control architecture. In *2013 IEEE International Conference on Robotics and Automation*, pages 4000–4007. IEEE.

[78] Girão, P. S., Ramos, P. M. P., Postolache, O., and Pereira, J. M. D. (2013). Tactile sensors for robotic applications. *Measurement*, 46(3):1257–1271.

[79] Gu, Q., Yang, Y. E., and Tassoudji, M. A. (1993a). Modeling and analysis of vias in multilayered integrated circuits. *IEEE Transactions on Microwave Theory and Techniques*, 41(2):206–214.

[80] Gu, Q., Yang, Y. E., and Tassoudji, M. A. (1993b). Modeling and analysis of vias in multilayered integrated circuits. *IEEE Transactions on Microwave Theory and Techniques*, 41(2):206–214.

[81] Guelcher, S. A. and Sterling, J. A. (2011). Contribution of bone tissue modulus to breast cancer metastasis to bone. *Cancer Microenvironment*, 4(3):247–259.

[82] Gul, J. Z., Sajid, M., Rehman, M. M., Siddiqui, G. U., Shah, I., Kim, K.-H., Lee, J.-W., and Choi, K. H. (2018). 3d printing for soft robotics–a review. *Science and technology of advanced materials*, 19(1):243–262.

[83] Guo, R., Yu, Y., Xie, Z., Liu, X., Zhou, X., Gao, Y., Liu, Z., Zhou, F., Yang, Y., and Zheng, Z. (2013). Matrix-assisted catalytic printing for the fabrication of multiscale, flexible, foldable, and stretchable metal conductors. *Advanced Materials*, 25(24):3343–3350.

[84] Gupta, S., Heidari, H., Vilouras, A., Lorenzelli, L., and Dahiya, R. (2016). Device modelling for bendable piezoelectric fet-based touch sensing system. *IEEE Transactions on Circuits and Systems I: Regular Papers*, 63(12):2200–2208.

[85] Haddadin, S., Albu-Schaffer, A., De Luca, A., and Hirzinger, G. (2008). Collision detection and reaction: A contribution to safe physical human-robot interaction. In *2008 IEEE/RSJ International Conference on Intelligent Robots and Systems*, pages 3356–3363. IEEE.

[86] Hammond, F. L., Kramer, R. K., Wan, Q., Howe, R. D., and Wood, R. J. (2012). Soft tactile sensor arrays for micromanipulation. In *2012 IEEE/RSJ International Conference on Intelligent Robots and Systems*, pages 25–32. IEEE.

[87] Harmon, L. D. (1982). Automated tactile sensing. *The International Journal of Robotics Research*, 1(2):3–32.

[88] Hemmilä, S., Cauich-Rodríguez, J. V., Kreutzer, J., and Kallio, P. (2012). Rapid, simple, and cost-effective treatments to achieve long-term hydrophilic pdms surfaces. *Applied Surface Science*, 258(24):9864–9875.

[89] Hossain, S. Z., Luckham, R. E., Smith, A. M., Lebert, J. M., Davies, L. M., Pelton, R. H., Filipe, C. D., and Brennan, J. D. (2009). Development of a bioactive paper sensor for detection of neurotoxins using piezoelectric inkjet printing of sol- gel-derived bioinks. *Analytical chemistry*, 81(13):5474–5483.

[90] Hsieh, M.-L., Yeh, S.-K., Lee, J.-H., Lin, P.-S., Lai, M.-F., and Fang, W. (2019). Vertically integrated multiple electrode design for sensitivity enhancement of cmos-mems capacitive tactile sensor. In *2019 20th International Conference on Solid-State Sensors, Actuators and Microsystems & Eurosensors XXXIII (TRANSDUCERS & EUROSENSORS XXXIII)*, pages 2174–2177. IEEE.

[91] Hu, X., Zhang, X., Liu, M., Chen, Y., Li, P., Pei, W., Zhang, C., and Chen, H. (2014). A flexible capacitive tactile sensor array with micro structure for robotic application. *Science China Information Sciences*, 57(12):1–6.

[92] Islam, G. N., Ali, A., and Collie, S. (2020). Textile sensors for wearable applications: A comprehensive review. *Cellulose*, 27(11):6103–6131.

[93] Jain, A., Killpack, M. D., Edsinger, A., and Kemp, C. C. (2013). Reaching in clutter with whole-arm tactile sensing. *The International Journal of Robotics Research*, 32(4):458–482.

[94] Jen, Y.-H., Mo, C.-T., Chen, Y.-W., Martincic, E., Yamane, D., Chang, T.-F. M., Sone, M., and Lo, C.-Y. (2020). Development and characterization of vertically stacked tactile sensor with hollow structure. *IEEE Sensors Journal*, 21(5):5809–5818.

[95] Jensen, G. C., Krause, C. E., Sotzing, G. A., and Rusling, J. F. (2011). Inkjet-printed gold nanoparticle electrochemical arrays on plastic. application to immunodetection of a cancer biomarker protein. *Physical Chemistry Chemical Physics*, 13(11):4888–4894.

[96] Jeong, H., Cui, Y., Tentzeris, M. M., and Lim, S. (2020). Hybrid (3d and inkjet) printed electromagnetic pressure sensor using metamaterial absorber. *Additive Manufacturing*, 35:101405.

[97] Jha, S., Wang, X.-H., and Faber, H. (2017). Touch sensor application of spray deposited zno films. In *2017 IEEE 26th International Symposium on Industrial Electronics (ISIE)*, pages 1412–1416. IEEE.

[98] Jiang, J., Bao, B., Li, M., Sun, J., Zhang, C., Li, Y., Li, F., Yao, X., and Song, Y. (2016). Fabrication of transparent multilayer circuits by inkjet printing. *Advanced Materials*, 28(7):1420–1426.

[99] Kamyshny, A., Ben-Moshe, M., Aviezer, S., and Magdassi, S. (2005). Ink-jet printing of metallic nanoparticles and microemulsions. *Macromolecular Rapid Communications*, 26(4):281–288.

[100] Kappassov, Z., Corrales, J.-A., and Perdereau, V. (2020). Touch driven controller and tactile features for physical interactions. *Robotics and Autonomous Systems*, 123:103332.

[101] Kathan, L. L. (2020). Study of a tactile sensor for robot hands.

[102] Kawahara, Y., Hodges, S., Cook, B. S., Zhang, C., and Abowd, G. D. (2013). Instant inkjet circuits: lab-based inkjet printing to support rapid prototyping of ubicomp devices. In *Proceedings of the 2013 ACM international joint conference on Pervasive and ubiquitous computing*, pages 363–372.

[103] Kawasaki, H., Komatsu, T., and Uchiyama, K. (2002). Dexterous anthropomorphic robot hand with distributed tactile sensor: Gifu hand ii. *IEEE/ASME transactions on mechatronics*, 7(3):296–303.

[104] Kaydanova, T., Miedaner, A., Perkins, J. D., Curtis, C., Alleman, J. L., and Ginley, D. S. (2007). Direct-write inkjet printing for fabrication of barium strontium titanate-based tunable circuits. *Thin Solid Films*, 515(7-8):3820–3824.

[105] Ke, S.-Y., Chen, Y.-W., and Lo, C.-Y. (2020). Novel response acquisition method for enhancing spatial resolution in capacitive tactile sensing array. *IEEE Sensors Journal*, 21(5):5895–5903.

[106] Khan, Y., Pavinatto, F. J., Lin, M. C., Liao, A., Swisher, S. L., Mann, K., Subramanian, V., Maharbiz, M. M., and Arias, A. C. (2016). Inkjet-printed flexible gold electrode arrays for bioelectronic interfaces. *Advanced Functional Materials*, 26(7):1004–1013.

[107] Khan, Y., Thielens, A., Muin, S., Ting, J., Baumbauer, C., and Arias, A. C. (2020). A new frontier of printed electronics: flexible hybrid electronics. *Advanced Materials*, 32(15):1905279.

[108] Khoshmanesh, F., Thurgood, P., Pirogova, E., Nahavandi, S., and Baratchi, S. (2021). Wearable sensors: At the frontier of personalised health monitoring, smart prosthetics and assistive technologies. *Biosensors and Bioelectronics*, 176:112946.

[109] Killpack, M. D., Kapusta, A., and Kemp, C. C. (2016). Model predictive control for fast reaching in clutter. *Autonomous Robots*, 40(3):537–560.

[110] Kim, D. and Moon, J. (2005). Highly conductive ink jet printed films of nanosilver particles for printable electronics. *Electrochemical and Solid State Letters*, 8(11):J30.

[111] Kim, S., Traille, A., Lee, H., Aubert, H., Yoshihiro, K., Georgiadis, A., Collado, A., and Tentzeris, M. M. (2013). Inkjet-printed sensors on paper substrate for agricultural applications. In *2013 European Microwave Conference*, pages 866–869. IEEE.

[112] Kim, S.-Y., Kim, K., Hwang, Y., Park, J., Jang, J., Nam, Y., Kang, Y., Kim, M., Park, H., Lee, Z., et al. (2016). High-resolution electrohydrodynamic inkjet printing of stretchable metal oxide semiconductor transistors with high performance. *Nanoscale*, 8(39):17113–17121.

[113] Kim, T., Song, H., Ha, J., Kim, S., Kim, D., Chung, S., Lee, J., and Hong, Y. (2014). Inkjet-printed stretchable single-walled carbon nanotube electrodes with excellent mechanical properties. *Applied Physics Letters*, 104(11):113103.

[114] Kim, U., Kim, Y. B., Seok, D.-Y., So, J., and Choi, H. R. (2017). A surgical palpation probe with 6-axis force/torque sensing capability for minimally invasive surgery. *IEEE Transactions on Industrial Electronics*, 65(3):2755–2765.

[115] Kim, Y. and Oh, J. H. (2020a). Recent progress in pressure sensors for wearable electronics: From design to applications. *Applied Sciences*, 10(18):6403.

[116] Kim, Y. and Oh, J. H. (2020b). Recent progress in pressure sensors for wearable electronics: From design to applications. *Applied Sciences*, 10(18):6403.

[117] Ko, E.-H., Kim, H.-J., Lee, S.-M., Kim, T.-W., and Kim, H.-K. (2017). Stretchable ag electrodes with mechanically tunable optical transmittance on wavy-patterned pdms substrates. *Scientific reports*, 7(1):1–12.

[118] Ko, S. H., Chung, J., Pan, H., Grigoropoulos, C. P., and Poulikakos, D. (2007). Fabrication of multilayer passive and active electric components on polymer using inkjet printing and low temperature laser processing. *Sensors and Actuators A: Physical*, 134(1):161–168.

[119] Komoda, N., Nogi, M., Suganuma, K., and Otsuka, K. (2012). Highly sensitive antenna using inkjet overprinting with particle-free conductive inks. *ACS applied materials & interfaces*, 4(11):5732–5736.

[120] Konstantinova, J., Stilli, A., and Althoefer, K. (2015). Force and proximity fingertip sensor to enhance grasping perception. In *2015 IEEE/RSJ International Conference on Intelligent Robots and Systems (IROS)*, pages 2118–2123. IEEE.

[121] Kordás, K., Mustonen, T., Tóth, G., Jantunen, H., Lajunen, M., Soldano, C., Talapatra, S., Kar, S., Vajtai, R., and Ajayan, P. M. (2006). Inkjet printing of electrically conductive patterns of carbon nanotubes. *Small*, 2(8-9):1021–1025.

[122] Kumaresan, Y., Ozioko, O., and Dahiya, R. (2021). Multifunctional electronic skin with a stack of temperature and pressure sensor arrays. *IEEE Sensors Journal*, 21(23):26243–26251.

[123] Kuniyoshi, Y., Yorozu, Y., Ohmura, Y., Terada, K., Otani, T., Nagakubo, A., and Yamamoto, T. (2004). From humanoid embodiment to theory of mind. In *Embodied artificial intelligence*, pages 202–218. Springer.

[124] Kwon, H.-J., Chung, S., Jang, J., and Grigoropoulos, C. P. (2016). Laser direct writing and inkjet printing for a sub-2 μm channel length mos2 transistor with high-resolution electrodes. *Nanotechnology*, 27(40):405301.

[125] LaCroix, A. S., Duenwald-Kuehl, S. E., Lakes, R. S., and Vanderby Jr, R. (2013). Relationship between tendon stiffness and failure: a metaanalysis. *Journal of Applied Physiology*, 115(1):43–51.

[126] Leboutet, Q., Dean-Leon, E., Bergner, F., and Cheng, G. (2019a). Tactile-based whole-body compliance with force propagation for mobile manipulators. *IEEE Transactions on Robotics*, 35(2):330–342.

[127] Leboutet, Q., Dean-Leon, E., Bergner, F., and Cheng, G. (2019b). Tactile-based whole-body compliance with force propagation for mobile manipulators. *IEEE Transactions on Robotics*, 35(2):330–342.

[128] Lee, H.-H., Chou, K.-S., and Huang, K.-C. (2005). Inkjet printing of nanosized silver colloids. *Nanotechnology*, 16(10):2436.

[129] Lee, H.-K., Chang, S.-I., and Yoon, E. (2006). A flexible polymer tactile sensor: Fabrication and modular expandability for large area deployment. *Journal of microelectromechanical systems*, 15(6):1681–1686.

[130] Lee, M. H. and Nicholls, H. R. (1999a). Review article tactile sensing for mechatronics—a state of the art survey. *Mechatronics*, 9(1):1–31.

[131] Lee, M. H. and Nicholls, H. R. (1999b). Review article tactile sensing for mechatronics—a state of the art survey. *Mechatronics*, 9(1):1–31.

[132] Lee, T., Kang, Y., Kim, K., Sim, S., Bae, K., Kwak, Y., Park, W., Kim, M., and Kim, J. (2021). All paper-based, multilayered, inkjet-printed tactile sensor in wide pressure detection range with high sensitivity. *Advanced Materials Technologies*, page 2100428.

[133] Lee, U. G., Kim, W.-B., Han, D. H., and Chung, H. S. (2019). A modified equation for thickness of the film fabricated by spin coating. *Symmetry*, 11(9):1183.

[134] Li, C.-Y. and Liao, Y.-C. (2016). Adhesive stretchable printed conductive thin film patterns on pdms surface with an atmospheric plasma treatment. *ACS applied materials & interfaces*, 8(18):11868–11874.

[135] Li, J., Bao, R., Tao, J., Peng, Y., and Pan, C. (2018a). Recent progress in flexible pressure sensor arrays: from design to applications. *Journal of Materials Chemistry C*, 6(44):11878–11892.

[136] Li, J., Bao, R., Tao, J., Peng, Y., and Pan, C. (2018b). Recent progress in flexible pressure sensor arrays: from design to applications. *Journal of Materials Chemistry C*, 6(44):11878–11892.

[137] Li, K., Wei, H., Liu, W., Meng, H., Zhang, P., and Yan, C. (2018c). 3d printed stretchable capacitive sensors for highly sensitive tactile and electrochemical sensing. *Nanotechnology*, 29(18):185501.

[138] Li, Q., Luo, S., and Wang, Q.-M. (2019). Piezoresistive thin film pressure sensor based on carbon nanotube-polyimide nanocomposites. *Sensors and Actuators A: Physical*, 295:336–342.

[139] Li, Q., Schürmann, C., Haschke, R., and Ritter, H. J. (2013). A control framework for tactile servoing. In *Robotics: Science and systems*. Citeseer.

[140] Li, Y., Torah, R., Beeby, S., and Tudor, J. (2012). An all-inkjet printed flexible capacitor on a textile using a new poly (4-vinylphenol) dielectric ink for wearable applications. In *SENSORS, 2012 IEEE*, pages 1–4. IEEE.

[141] Liana, D. D., Raguse, B., Gooding, J. J., and Chow, E. (2012). Recent advances in paper-based sensors. *sensors*, 12(9):11505–11526.

[142] Ling, H., Chen, R., Huang, Q., Shen, F., Wang, Y., and Wang, X. (2020). Transparent, flexible and recyclable nanopaper-based touch sensors fabricated via inkjet-printing. *Green Chemistry*, 22(10):3208–3215.

[143] Liu, C., Huang, N., Xu, F., Tong, J., Chen, Z., Gui, X., Fu, Y., and Lao, C. (2018). 3d printing technologies for flexible tactile sensors toward wearable electronics and electronic skin. *Polymers*, 10(6):629.

[144] Liu, Y., Cui, T., and Varahramyan, K. (2003). All-polymer capacitor fabricated with inkjet printing technique. *Solid-State Electronics*, 47(9):1543–1548.

[145] Lo, L.-W., Shi, H., Wan, H., Xu, Z., Tan, X., and Wang, C. (2020). Inkjet-printed soft resistive pressure sensor patch for wearable electronics applications. *Advanced Materials Technologies*, 5(1):1900717.

[146] Low, Z. W. K., Li, Z., Owh, C., Chee, P. L., Ye, E., Dan, K., Chan, S. Y., Young, D. J., and Loh, X. J. (2020). Recent innovations in artificial skin. *Biomaterials science*, 8(3):776–797.

[147] Ma, S., Liu, L., Bromberg, V., and Singler, T. J. (2014). Electroless copper plating of inkjet-printed polydopamine nanoparticles: A facile method to fabricate highly conductive patterns at near room temperature. *ACS applied materials & interfaces*, 6(22):19494–19498.

[148] Ma, S., Ribeiro, F., Powell, K., Lutian, J., Møller, C., Large, T., and Holbery, J. (2015). Fabrication of novel transparent touch sensing device via drop-on-demand inkjet printing technique. *ACS applied materials & interfaces*, 7(39):21628–21633.

[149] Ma, Z., Li, S., Wang, H., Cheng, W., Li, Y., Pan, L., and Shi, Y. (2019). Advanced electronic skin devices for healthcare applications. *Journal of Materials Chemistry B*, 7(2):173–197.

[150] MacCurdy, R., Katzschmann, R., Kim, Y., and Rus, D. (2016). Printable hydraulics: A method for fabricating robots by 3d co-printing solids and liquids. In *2016 IEEE International Conference on Robotics and Automation (ICRA)*, pages 3878–3885. IEEE.

[151] Magdassi, S., Bassa, A., Vinetsky, Y., and Kamyshny, A. (2003). Silver nanoparticles as pigments for water-based ink-jet inks. *Chemistry of Materials*, 15(11):2208–2217.

[152] Magrini, E. and De Luca, A. (2017). Human-robot coexistence and contact handling with redundant robots. In *2017 IEEE/RSJ International Conference on Intelligent Robots and Systems (IROS)*, pages 4611–4617. IEEE.

[153] Maiolino, P., Galantini, F., Mastrogiovanni, F., Gallone, G., Cannata, G., and Carpi, F. (2015). Soft dielectrics for capacitive sensing in robot skins: Performance of different elastomer types. *Sensors and Actuators A: Physical*, 226:37–47.

[154] Maiolino, P., Maggiali, M., Cannata, G., Metta, G., and Natale, L. (2013). A flexible and robust large scale capacitive tactile system for robots. *IEEE Sensors Journal*, 13(10):3910–3917.

[155] Maiolino, P., Mastrogiovanni, F., Cannata, G., et al. (2016). Skinning a robot: Design methodologies for large-scale robot skin. *IEEE Robotics & Automation Magazine*, 23(4):150–159.

[156] Majewski, C., Perkins, A., Faltz, D., Zhang, F., Zhao, H., and Xiao, W. (2017). Design of a 3d printed insole with embedded plantar pressure sensor arrays. In *Proceedings of the 2017 ACM International Joint Conference on Pervasive and Ubiquitous Computing and Proceedings of the 2017 ACM International Symposium on Wearable Computers*, pages 261–264.

[157] Mannsfeld, S. C., Tee, B. C., Stoltenberg, R. M., Chen, C. V., Barman, S., Muir, B. V., Sokolov, A. N., Reese, C., and Bao, Z. (2010a). Highly sensitive flexible pressure sensors with microstructured rubber dielectric layers. *Nature materials*, 9(10):859–864.

[158] Mannsfeld, S. C., Tee, B. C., Stoltenberg, R. M., Chen, C. V., Barman, S., Muir, B. V., Sokolov, A. N., Reese, C., and Bao, Z. (2010b). Highly sensitive flexible pressure sensors with microstructured rubber dielectric layers. *Nature materials*, 9(10):859–864.

[159] Manuelli, L. and Tedrake, R. (2016). Localizing external contact using proprioceptive sensors: The contact particle filter. In *2016 IEEE/RSJ International Conference on Intelligent Robots and Systems (IROS)*, pages 5062–5069. IEEE.

[160] Martin, T. B., Ambrose, R. O., Diftler, M. A., Platt, R., and Butzer, M. (2004). Tactile gloves for autonomous grasping with the nasa/darpa robonaut. In *IEEE International Conference on Robotics and Automation, 2004. Proceedings. ICRA'04. 2004*, volume 2, pages 1713–1718. IEEE.

[161] Mastrogiovanni, F. and Guo, X. (2019). The robot skin placement problem: a new technique to place triangular modules inside polygons. *Intelligent Service Robotics*, 12(1):27–43.

[162] McCoul, D., Rosset, S., Schlatter, S., and Shea, H. (2017). Inkjet 3d printing of uv and thermal cure silicone elastomers for dielectric elastomer actuators. *Smart Materials and Structures*, 26(12):125022.

[163] McKinley, S., Garg, A., Sen, S., Kapadia, R., Murali, A., Nichols, K., Lim, S., Patil, S., Abbeel, P., Okamura, A. M., et al. (2015). A single-use haptic palpation probe for locating subcutaneous blood vessels in robot-assisted minimally invasive surgery. In *2015 IEEE International Conference on Automation Science and Engineering (CASE)*, pages 1151–1158. Ieee.

[164] Mikkonen, R., Koivikko, A., Vuorinen, T., Sariola, V., and Mantysalo, M. (2021). Inkjet-printed, nanofiber-based soft capacitive pressure sensors for tactile sensing. *IEEE Sensors Journal*.

[165] Mikkonen, R. and Mantysalo, M. (2020). Inkjettable, polydimethylsiloxane based soft electronics. In *2020 IEEE International Conference on Flexible and Printable Sensors and Systems (FLEPS)*, pages 1–3. IEEE.

[166] Mikkonen, R., Puistola, P., Jonkkari, I., and Mantysalo, M. (2020a). Inkjet printable polydimethylsiloxane for all-inkjet-printed multilayered soft electrical applications. *ACS applied materials & interfaces*, 12(10):11990–11997.

[167] Mikkonen, R., Puistola, P., Jonkkari, I., and Mantysalo, M. (2020b). Inkjet printable polydimethylsiloxane for all-inkjet-printed multilayered soft electrical applications. *ACS applied materials & interfaces*, 12(10):11990–11997.

[168] Minemawari, H., Yamada, T., Matsui, H., Tsutsumi, J., Haas, S., Chiba, R., Kumai, R., and Hasegawa, T. (2011). Inkjet printing of single-crystal films. *Nature*, 475(7356):364–367.

[169] Mishra, R. B., El-Atab, N., Hussain, A. M., and Hussain, M. M. (2021). Recent progress on flexible capacitive pressure sensors: From design and materials to applications. *Advanced materials technologies*, 6(4):2001023.

[170] Mittendorfer, P. and Cheng, G. (2011). Humanoid multimodal tactile-sensing modules. *IEEE Transactions on robotics*, 27(3):401–410.

[171] Modayil, J. (2010). Discovering sensor space: Constructing spatial embeddings that explain sensor correlations. In *2010 IEEE 9th International Conference on Development and Learning*, pages 120–125. IEEE.

[172] Montero, K. L., Laurila, M.-M., and Mäntysalo, M. (2020). All printed flexible piezoelectric pressure sensor with interdigitated electrodes. In *2020 IEEE 8th Electronics System-Integration Technology Conference (ESTC)*, pages 1–6. IEEE.

[173] Morales, A., Prats, M., Sanz, P., and Pobil, A. P. (2007). An experiment in the use of manipulation primitives and tactile perception for reactive grasping. In *Robotics: Science and Systems, Workshop on Robot Manipulation: Sensing and Adapting to the Real World, Atlanta, USA*.

[174] Mousavi, S., Howard, D., Wu, S., and Wang, C. (2018). An ultrasensitive 3d printed tactile sensor for soft robotics. *arXiv preprint arXiv:1810.09236*.

[175] Mukai, T., Onishi, M., Odashima, T., Hirano, S., and Luo, Z. (2008). Development of the tactile sensor system of a human-interactive robot "ri-man". *IEEE Transactions on robotics*, 24(2):505–512.

[176] Muth, J. T., Vogt, D. M., Truby, R. L., Mengüç, Y., Kolesky, D. B., Wood, R. J., and Lewis, J. A. (2014). Embedded 3d printing of strain sensors within highly stretchable elastomers. *Advanced materials*, 26(36):6307–6312.

[177] Nicholls, H. R. and Lee, M. H. (1989a). A survey of robot tactile sensing technology. *The International Journal of Robotics Research*, 8(3):3–30.

[178] Nicholls, H. R. and Lee, M. H. (1989b). A survey of robot tactile sensing technology. *The International Journal of Robotics Research*, 8(3):3–30.

[179] Noda, T., Miyashita, T., Ishiguro, H., and Hagita, N. (2012). Super-flexible skin sensors embedded on the whole body self-organizing based on haptic interactions. *Human-Robot Interaction in Social Robotics*, page 183.

[180] Noh, Y., Sareh, S., Back, J., Würdemann, H. A., Ranzani, T., Secco, E. L., Faragasso, A., Liu, H., and Althoefer, K. (2014). A three-axial body force sensor for flexible manipulators. In *2014 IEEE International Conference on Robotics and Automation (ICRA)*, pages 6388–6393. IEEE.

[181] Ohmura, Y. and Kuniyoshi, Y. (2007). Humanoid robot which can lift a 30kg box by whole body contact and tactile feedback. In *2007 IEEE/RSJ International Conference on Intelligent Robots and Systems*, pages 1136–1141. IEEE.

[182] Olberding, S., Gong, N.-W., Tiab, J., Paradiso, J. A., and Steimle, J. (2013). A cuttable multi-touch sensor. In *Proceedings of the 26th annual ACM symposium on User interface software and technology*, pages 245–254.

[183] Ozioko, O. and Dahiya, R. (2021). Smart tactile gloves for haptic interaction, communication, and rehabilitation. *Advanced Intelligent Systems*, page 2100091.

[184] Pang, G., Deng, J., Wang, F., Zhang, J., Pang, Z., and Yang, G. (2018). Development of flexible robot skin for safe and natural human–robot collaboration. *Micromachines*, 9(11):576.

[185] Park, S.-H., Lee, H. B., Yeon, S. M., Park, J., and Lee, N. K. (2016). Flexible and stretchable piezoelectric sensor with thickness-tunable configuration of electrospun nanofiber mat and elastomeric substrates. *ACS applied materials & interfaces*, 8(37):24773–24781.

[186] Payne, C. J., Marcus, H. J., and Yang, G.-Z. (2015). A smart haptic hand-held device for neurosurgical microdissection. *Annals of biomedical engineering*, 43(9):2185–2195.

[187] Peng, Y., Xiao, S., Yang, J., Lin, J., Yuan, W., Gu, W., Wu, X., and Cui, Z. (2017). The elastic microstructures of inkjet printed polydimethylsiloxane as the patterned dielectric layer for pressure sensors. *Applied Physics Letters*, 110(26):261904.

[188] Perelaer, J., De Gans, B.-J., and Schubert, U. S. (2006). Ink-jet printing and microwave sintering of conductive silver tracks. *Advanced materials*, 18(16):2101–2104.

[189] Perelaer, J., Hendriks, C. E., de Laat, A. W., and Schubert, U. S. (2009). One-step inkjet printing of conductive silver tracks on polymer substrates. *Nanotechnology*, 20(16):165303.

[190] Pierce, D. and Kuipers, B. J. (1997). Map learning with uninterpreted sensors and effectors. *Artificial Intelligence*, 92(1-2):169–227.

[191] Ponraj, G., Kirthika, S. K., Lim, C. M., and Ren, H. (2018). Soft tactile sensors with inkjet-printing conductivity and hydrogel biocompatibility for retractors in cadaveric surgical trials. *IEEE Sensors Journal*, 18(23):9840–9847.

[192] Puangmali, P., Liu, H., Seneviratne, L. D., Dasgupta, P., and Althoefer, K. (2011). Miniature 3-axis distal force sensor for minimally invasive surgical palpation. *Ieee/Asme Transactions On Mechatronics*, 17(4):646–656.

[193] Qin, D., Xia, Y., and Whitesides, G. M. (2010). Soft lithography for micro-and nanoscale patterning. *Nature protocols*, 5(3):491.

[194] Rausch, J., Salun, L., Griesheimer, S., Ibis, M., and Werthschützky, R. (2011). Printed resistive strain sensors for monitoring of light-weight structures. In *Smart Sensor Phenomena, Technology, Networks, and Systems 2011*, volume 7982, page 79820H. International Society for Optics and Photonics.

[195] Ren, P. and Dong, J. (2021a). Direct fabrication of via interconnects by electrohydrodynamic printing for multi-layer 3d flexible and stretchable electronics. *Advanced Materials Technologies*, page 2100280.

[196] Ren, P. and Dong, J. (2021b). Direct fabrication of via interconnects by electrohydrodynamic printing for multi-layer 3d flexible and stretchable electronics. *Advanced Materials Technologies*, 6(9):2100280.

[197] Röddiger, T., Beigl, M., Wolffram, D., Budde, M., and Sun, H. (2020). Pdmskin: On-skin gestures with printable ultra-stretchable soft electronic second skin. In *Proceedings of the Augmented Humans International Conference*, pages 1–9.

[198] Rozenberg, G. G., Bresler, E., Speakman, S. P., Jeynes, C., and Steinke, J. H. (2002). Patterned low temperature copper-rich deposits using inkjet printing. *Applied physics letters*, 81(27):5249–5251.

[199] Salim, A. and Lim, S. (2017). Review of recent inkjet-printed capacitive tactile sensors. *Sensors*, 17(11):2593.

[200] Salim, A., Naqvi, A. H., Park, E., Pham, A. D., and Lim, S. (2019). Inkjet printed kirigami inspired split ring resonator for disposable, low cost strain sensor applications. *Smart Materials and Structures*, 29(1):015016.

[201] Sánchez, M., Moriche, R., Sanchez-Romate, X. F., Prolongo, S., Rams, J., and Ureña, A. (2019). Effect of graphene nanoplatelets thickness on strain sensitivity of nanocomposites: A deeper theoretical to experimental analysis. *Composites Science and Technology*, 181:107697.

[202] Schmitz, A., Maiolino, P., Maggiali, M., Natale, L., Cannata, G., and Metta, G. (2011). Methods and technologies for the implementation of large-scale robot tactile sensors. *IEEE Transactions on Robotics*, 27(3):389–400.

[203] Sekine, T., Sugano, R., Tashiro, T., Sato, J., Takeda, Y., Matsui, H., Kumaki, D., Domingues Dos Santos, F., Miyabo, A., and Tokito, S. (2018). Fully printed wearable vital sensor for human pulse rate monitoring using ferroelectric polymer. *Scientific reports*, 8(1):1–10.

[204] Senthil Kumar, K., Chen, P.-Y., and Ren, H. (2019). A review of printable flexible and stretchable tactile sensors. *Research*, 2019.

[205] Sette, D., Mercier, D., Brunet-Manquat, P., Poulain, C., and Blayo, A. (2013). Micro pirani pressure sensor fabricated by inkjet printing of silver nanoparticles. In *2013 Transducers & Eurosensors XXVII: The 17th International Conference on Solid-State Sensors, Actuators and Microsystems (TRANSDUCERS & EUROSENSORS XXVII)*, pages 1783–1786. IEEE.

[206] Shahariar, H., Kim, I., Soewardiman, H., and Jur, J. S. (2019). Inkjet printing of reactive silver ink on textiles. *ACS applied materials & interfaces*, 11(6):6208–6216.

[207] Shen, W., Zhang, X., Huang, Q., Xu, Q., and Song, W. (2014). Preparation of solid silver nanoparticles for inkjet printed flexible electronics with high conductivity. *Nanoscale*, 6(3):1622–1628.

[208] Sherwani, F., Asad, M. M., and Ibrahim, B. (2020). Collaborative robots and industrial revolution 4.0 (ir 4.0). In *2020 International Conference on Emerging Trends in Smart Technologies (ICETST)*, pages 1–5. IEEE.

[209] Shi, H., Liu, C., Jiang, Q., and Xu, J. (2015). Effective approaches to improve the electrical conductivity of pedot: Pss: a review. *Advanced Electronic Materials*, 1(4):1500017.

[210] Siciliano, B., Khatib, O., and Kröger, T. (2008). *Springer handbook of robotics*, volume 200. Springer.

[211] Simaite, A., Mesnilgrente, F., Tondu, B., Souères, P., and Bergaud, C. (2016). Towards inkjet printable conducting polymer artificial muscles. *Sensors and Actuators B: Chemical*, 229:425–433.

[212] Singh, M., Haverinen, H. M., Dhagat, P., and Jabbour, G. E. (2010). Inkjet printing—process and its applications. *Advanced materials*, 22(6):673–685.

[213] Sirringhaus, H., Kawase, T., Friend, R., Shimoda, T., Inbasekaran, M., Wu, W., and Woo, E. (2000). High-resolution inkjet printing of all-polymer transistor circuits. *Science*, 290(5499):2123–2126.

[214] Sommer, N. and Billard, A. (2016). Multi-contact haptic exploration and grasping with tactile sensors. *Robotics and autonomous systems*, 85:48–61.

[215] Srichan, C., Saikrajang, T., Lomas, T., Jomphoak, A., Maturos, T., Phokaratkul, D., Kerdcharoen, T., and Tuantranont, A. (2009). Inkjet printing pedot: Pss using desktop inkjet printer. In *2009 6th International Conference on Electrical Engineering/Electronics, Computer, Telecommunications and Information Technology*, volume 1, pages 465–468. IEEE.

[216] Stříteskỳ, S., Marková, A., Víteček, J., Šafaříková, E., Hrabal, M., Kubáč, L., Kubala, L., Weiter, M., and Vala, M. (2018). Printing inks of electroactive polymer pedot: Pss: The study of biocompatibility, stability, and electrical properties. *Journal of Biomedical Materials Research Part A*, 106(4):1121–1128.

[217] Sun, J., Jiang, J., Bao, B., Wang, S., He, M., Zhang, X., and Song, Y. (2016). Fabrication of bendable circuits on a polydimethylsiloxane (pdms) surface by inkjet printing semi-wrapped structures. *Materials*, 9(4):253.

[218] Sun, X., Liu, T., Zhou, J., Yao, L., Liang, S., Zhao, M., Liu, C., and Xue, N. (2021). Recent applications of different microstructure designs in high performance tactile sensors: A review. *IEEE Sensors Journal*.

[219] Sung, Y.-L., Jeang, J., Lee, C.-H., and Shih, W.-C. (2015). Fabricating optical lenses by inkjet printing and heat-assisted in situ curing of polydimethylsiloxane for smartphone microscopy. *Journal of biomedical optics*, 20(4):047005.

[220] Sweeney, J. and Ward, I. M. (2012). *Mechanical properties of solid polymers*. John Wiley and Sons.

[221] Talasaz, A., Trejos, A. L., and Patel, R. V. (2016). The role of direct and visual force feedback in suturing using a 7-dof dual-arm teleoperated system. *IEEE transactions on haptics*, 10(2):276–287.

[222] Tas, M. O., Baker, M. A., Masteghin, M. G., Bentz, J., Boxshall, K., and Stolojan, V. (2019). Highly stretchable, directionally oriented carbon nanotube/pdms conductive films with enhanced sensitivity as wearable strain sensors. *ACS applied materials & interfaces*, 11(43):39560–39573.

[223] Teichler, A., Perelaer, J., and Schubert, U. S. (2013). Inkjet printing of organic electronics–comparison of deposition techniques and state-of-the-art developments. *Journal of Materials Chemistry C*, 1(10):1910–1925.

[224] Thompson, M. K., Moroni, G., Vaneker, T., Fadel, G., Campbell, R. I., Gibson, I., Bernard, A., Schulz, J., Graf, P., Ahuja, B., et al. (2016). Design for additive manufacturing: Trends, opportunities, considerations, and constraints. *CIRP annals*, 65(2):737–760.

[225] Thuau, D., Kallitsis, K., Dos Santos, F. D., and Hadziioannou, G. (2017). All inkjet-printed piezoelectric electronic devices: energy generators, sensors and actuators. *Journal of Materials Chemistry C*, 5(38):9963–9966.

[226] Tiwana, M. I., Redmond, S. J., and Lovell, N. H. (2012a). A review of tactile sensing technologies with applications in biomedical engineering. *Sensors and Actuators A: physical*, 179:17–31.

[227] Tiwana, M. I., Redmond, S. J., and Lovell, N. H. (2012b). A review of tactile sensing technologies with applications in biomedical engineering. *Sensors and Actuators A: physical*, 179:17–31.

[228] Tobjörk, D. and Österbacka, R. (2011). Paper electronics. *Advanced materials*, 23(17):1935–1961.

[229] Tomchenko, A. A. (2006). Printed chemical sensors: From screen-printing to micro-printing. *Encycl. Sens*, 10:279–290.

[230] Van Osch, T. H., Perelaer, J., De Laat, A. W., and Schubert, U. S. (2008). Inkjet printing of narrow conductive tracks on untreated polymeric substrates. *Advanced Materials*, 20(2):343–345.

[231] Vatani, M., Lu, Y., Engeberg, E. D., and Choi, J.-W. (2015). Combined 3d printing technologies and material for fabrication of tactile sensors. *International Journal of Precision Engineering and Manufacturing*, 16(7):1375–1383.

[232] Vu, C. C., Kim, S. J., and Kim, J. (2021). Flexible wearable sensors-an update in view of touch-sensing. *Science and Technology of Advanced Materials*, 22(1):26–36.

[233] Wang, S., Lin, L., and Wang, Z. L. (2015a). Triboelectric nanogenerators as self-powered active sensors. *Nano Energy*, 11:436–462.

[234] Wang, X., Dong, L., Zhang, H., Yu, R., Pan, C., and Wang, Z. L. (2015b). Recent progress in electronic skin. *Advanced Science*, 2(10):1500169.

[235] Wang, X., Li, J., Song, H., Huang, H., and Gou, J. (2018). Highly stretchable and wearable strain sensor based on printable carbon nanotube layers/polydimethylsiloxane composites with adjustable sensitivity. *ACS applied materials & interfaces*, 10(8):7371–7380.

[236] Wang, X., Liu, Z., and Zhang, T. (2017). Flexible sensing electronics for wearable/attachable health monitoring. *Small*, 13(25):1602790.

[237] Wang, Y., Bokor, J., and Lee, A. (2004). Maskless lithography using drop-on-demand inkjet printing method. In *Emerging Lithographic Technologies VIII*, volume 5374, pages 628–636. International Society for Optics and Photonics.

[238] Wasserfall, F. (2018). Topology-aware routing of electric wires in fdm-printed objects. In *Proceedings of the 29th International Solid Freeform Fabrication Symposium*, pages 1649–1659.

[239] Watson, N., Meisel, N. A., Bilén, S., Duarte, J., and Nazarian, S. (2019). Large-scale additive manufacturing of concrete using a 6-axis robotic arm for autonomous habitat construction. In *2019 International Solid Freeform Fabrication Symposium*. University of Texas at Austin.

[240] Wei, X., Joneja, A., and Tang, K. (2014). An improved algorithm for the automated design of large-scaled robot skin. *IEEE Transactions on Automation Science and Engineering*, 12(1):372–377.

[241] Windecker, R. and Tiziani, H. J. (1999). Optical roughness measurements using extended white-light interferometry. *Optical engineering*, 38(6):1081–1087.

[242] Wong, K. V. and Hernandez, A. (2012). A review of additive manufacturing. *International scholarly research notices*, 2012.

[243] Woo, K., Kim, D., Kim, J. S., Lim, S., and Moon, J. (2009). Ink-jet printing of cu-ag-based highly conductive tracks on a transparent substrate. *Langmuir*, 25(1):429–433.

[244] Wu, J., Roberts, R., Tien, N. C., and Li, D. (2014). Inkjet printed silver patterning on pdms to fabricate microelectrodes for microfluidic sensing. In *SENSORS, 2014 IEEE*, pages 1100–1103. IEEE.

[245] Wu, J., Wang, R., Yu, H., Li, G., Xu, K., Tien, N. C., Roberts, R. C., and Li, D. (2015a). Inkjet-printed microelectrodes on pdms as biosensors for functionalized microfluidic systems. *Lab on a Chip*, 15(3):690–695.

[246] Wu, J., Wang, R., Yu, H., Li, G., Xu, K., Tien, N. C., Roberts, R. C., and Li, D. (2015b). Inkjet-printed microelectrodes on pdms as biosensors for functionalized microfluidic systems. *Lab on a Chip*, 15(3):690–695.

[247] Wu, J., Yao, Y., Zhang, Y., Shao, T., Wu, H., Liu, S., Li, Z., and Wu, L. (2020). Rational design of flexible capacitive sensors with highly linear response over a broad pressure sensing range. *Nanoscale*, 12(41):21198–21206.

[248] Wu, J.-T., Hsu, S. L.-C., Tsai, M.-H., and Hwang, W.-S. (2009). Conductive silver patterns via ethylene glycol vapor reduction of ink-jet printed silver nitrate tracks on a polyimide substrate. *Thin Solid Films*, 20(517):5913–5917.

[249] Xu, K., Lu, Y., and Takei, K. (2019). Multifunctional skin-inspired flexible sensor systems for wearable electronics. *Advanced Materials Technologies*, 4(3):1800628.

[250] Xu, Y., Wu, X., Guo, X., Kong, B., Zhang, M., Qian, X., Mi, S., and Sun, W. (2017). The boom in 3d-printed sensor technology. *Sensors*, 17(5):1166.

[251] Yang, L., Rida, A., Vyas, R., and Tentzeris, M. M. (2007). Rfid tag and rf structures on a paper substrate using inkjet-printing technology. *IEEE transactions on microwave theory and techniques*, 55(12):2894–2901.

[252] Yang, T., Xie, D., Li, Z., and Zhu, H. (2017a). Recent advances in wearable tactile sensors: Materials, sensing mechanisms, and device performance. *Materials Science and Engineering: R: Reports*, 115:1–37.

[253] Yang, T., Xie, D., Li, Z., and Zhu, H. (2017b). Recent advances in wearable tactile sensors: Materials, sensing mechanisms, and device performance. *Materials Science and Engineering: R: Reports*, 115:1–37.

[254] Yeo, L., Lok, B., Nguyen, Q., Lu, C., and Lam, Y. (2014). Selective surface modification of pet substrate for inkjet printing. *The International Journal of Advanced Manufacturing Technology*, 71(9-12):1749–1755.

[255] Yilbas, B., Al-Sharafi, A., and Ali, H. (2019). *Self-cleaning of surfaces and water droplet mobility*. Elsevier.

[256] Yin, Z. (2010). Y. a. huang, nb bu, xm wang, yl xiong, inkjet printing for flexible electronics: Materials, processes and equipments. *Chinese Sci. Bull*, 55(30):3383–3407.

[257] Yin, Z., Huang, Y., Bu, N., Wang, X., and Xiong, Y. (2010). Inkjet printing for flexible electronics: Materials, processes and equipments. *Chinese Science Bulletin*, 55(30):3383–3407.

[258] Yun, T., Eom, S., and Lim, S. (2016). Based capacitive touchpad using home inkjet printer. *Journal of Display Technology*, 12(11):1411–1416.

[259] Zhang, F., Tuck, C., Hague, R., He, Y., Saleh, E., Li, Y., Sturgess, C., and Wildman, R. (2016). Inkjet printing of polyimide insulators for the 3 d printing of dielectric materials for microelectronic applications. *Journal of Applied Polymer Science*, 133(18).

[260] Zhang, Q., Leonardi, F., Pfattner, R., and Mas-Torrent, M. (2019a). A solid-state aqueous electrolyte-gated field-effect transistor as a low-voltage operation pressure-sensitive platform. *Advanced Materials Interfaces*, 6(16):1900719.

[261] Zhang, T., Li, Z., Li, K., and Yang, X. (2019b). Flexible pressure sensors with wide linearity range and high sensitivity based on selective laser sintering 3d printing. *Advanced Materials Technologies*, 4(12):1900679.

[262] Zhang, Y.-R., Jen, Y.-H., Mo, C.-T., Chen, Y.-W., Al-Romaithy, M., Martincic, E., and Lo, C.-Y. (2020). Realization of multistage detection sensitivity and dynamic range in capacitive tactile sensors. *IEEE Sensors Journal*, 20(17):9724–9732.

[263] Zhao, X., Zhang, Z., Liao, Q., Xun, X., Gao, F., Xu, L., Kang, Z., and Zhang, Y. (2020). Self-powered user-interactive electronic skin for programmable touch operation platform. *Science advances*, 6(28):eaba4294.

[264] Zhou, L.-y., Fu, J.-z., Gao, Q., Zhao, P., and He, Y. (2020). All-printed flexible and stretchable electronics with pressing or freezing activatable liquid-metal–silicone inks. *Advanced Functional Materials*, 30(3):1906683.

[265] Zhou, X. and Lee, P. S. (2021). Three-dimensional printing of tactile sensors for soft robotics. *MRS Bulletin*, 46(4):330–336.

[266] Zhuang, J.-L., Ar, D., Yu, X.-J., Liu, J.-X., and Terfort, A. (2013). Patterned deposition of metal-organic frameworks onto plastic, paper, and textile substrates by inkjet printing of a precursor solution. *Advanced materials*, 25(33):4631–4635.

[267] Zou, L., Ge, C., Wang, Z. J., Cretu, E., and Li, X. (2017). Novel tactile sensor technology and smart tactile sensing systems: A review. *Sensors*, 17(11):2653.

Appendix A

Generalization of the mathematical model in the case of an N-layer stack

As shown in Section 2.1, if we consider the case $N = 2$, where N is a design specification related to the number of layers of the stack, the optimal thickness allocation is t_{min}, $\Delta - t_{min}$, where Δ is the total transducer thickness intended also as a design specification as shown in Figure A.1 and t_{min} is a technological constraint representing the minimum possible layer thickness.

Figure A.1 Generalization for N layers.

$N \cdot t \leq \Delta$ is the feasibility constraint ensuring the possibility of implementing an N-stack capacitor and of course the interesting case is when $N \cdot t < \Delta$ or even $\Delta \gg N \cdot t$.

Let assume Δ is given and, by induction, let assume that for a $N - 1$ layers stack, the maximum capacitance is obtained using the configuration explained in Equation 20.

$$\begin{cases} x_1 = t_{min} \\ x_{N-2} = t_{min} \\ x_{N-1} = \Delta - (N-2) \cdot t_{min} \end{cases} \tag{A.1}$$

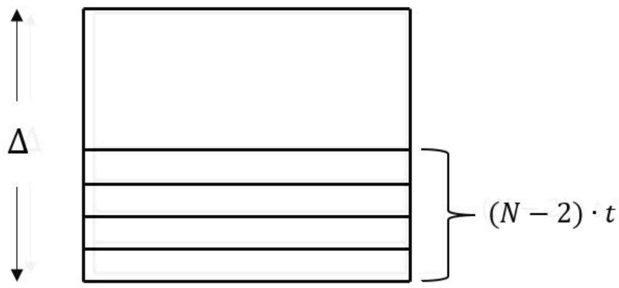

Figure A.2 Case for N-1 layers stack.

In the case of N layers we can observe that the distribution of Equation 20 maximises the capacitance for a vertical space budget $\Delta_{N-2} = (N-2) \cdot t_{min}$. Therefore, for the allocation of the remaining two layers there is a space budget equal to $\Delta - (N-2) \cdot t_{min}$.

This corresponds to the problem of maximizing the capacitance of a 2 layers stack for an available space $\bar{\Delta} = \Delta - (N-2) \cdot t_{min}$ which leads to the following allocation:

$$\begin{cases} x_{N-1} = t_{min} \\ x_N = \Delta - (N-2) \cdot t_{min} + t_{min} \end{cases} \tag{A.2}$$